A probabilistic framework for the quantification of vegetation effects on the failure mechanisms of Dutch river dikes

L. M. Wopereis

A probabilistic framework for the quantification of vegetation effects on the failure mechanisms of Dutch river dikes

by

L. M. Wopereis

to obtain the degree of Master of Science

at the Delft University of Technology,

to be defended publicly on 12 January, 2021 at 09:00 AM.

Student number:	4393600	
Project duration:	November 30, 2019 – November 30, 2020	
Thesis committee:	Dr. R. C. Lanzafame,	TU Delft, Daily supervisor
	Dr. J. P. Aguilar-López,	TU Delft, Chair person
	Dr. D. Kurowicka,	TU Delft, External Supervisor
	Dr. E. Penning,	Deltares, Company Supervisor

TU Delft

Preface

This thesis is part of my Masters degree in Civil Engineering with specialization “Flood Risk” at the Delft University of Technology. It focuses on the creation of a probabilistic framework for quantifying vegetation effects on dike failure mechanisms. The approach is applied to three river dikes in the Netherlands.

I chose this topic because I believe that most of our problems can be solved in a sustainable way by observing and learning from nature. This holds true for one of our most important problems caused by climate change: an increase in the risk of flooding. This concerns the majority of the biggest cities around the world, due to their location near a sea, ocean, or river. This means that attention to flood defences will become even more important in the future and that is certainly true for a low-lying country like the Netherlands. It will be crucial to include nature-based options when considering dike strengthening and maintenance because this may reduce their environmental footprint considerably.

I hope you will enjoy reading this thesis and that it will contribute to greener and safer dikes in the Netherlands - with vegetation welcoming a variety of birds and fish thereby contributing to a cleaner, healthier and friendlier environment. I sincerely hope that this thesis is a step towards achieving that vision.

L. M. Wopereis
Delft, November 2020

Acknowledgments

I would like to provide my sincere gratitude to my four supervisors: Robert Lanzafame, Juan Aguilar-López, Dorota Kurowicka, and Ellis Penning.

It was a pleasure to work with all of you and your different backgrounds made this whole experience extremely interesting. I truly appreciate the effort all of you put into this study.

Thank you, Robert, for all the interesting talks about the different vegetation effects, for helping me set up the topic and debugging my codes, and for your critical feedback on my reports.

Juan, thank you for always being enthusiastic and taking the time to explain everything in detail. I appreciated you sharing your knowledge of Pomegranate, which was essential for this research.

Dorota, thanks a lot for your advice to help me set up the model, for your critical feedback on the report, and for your always-practical views. You certainly steered this thesis in the right direction.

Last but not least, Ellis, thank you for contacting multiple water authorities for me and introducing me to so many useful people, and for all our discussions. Your feedback really helped in adding a practical view to this topic.

My gratitude also goes to Jan Gruppen and Marten Hoeksema from the water authorities "Drents Overijsselse Delta" and "Vallei en Veluwe" for their help in providing me with essential information and data for the research.

Furthermore, I would like to give my special gratitude to my boyfriend Roberto, in particular for his patience with me during the writing of this thesis. I look forward to taking on the next challenge together with you. Thanks a lot to my family, my parents, sister Tamika, and brother Guido for all their love, support, and feedback. A special thanks goes to my dearest friends Shakthi and Jason: you always knew what to say to bring down stress levels and make me smile.

Summary

River floods are becoming increasingly devastating due to the effects of climate change (more frequent and extreme rainfall), population growth and the increasing economic importance of river basins. The Netherlands is particularly affected because a quarter of its land area lies below sea level and more than half is vulnerable to flooding. This situation requires maintenance and strengthening of flood-defence systems. For dikes, this is traditionally done by increasing their width and height (also known as crest). This approach entails high costs and may be difficult to implement because of space constraints.

Adding certain types of vegetation at precise locations for their positive impact may be a cheaper, more flexible, and more environment-friendly way to strengthen dikes than the traditional increase in height. However, this nature-based (NB) option is not yet widely implemented due to the lack of precise knowledge of the potential of vegetation effects (which can also be negative) and their uncertainty (caused by seasonal variations in growth or vulnerability to diseases or attacks by animals). Therefore, to allow for the safe use of NB flood defences, it is essential to fully understand the effects of vegetation on individual dike failure mechanisms and their overall impact on the total failure probability of a dike.

This study uses a probabilistic method for including vegetation effects in the computation of the failure probability of river dikes. This was done for two different failure mechanisms: overtopping/overflow and internal erosion, and could be extended to more failure mechanisms. Three types of vegetation were considered: woody vegetation (e.g. trees and bushes), reed beds (tall, grass-like plants of wetlands) and scrubs (low woody plants), and herbaceous vegetation (low vegetation). In addition, different locations for these types of vegetation were evaluated. From these vegetation types and locations, a list of five potential vegetation effects on one or both failure mechanisms was composed: (1) increase in water level due to extra woody vegetation, reed beds and scrubs added on the floodplain or foreshore, (2) increase in erosion resistance due to herbaceous vegetation on the outer slope, (3) reduction in wave height due to large vegetation on the local foreshore, (4) increase in surface roughness due to herbaceous vegetation on the inner slope, and (5) decrease of the dike's strength due to woody vegetation toppling over on the hinterland. A primary assessment determined the main parameters of the limit state functions (regarding the failure mechanisms of overtopping/overflow and internal erosion) that could be influenced by these effects. The core idea of the probabilistic approach employed in this thesis is to estimate the variations in these parameters due to the presence of vegetation, and using the same limit state functions, to compute the failure probability of a dike given the presence of this vegetation.

A framework was established to combine all these vegetation effects simultaneously in the computation of the total failure probability, considering different magnitudes of each effect. This enabled the consideration of a wide range of vegetation scenarios. Bayesian Belief Networks (BBNs), which are acyclic graphical probabilistic models that provide a visual representation of dependencies between a set of continuous or discrete variables, were employed for this pur-

pose. This tool was selected due to its graphical visualization and its ability to store a great amount of information and, therefore, compute a large number of failure probability scenarios. This framework estimated the overall impact of certain vegetation scenarios, which allowed to conclude whether their effect was positive, negative, or negligible.

To evaluate the performance of the framework, three case studies located in the upper-river areas of the Netherlands (Culemborg, Grebbedijk, and Duursche Waarden) were used. Due to the lack of data, the different magnitudes of each vegetation effect were assumed and considered as similar for all case studies, therefore, they do not represent the actual conditions. With these assumptions, all three case studies showed similar trends and conclusions. In general, it was observed that from all the vegetation effects considered, an increase in water level of up to 0.1 m had the strongest and negative impact on both failure mechanisms leading to an approximate 30% increase in total failure probability. However, this increase in water level is overly-conservative; achieving a 0.1 m increase in water level requires a very high amount of extra vegetation added to the already existing vegetation present on the floodplains.

In case overtopping/overflow is the dominant failure mechanism present on a dike, i.e. the failure mechanism with the highest failure probability, this negative effect of an increase in water level could be compensated by an increase in erosion resistance due to the root strength of herbaceous vegetation located on the inner slope. This result shows the high potential of vegetation with strong roots, which is often overlooked. Further research on this type of vegetation is highly encouraged. In general, however, the failure mechanism of internal erosion was dominant in all case studies and, hence, the potential increase in water level could not be compensated.

The focus of this thesis was limited to Dutch river dikes but the main conclusions mentioned above could be extended to other situations. Given its versatility, the framework established in this study can be extended to include additional vegetation effects and more failure mechanisms, provided that their effects on the dike parameters are properly accounted for in the limit state functions. The accuracy of the predictions of this approach can be improved by in-depth studies of the effect of vegetation characteristics on the parameters of the limit-state functions. Overall, this thesis provides a useful and versatile tool for assessing the influence of vegetation on the failure probability of dikes that has a lot of potential and can be easily enhanced in the future.

Contents

List of Figures

List of Tables

1 Introduction

1.1. Motivation

The majority of the biggest cities around Europe, and also the world, are located near a sea, ocean, or river, which, implies a high risk of flooding. Despite this fact, the population and economic value of these cities are still continuously growing. Climate change is expected to worsen the situation due to sea-level rise, an increase in the frequency and intensity of storms, and more extreme droughts. Flooding is, therefore, an increasingly important issue in coastal areas but also in river areas. The Intergovernmental Panel on Climate Change (IPCC) predicts a rise in river floods risk in Europe, mainly due to this increase in population and economic growth along river areas (Kovats and Valentini, 2014), but also due to the increase in the frequency of extreme rainfalls. If no adaptive measures are taken, the population and economic damages could be significant. It is predicted that by 2080, the number of people in EU15 (European Union of 15 Countries) affected by floods could more than double, with 250,000 to 400,000 additional people affected when considering the climate change scenarios A2 and B2 respectively of the Special Report on Emissions and Scenarios (Nakicenovic, 2000). Central, Northern Europe, and the UK would be the most affected. In Northern Europe, on a local scale, an increase in extreme river discharge was already observed according to the fifth Annual Report on Impacts, Adaptation, and vulnerability (working group II) (Jiménez Cisneros and Oki, 2014).

Nevertheless, even with this high risk of flooding, a few countries have not been affected by floods for several years. A good example of this is the Netherlands, despite being a very low lying country with approximately 26% of the country's land below the sea level and 55% of it prone to flooding ("Correction wording flood risks for the Netherlands in IPCC report", 2017). The Dutch have equipped themselves with dikes for several centuries due to several disastrous flooding events that happened in the past, the most recent ones are those in 1916 and 1953. This made the country gather enough experience to create its current elaborate flood defence system consisting of 95 dike ring areas protected by dunes, dikes, dams, and/or hydraulic structures ("Waterveiligheidsportaal", 2020). Only 4% of the Dutch land surface is situated outside the dike rings areas ("Correction wording flood risks for the Netherlands in IPCC report", 2017). It is, therefore, interesting and relevant to study the experience of this country. However, the current defence system along river areas does not account for the potential effects of an increase

in river discharges due to climate change. To counteract this effect, higher and wider dikes are needed, which are costly and require a large amount of space, often not available. Furthermore, dikes are starting to be criticized due to their potential negative effects. For example, van Wesenbeeck et al., 2014 mention that dikes block the natural flow of water, leading to the settlement of polluting substances on the river bed. Moreover, designing high dikes has become not only financially unattractive but also ecologically untenable. Protecting natural areas and biodiversity is becoming increasingly important. The high environmental impact of dikes points to the need for a new, more nature-friendly flood defence system in the Netherlands.

An innovative solution, offering environmentally-friendly and flexible dikes are Nature-Based (NB) flood defences, which refer to dikes with some natural elements, usually, some types of vegetation that acquire a function in the flood defence (B. de Groot and Hordijk, 2015; de Vries and Dekker, 2009; Vuik et al., 2018). The vegetation, depending on its location and quantity, allows for an increase in the strength or a reduction in the load of the dike. This makes NB flood defences more natural and less intrusive to the landscape thanks to the several advantages that Nature can provide, such as:

- Creation of ecological and social services, which increase terrestrial and aquatic habitat and biodiversity.
- Better water and air quality (it can absorb CO_2 and generate oxygen), which has been an increasingly important issue along several Dutch rivers (S. de Groot, 2002).
- Stabilization of riverbanks and increase in water retention capacity.
- Increase in soil productivity and the fertility of the land (Leyer et al., 2012).
- Increase in recreational activities and social welfare (Zanetti et al., 2009).

To implement NB flood defences, a good understanding of all types of vegetation located on or near them, and their effects is required. Guidelines are needed to determine the optimal amount and location for a vegetation type to be placed in order to achieve a positive effect on the flood defence. Detailed information on the uncertainties brought by vegetation due to their unreliability is also necessary.

An example of a possible NB flood defence is to place salt marshes in front of sea dikes, which have proven to be very effective in reducing wave heights, and thus, reducing the overtopping load on sea dikes (Vuik et al., 2018). The same effect was found for willow trees in front (on the foreshore) of the river dike at Fort Steurgat (de Vries et al., 2015), which allowed the crest of the dike to be lowered by approximately 0.5 m because of the 60% reduction of the wave height achieved (de Vries and Dekker, 2009; Venema et al., 2014a, 2014b). Another example includes placing reed beds, scrubs, or herbaceous vegetation on the outer slope of the dike, which would increase the roughness and, therefore, decrease its overtopping load, although this effect has not been applied anywhere in practice yet (Klein Breteler et al., 2016). Furthermore, on the inner slope, the roots of herbaceous vegetation can increase cohesion and, thus, the strength of the dike, by improving erosion resistance, and slope instability (Fathi-Maghadam and Kouwen, 1997; Järvelä, 2002a). Grass revetment is currently being used for erosion resistance. However, other types of herbaceous vegetation with stronger roots could also be employed (Berendse et al., 2015; Stuip et al., 1999). It is, thus, beneficial to understand, study, and quantify the multiple effects of different types and locations of vegetation, to take them into account when designing and assessing dikes. This allows for a lower crest height due to either an increase in the dike's strength or a decrease in its load, with as consequence

saving in the amount of material required.

However, taking these positive effects into account when designing dikes is not yet common practice, because water authorities remain reluctant to keep any vegetation type on or near dikes. Most types of vegetation around and on dikes are removed because of fear for their potential negative effects. For example, if vegetation on the foreshore is added to reduce wave height it can also increase the water level (Zanetti et al., 2009). Moreover, some studies also suggest that roots of vegetation can increase seepage, especially dead roots, which counteracts the positive increased cohesion effect (Zanetti et al., 2009). Other potential negative effects are hindering maintenance and flood fighting, creating habitats for burrowing animals, and vegetation close to the dike's toe can create shadows on the grass revetment that can reduce its quality or debris of vegetation damaging revetments. Assessing and quantifying both negative and positive effects of vegetation on the failure probability of dikes is critical.

Water authorities also fear the uncertainty of vegetation. Nature itself is not easily predictable and has a high amount of uncertainty. This is due to expected reasons, such as seasonal variations, or unexpected ones like plant diseases or animals that feed on the plants, potentially damaging them. There is a lack of knowledge and guidelines on how to take vegetation and its uncertainties into account. This underlines the importance of further studying and quantifying vegetation effects on dikes.

Another reason why it is important to study the effects of vegetation is that current dikes are not completely vegetation-free. Public opinion is often against removing trees or other types of vegetation for cultural and aesthetic reasons. Their effects need to be understood to safely maintain this vegetation without jeopardizing safety

Until now, most studies focused on modeling and quantifying single effects of vegetation, for example, the amount of wave reduction that can be achieved with a certain amount of vegetation or how much root strength a certain type of vegetation has (De Baets et al., 2006; de Vries et al., 2015). Most of the research is still ongoing. However, there is also a need to take these already quantified vegetation effects into account in the computation of the failure probabilities of dikes. This would enable to combine multiple effects and achieve a better understanding of the overall impact of vegetation, such as the dominant effects and whether the overall impact is positive or negative. Finding a way to include the effects of different types, quantities, and locations of vegetation in the computation of the failure probability of a dike allows to eventually include them in the official guidelines of assessing and designing dikes and optimizing the placement of certain vegetation types to achieve the optimal benefit they can offer.

The aim of this study is, therefore, to explore a new way of considering multiple vegetation effects into the computation of failure probabilities of Dutch river dikes and, eventually, in the Dutch assessment methods. This was done by establishing an innovative framework that allows to combine both the different effects of vegetation and different vegetation scenarios when computing the failure probability. Through this new approach, a first approximation can be made of the optimal amount of vegetation that can be planted or kept on dikes and its ideal location. It also enables the inclusion of uncertainty by calculating the failure probability if, for example, only a portion of the vegetation is left.

1.2. Research objectives

This study focuses on the development of a framework enabling to compute the failure probability of a Dutch river dike, including the presence of different types of vegetation grown on or near this dike, considering two failure mechanisms: overtopping/overflow and internal erosion. The framework is exploratory in nature and offers model-based statistical insight in the order of magnitude of the effects of vegetation on the total failure probability. It uses Bayesian Belief Networks (BBN) to create the framework for the following reasons:

- BBNs are graphical tools that are useful to visualize the problem.
- They facilitate computation by storing a lot of information in conditional probability tables, which allows for multiple different quantities of vegetation to be considered in a short amount of time.
- They are very flexible and easily allow for the addition and removal of vegetation effects, failure mechanisms, or inter-dependencies. This enables the eventual consideration of a whole spectrum of vegetation effects when assessing and designing dikes.

In this report, the term vegetation includes woody vegetation (e.g. trees and bushes), reed beds (tall, grass-like plants of wetlands) and scrubs (which are low woody plants), and herbaceous vegetation (low vegetation) because these types have been studied in detail and, therefore, have enough data available in the literature to allow their effects to be approximately quantified (de Vries et al., 2015; Klein Breteler et al., 2016; Lanzafame and Sitar, 2018). The vegetation effects considered are the following: increase in water level (negative effect), change in erosion resistance of the inner slope (negative or positive effect), wave height reduction (positive effect), increase in roughness of the outer slope (positive effect), and a potential tree toppling over on the hinterland (negative effect).

To evaluate the framework, three case studies located in the upper river areas of the Netherlands were used. The actual amount of vegetation on these case studies and their translation, based on their characteristics (height, density, etc.), into quantified effects are not the focus of this study. Instead, all case studies were assigned the same range of quantities of vegetation effects based on realistic and achievable values obtained from the literature (de Vries et al., 2015). Therefore, the framework does not provide any accurate physical meaning to the quantity of vegetation effects employed and, hence, the results obtained from these case studies should be considered as indicative. This means that the amount of vegetation required to obtain, for example, a 50% wave height reduction is unknown and not the focus of this research. As such, this study aims at answering the following general research question:

How can multiple, already quantified, effects of vegetation be combined when computing the failure probability of a Dutch river dike considering overtopping/overflow and internal erosion?

Additionally, the following sub-questions are formulated:

- Which parameters in the limit state functions of overtopping/overflow and internal erosion are affected by the vegetation effects under study? How can they be modified to include these effects?
- How can the failure probability of a Dutch river dike cross-section be computed using a Bayesian Belief Network (BBN) considering the aforementioned two failure mechanisms? How can the effects of vegetation be implemented into this BBN?

1.3. Thesis outline

Chapter 2 discusses the structure of the official Dutch guidelines for assessing river dikes and explains the two failure mechanisms considered in this study: overtopping/overflow and internal erosion, describing their physical processes and mathematical translations into limit state functions. This chapter also explains the role of vegetation in the current safety assessment. Chapter 3 discusses the five vegetation effects that are studied, defining the way they affect each failure mode and providing a brief explanation of the vegetation characteristics that create such effect. Details on how vegetation effects were modeled are provided. Chapter 4 provides a brief introduction of Bayesian Belief Networks, and of Pomegranate, the Python package used to model the framework, followed by a detailed presentation of the framework itself, an explanation of how the results are presented, and the assumptions of this research. Chapter 5 provides an overview of the three case studies used to apply and evaluate the framework. Chapter 6 discusses the main computational results obtained with the framework. Conclusions and recommendations are presented in Chapter 7.

2

Current Dutch safety assessment

2.1. General procedure

The elaborate flood defence system of the Netherlands currently consists of 95 dike ring areas, which are composed of dunes, hydraulic structures, dams, or primary dikes ("Waterveiligheidsportaal", 2020). The latter are divided into dike segments depending on the land behind them (see Figure 2.1) and are the focus of this research (Kok et al., 2016). Figure 2.2 shows the terminology for dikes employed throughout this study. Each of these dike segments is subject to a Dutch law called the Water Act ("*Water wet*" in Dutch), in which safety standards are defined together with the responsible bodies that maintain the system. This law aims to guarantee the country's safety against flooding at all times and, therefore, it is regularly updated. The latest update took place after the consecutive extremely high water levels of 1995 and 1996, which led to the new 2017 safety standards (Jongenjan, 2017).

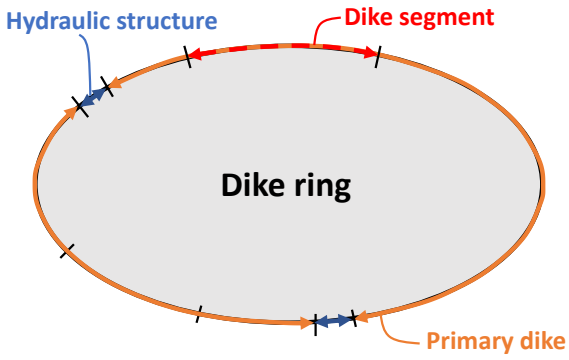

Figure 2.1: Example of a dike ring in the Netherlands consisting of two hydraulic structures and two primary dikes. The latter are both divided into three dike segments.

In total, there are 234 primary dike segments in the Netherlands, see Figure 2.3 for an overview, each managed and maintained by either a water authority (organization responsible for dike maintenance) or by the Rijkswaterstaat (Directorate-General for Public Works and Water Management of the Netherlands). These segments are, according to the Water Act, subject to safety standards, which are currently expressed in terms of failure probability based on a reference

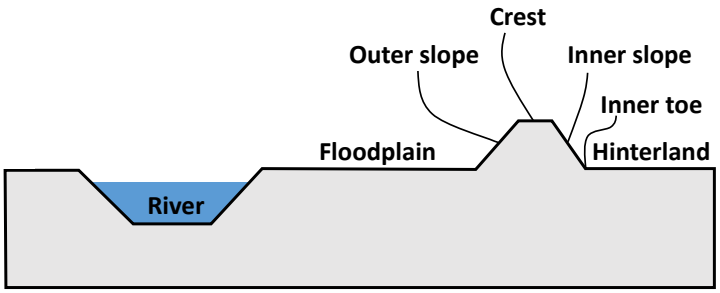

Figure 2.2: Terminology for dikes employed throughout this study and locations of vegetation taken into account in the current safety assessment of Dutch dikes.

period of one year. Therefore, the safety standards express the number of times per year a dike *is allowed to fail*. The required failure probability is based on the individual, societal, and economical risks of the land protected by the dike. More information on how to calculate these risks can be found in "The national flood risk analysis for the Netherlands", referred to as VNK ("*De veiligheid van Nederland in kaart*" in Dutch) (Vergouwe, 2016). Each dike segment has its own required failure probability, which can range from 1/300 to 1/1,000,000. The higher the risk, the lower the required failure probability. The safety standards also consist of a maximum required failure probability, which is approximately three times the required one and is used for assessing dikes.

Figure 2.3: Location of the primary dike segments according to the new safety standards of 2017. Obtained from the website *Waterveiligheidsportaal* ("Waterveiligheidsportaal", 2020).

To make sure the dike segments fulfill their safety standards at all times, they have to be assessed by their respective water authority or Rijkswaterstaat every 12 years (Kok et al., 2016;

Vergouwe, 2016). A full description on how to perform a safety assessment can be found in the statutory assessment instrument ("*Wettelijk Beoordelingsintrumentarium*" in Dutch), referred to as the WBI2017 (*WBI2017 Handboek voor de toezichthouder*, 2017), and the flood risk assessment tool ("*Wettelijk Toetsinstrumentarium*" in Dutch), referred to as WTI2017 (Chbab, 2015). There are several assessment methods, ranging from the most simple ("*Eenvoudige toets*" in Dutch) to more complicated ones ("*Toets op maat*" in Dutch) which compute the current failure probabilities of dike segments using a semi-probabilistic or full probabilistic approach. The latter usually employ official software, such as *PC-ring* (Vrouwenvelder, 1999) or the most recent one, *Riskeer* (*Riskeer*, 2019). In this study, the focus was placed on adding the effects of different types of vegetation, depending on their location, to the more complicated assessment methods which compute the current failure probability of a dike segment. All computations were performed using Python rather than the existing software to be able to add these effects (Van Rossum and Drake Jr, 1995).

To calculate the actual failure probability of a dike segment, the limit state of the dike is evaluated, which is "the transition between the desired situation, whereby the flood defences function properly, and a situation in which this is no longer the case", according to Kok et al., 2016. A dike can stop functioning, thus fail, in multiple manners, which are called failure mechanisms. An overview of the most common failure mechanisms according to "Technical Advisory Committee on Flood Defences" is included in Figure 2.4 (Schiereck and Van der Kleij, 1998). The actual failure probability of a dike segment is the probability that at least one of the failure mechanisms occurs. Therefore, the failure probability of each failure mechanism needs to be computed and then combined to obtain the total current failure probability. In general, the combination of all failure mechanisms provides a probability that is lower than their sum, because of the interdependencies between some failure mechanisms. A fault tree illustrating how a dike is assessed considering all failure mechanisms can be found in Figure 2.5 (Kok et al., 2016).

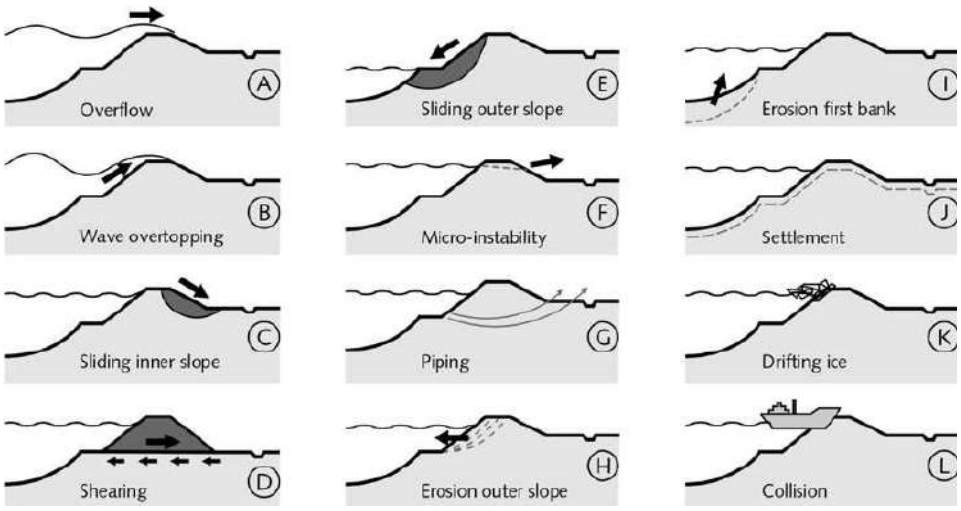

Figure 2.4: Overview of the most common failure mechanisms according to TAW (Schiereck and Van der Kleij, 1998).

To assess the failure probability for a certain failure mechanism, the dike first needs to be divided into sections (see Figure 2.5), which is done depending on the failure mechanism under study. The failure probabilities of each section are computed and then combined using a pa-

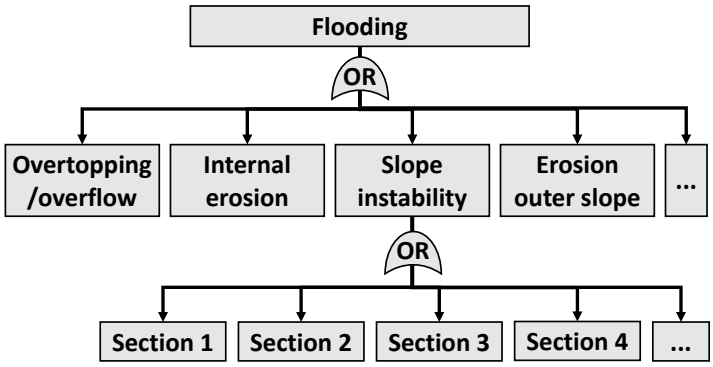

Figure 2.5: Fault tree of a dike segment.

rameter called the length effect, which states that the longer the dike, the higher the failure probability (Jongejan, 2016). A summary of the assessment process is presented in Figure 2.6: the dike segment needs to be assessed per failure mechanism (denoted in orange color in Figure 2.6). In order to do that, it has to be divided into sections and the respective failure probabilities of each section need to be computed, and then combined (denoted in blue color in Figure 2.6). Once the combined failure probabilities of all sections are computed (per failure mechanism), those can then be combined to determine the total actual failure probability of the dike segment (denoted in green color in Figure 2.6).

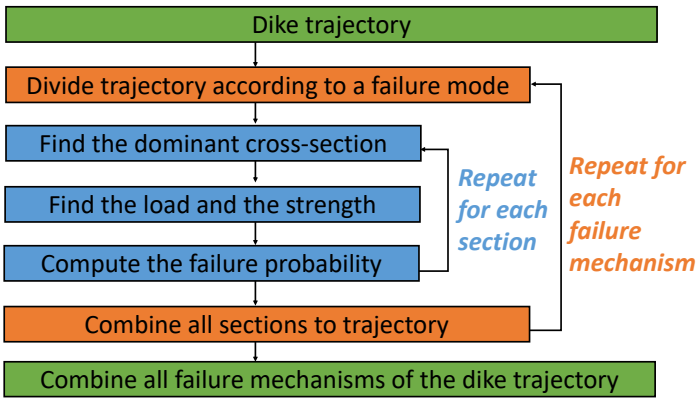

Figure 2.6: Schematization of the assessment method for computing the failure probability of a dike segment considering multiple failure mechanism.

This thesis focuses on the blue elements of Figure 2.6, i.e. the cross-sectional level. The failure probability of a dike's cross-section when considering a single failure mechanism depends on the combination of its strength and load. The strength of a dike depends on the failure mechanism under study and typically consists of either its height, its friction angle, or geotechnical parameters which can be calculated using models, which can range from very simplified to very sophisticated. The loads on a dike also depend on the failure mechanism under study, it can be the pressure caused by the difference between the water level on the riverside and the phreatic level on the land side, the force acting on the dike due to waves, or the flow of water along, through, or under the dike (Kok et al., 2016). Both the strength and the load of a dike have some uncertainties. Two types of uncertainties exist: inherent and epistemic. The former, also known as aleatory uncertainty, is due to the purely random nature of an event, such as the

natural variability of the seawater levels, and, therefore, cannot be reduced by further analysis or data collection. Epistemic uncertainty, on the other hand, is caused by a lack of knowledge and, thus, can be reduced by further analysis and data collection. The strength and load of dikes are uncertain, the former mainly due to epistemic uncertainty and, the latter due to inherent uncertainties. To take both uncertainties into account strength and load parameters, such as the hydraulic conductivity, the water level or wind speed are represented with a distribution (Kok et al., 2016).

Within a failure mechanism, there are many ways a dike can fail due to the uncertainties causing different possible combinations of load and strength values. These combinations are taken into account with a limit state function (often referred to as a Z-function), which allows the dike's failure prediction, for every possible combination of load and strength properties. Z-functions normally express the difference between the strength and load of a dike and differ per failure mechanism. The transition from a working dike to failure occurs when the limit state function becomes negative, i.e. the load becomes greater than the strength (Kok et al., 2016). Failure is thus defined as the moment the limit state function becomes negative, which does not necessarily mean flooding occurs due to the extra strength a dike can have ("*Reststerkte*" in Dutch). Using reliability methods (see Appendix A), such as Monte Carlo simulations, and a limit state function, the failure probability according to a certain failure mechanism and cross-section can be computed.

This failure probability needs to be compared to the required failure probability for a failure mechanism considering a cross-section, to check if the dike satisfies its safety standard. Usually, the maximum required failure probability is used in assessment, also referred to as the lower limit. To do this, the required maximum failure probability needs to be reduced to a failure probability for a failure mechanism and a cross-section. This is done in two steps:

- First, the lower limit is reduced to a value specific to the failure mechanism of interest. Because not all failure mechanisms contribute to the same degree to the total failure probability of the system (they do not all have the same probability of occurence), the lower limit is multiplied by a contribution factor ("*Faalkansruimtefactor*" in Dutch). This contribution factor increases for an increasing contribution of a failure mechanism to the total failure probability. For example, a value of 0.24 is recommended by the WBI2017 for the failure modes overtopping/overflow and internal erosion, whereas, grass erosion on the outer slope has a contribution factor of only 0.05.
- The second step is to reduce it to a specific cross-section. To achieve this, a process known as the length effect needs to be taken into account, which is based on the fact that the probability that a dike will fail at a certain location is smaller than the probability that it will fail anywhere in the system. The longer the dike trajectory, the more variation and the greater this effect will be. A simple example to illustrate this concept is that if somebody is inspecting a dike during a storm, each section may have the same probability of failure, but the more sections that person inspects, the higher the probability that a problem will be found (Jongejan, 2016). The magnitude of this phenomenon differs per failure mechanism because the homogeneity of their load and strength differ. For example, the load of the failure mechanism overtopping is the wave height which only varies slightly over the trajectory, and the strength is mainly the height of the dike which also differs marginally. Therefore, the difference between the failure probability of one section and the total failure probability does not change much for this failure mecha-

nism and, hence, the length effect is small. For internal erosion, on the other hand, the strength of the dike is based on the composition of the subsoil, which can change every 100 meters (Vergouwe, 2016). Thus, the exact location where internal erosion can occur is difficult to predict and the failure probability of a section and of the whole dike trajectory can differ significantly and, therefore, the length effect is high. For overtopping and overflow, the WBI2017 suggests to take a length effect factor N between 1 and 3, for internal erosion, it can be computed with Equation (2.1).

$$N = 1 + \frac{a\,L}{b}, \tag{2.1}$$

where:

- N [-]: length effect factor.
- L [m]: length of the dike trajectory.
- a [-]: fraction of the dike trajectory that is sensitive to the failure mechanism under study. In this case, a value of 0.9 is considered for internal erosion.
- b [m]: order of magnitude of the impact of the length effect of the considered failure mechanism. It takes a value of 300 m for internal erosion.

The required failure probability for a cross-section and a failure mechanism is thus computed following the two steps mentioned above, which are summarized in Equation (2.2). Once found, this required failure probability needs to be compared to the actual failure probability computed previously, if the required one is larger, the dike trajectory is safe.

$$P_{req,\,cs} = \frac{P_{ll}\,\omega}{N}, \tag{2.2}$$

where:

- $P_{req,\,cs}$: required failure probability for a specific failure mechanism of a dike cross section.
- P_{ll}: required lower limit failure probability.
- ω: contribution factor specific to each failure mechanism.
- N: length effect factor.

2.2. Failure mechanisms under study

2.2.1. Overtopping and overflow

The failure mechanisms of overtopping and overflow are referred to in the WBI as "*Grasbekleding erosie kruin en binnentalud" (GEKB)*, which translates as the erosion of the grass revetment on the crest and inner slope (*Schematiseringshandleiding grasbekleding*, 2019). This combined mechanism is one of the four related to grass revetment and it is the most common failure mechanism for Dutch coastal dikes due to their high wave heights. It is less common in river dikes due to their limited fetch, which leads to small waves and high design water levels, i.e. there is a very low probability that the water level would be close to the crest.

This failure mechanism occurs due to water flowing over the crest of the dike. The main danger is not the water pouring in the land side of the dike itself, since the amount of water is typically negligible. Instead, failure occurs before, when the water starts flowing over the inner slope of

the dike. The risk lies in the maximum water velocity exceeding the root strength of the grass revetment, creating erosion (see Figure 2.7). According to the WBI, failure is defined as the moment when a portion of at least 0.2 m of the top layer is eroded. The under-layer is then considered no longer protected and will eventually slide away and generate failure (Rijkswaterstaat, 2017a).

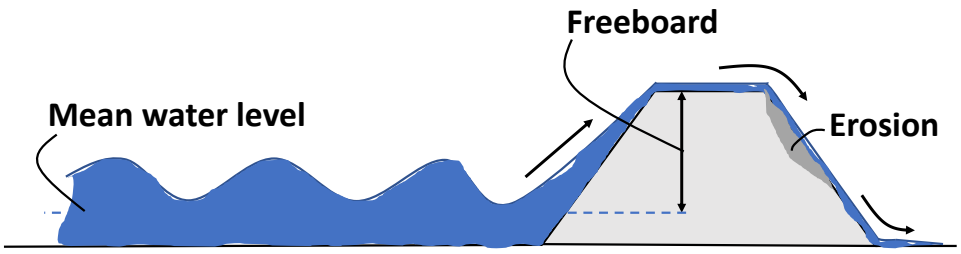

Figure 2.7: Illustration of the concept of overtopping failure mechanism.

The failure mechanism of overtopping/overflow is composed of two mechanisms, as its name suggests: overtopping and overflow. Their occurrence depends on a parameter called freeboard, which is the difference between the crest height and the water level, see Equation 2.3. The mechanism of overtopping occurs when the freeboard is positive, i.e. when the water level is below the crest height, and waves are high enough to topple over the dike, water then flows over the crest of the dike in a non-continuous manner. Overflow, on the other hand, occurs during a negative freeboard, i.e. the water levels are higher than the crest level, and there is a continuous flow of water over the dike. When the freeboard is close to zero, water levels are close to the crest height, and there is a transition period in which both mechanisms occur.

$$R_c = h_c - h_w, \tag{2.3}$$

where:

- R_c [m]: freeboard of the dike.
- h_c [m]: crest height of the dike.
- h_w [m]: river water level.

The strength of the dike in this failure mechanism mostly depends on its height, the outer slope's angle and roughness, and the strength of the grass on the inner slope of the dike. Thus, here the effect of herbaceous vegetation on the inner slope is currently taken into account in the design and assessment of dikes: increased cohesion due to the strength of its roots. The load considered in this failure mechanism is the water flowing along the dike, thus, the water discharge going over the crest of the dike. This load depends on the water levels at the toe of the dike, which are computed by *WAQUA* (*Users Guide WAQUA: General Information*, 2016),

a hydraulic model that considers the geometry of the river channel and its roughness caused by the vegetation currently present. Therefore, for the load, the effect of all the vegetation now present on and around the rivers on the water level is already taken into account.

The limit state function is defined as the strength, the critical discharge, which is the amount of water allowed to flow over the inner slope without creating erosion, minus the load, the actual overtopping/overflowing discharge, see Equation 2.4.

$$Z_{OT/OF} = q_c - q_{storm}, \tag{2.4}$$

where:

- $Z_{OT/OF}$ [l/(s m)]: limit state function of overtopping/overflow.
- q_c [l/(s m)]: critical discharge.
- q_{storm} [l/(s m)]: actual discharge going over the dike during a storm.

The actual discharge depends on the sign of the freeboard. If the freeboard is positive there is only overtopping, if close to zero (between $R_c = 0$ and $R_c/H_{m0} > -0.3$ according to the EuroTop manual (van der Meer et al., 2018)) both overtopping and overflow occur, and if negative enough ($R_c/H_{m0} < -0.3$) there is only overflow (van der Meer et al., 2018).

$$q_{storm} = \begin{cases} q_{overtopping}, & \text{if } R_c \geq 0, \\ q_{overtopping} + q_{overflow}, & \text{if } \frac{R_c}{H_{m0}} \geq -0.3, \\ q_{overflow}, & \text{if } \frac{R_c}{H_{m0}} < -0.3. \end{cases} \tag{2.5}$$

where:

- $q_{overtopping}$ [l/(s m)]: overtopping discharge.
- $q_{overflow}$ [l/(s m)]: overflowing discharge.

The overtopping and overflow discharges are calculated based on the empirical formulae found in the EuroTop manual for assessing and designing dikes (van der Meer et al., 2018). These formulae were fitted using experimental model data from studies around the world, which were conducted to formulate and validate the equation and were performed with specific dike geometries and wave conditions. The equation was refined several times over the years and is still based on the original work of Owen (1980), who proposed that the overtopping discharge decreases exponentially as the freeboard increases (van der Meer et al., 2018). The most recent formula has, in addition to this equation, a few more factors, such as the angle of the outer slope, the type of wave breaking, and four factors to account for the roughness, the presence of a berm, of a vertical wall, and the obliquity of the wave attack. Finally, in the new formula, an exponent was added to better model the overtopping discharge when the freeboard is close to zero. These changes lead to the currently used formula shown in Equation 2.6 with a maximum presented in Equation 2.7. The equation for the overflow discharge is more simple and only depends on the freeboard, see Equation 2.9.

$$\frac{q}{\sqrt{g\,H_{m0}^3}} = \frac{0.026}{\sqrt{\tan\alpha}}\,\xi_{m-1,0}\,\exp\left[-\left(2.5\frac{R_c}{\gamma_b\,\gamma_f\,\gamma_\beta\,\gamma_v\,\xi_{m-1,0}\,H_{m0}}\right)^{1.3}\right] \quad \text{for } R_c > 0, \tag{2.6}$$

$$\frac{q_{max}}{\sqrt{g\,H_{m0}^3}} = 0.1035\,\exp\left[-\left(1.35\frac{R_c}{\gamma_f\,\gamma_\beta\,\gamma_v\,H_{m0}}\right)^{1.3}\right] \quad \text{for } R_c > 0, \tag{2.7}$$

$$q_{overtopping} = min(q,\, q_{max}) \tag{2.8}$$

$$q_{overflow} = 0.54\sqrt{g|R_c^3|} \quad \text{for } R_c < 0, \tag{2.9}$$

where:

- q [l/(s m)]: water discharge.
- q_{max} [l/(s m)]: maximum overtopping discharge.
- H_{m0} [m]: significant wave height.
- α [deg]: slope angle of outer slope.
- $\xi_{m-1,0}$ [s/$\sqrt{m}$]: breaker parameter.
- g [m/s^2]: gravitational constant, here taken as 9.81 m/s^2.
- γ_f [-]: influence factor for the permeability and roughness of the outer slope.
- γ_v [-]: influence factor for a vertical wall on top of the crest.
- γ_b [-]: influence factor for a berm
- γ_β [-]: influence factor for oblique wave attack (γ_β = 1 - 0.0033|O|, with O the wave angle in degrees).

For river dikes, the dominant waves in case of a storm are wind waves. Their parameters (wave height and wave period) can be computed with the equations of Young and Verhagen (1996) (see Appendix B). They depend on the water level, bottom level, fetch, and wind speed. The breaker parameter (see equation in Appendix B) depends on these wave parameters and defines the way waves break on the slope of the dike.

A summary of the parameters relevant for this failure mechanism is shown graphically in Figure 2.8 and in more detail in Table 2.1. In this study, the stochastic variables in the limit state function are the water level, the critical discharge, the wind speed, and the bottom level. The water level and the wind speed have a distribution because they are load parameters with inherent uncertainties. The critical discharge and bottom level are strength parameters that were given a distribution due to epistemic uncertainty. The respective parameters of the stochastic variables are case dependent, except for the parameters of the critical discharge, which are based on the strength of grass and the wave height.

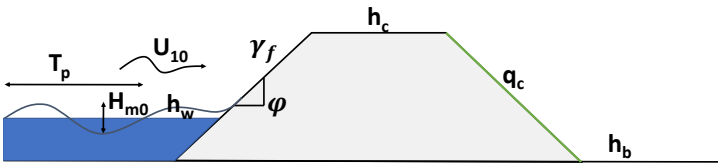

Figure 2.8: Graphical representation of the parameters for the failure mechanism overtopping/overflow.

Table 2.1: Parameters needed for the computation of the overtopping/overflow failure probability.

Variable	Symbol	Type	Distribution
Bottom level [m]	h_b	Strength	Normal
Crest height [m]	h_c	Strength	Deterministic
Critical discharge [l/(s m)]	q_c	Strength	Log-normal
Fetch [m]	F	Load	Determinsitic
Roughness factor [-]	γ_f	Strength	Deterministic
Slope angle [-]	α	Strength	Deterministic
Water level [m]	h_w	Load	Gumbel or empirical
Wind speed [m/s]	U_{10}	Load	Weibull

The critical discharge represents the amount of water that can flow over the dike without exceeding its strength, which originates from the roots of the grass (Smale, 2019). According to the WBI, the parameters of these stochastic variables depend on the quality of the grass and the wave height (see Table 2.2) (*Schematiseringshandleiding grasbekleding*, 2019; *WBI2017 Handboek voor de toezichthouder*, 2017). The stochastic nature of the critical discharge is meant to take into account the varying impact of a discharge flowing on the grass revetment. If the volume of water is composed of multiple small waves, the grass will not erode much. However, if the volume originates from one large wave, then the grass cover might not survive (Trung, 2014).

Table 2.2: Parameters (in l/(s m)) of the critical discharge depending on the wave height and the quality of the grass (*Schematiseringshandleiding grasbekleding*, 2019).

Wave height	Closed divot	Open divot
0 - 1 m	$\mu = 225, \sigma = 250$	$\mu = 100, \sigma = 120$
1 - 2 m	$\mu = 100, \sigma = 120$	$\mu = 70, \sigma = 80$
2 - 3 m	$\mu = 70, \sigma = 80$	$\mu = 40, \sigma = 50$

2.2.2. Internal erosion

Internal erosion is referred to in the WBI as *"Opbarsten, heave en piping (STPH)"* and is one of the geotechnical failure mechanisms and a common failure mechanism for Dutch river dikes.

Internal erosion occurs due to pressure differences across the dike, i.e. high water on one side and low water at the other (Rijkswaterstaat, 2017b). River dikes are more vulnerable to this failure mechanism because they typically have longer-lasting floods, which makes it easier for pressure to accumulate on one side of the dike. One condition for this pressure to accumulate is the presence of an impermeable layer, clay or silt (called aquitard or blanket layer), acting as a barrier for groundwater and resting on top of a very porous, permeable layer of sub-soil, typically sand (called aquifer). Therefore, internal erosion does not occur on sand dikes built on a sandy subsoil, as then no pressure can build up (Rijkswaterstaat, 2017b).

Within this failure mechanism, at least three events must occur for failure to happen (see Figure 2.9): First, the blanket layer, must be "lifted" in a process called "uplift", creating a crack from which water starts to flow out. This happens at the thinnest spot of the blanket layer in combination with high pore pressure. Its location is referred to as the exit point and is usually close to the landwards toe of the dike. Then, sand particles must start flowing out with the water, creating sand boils in a process called "heave". Finally, an erosion channel is created in the aquitard that moves towards the riverside until it makes its way through the whole length of the dike. This is the actual piping process and the dike can be washed away. This failure mechanism is considered a fully dependent, mutually-exclusive, parallel system in the WBI: all three must occur to have failure (see Figure 2.10). Therefore, the failure probability is equal to that of the sub-mechanism with the lowest failure probability. Currently, only the effect of vegetation already present on and around the rivers on the water level is taken into account in this failure mechanism.

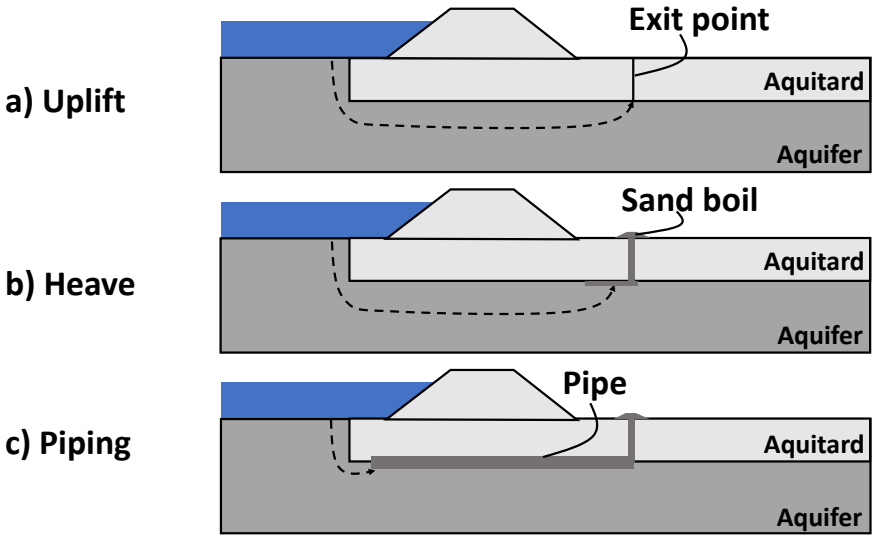

Figure 2.9: Illustration of the three steps required for internal erosion to occur. The color blue represents water, gray is for the dike core and the blanket layer (impermeable layer), and dark gray is a permeable layer.

Numerous laboratory tests were performed in Germany and the Netherlands to better understand this complex failure mechanism (Rijkswaterstaat, 2017b; Schweckendiek et al., 2014). These tests were mainly based on visual observations where the hydraulic head difference was gradually increased until sand boils appeared, and increased further until the seepage flow reached a critical value and the sandy aquifer failed. Based on these tests, Sellmeijer proposed a conceptual model, which was further improved to the current limit state functions (Sellmeijer et al., 2011), one for each sub-mechanisms: uplift, heave, and piping. Each limit state func-

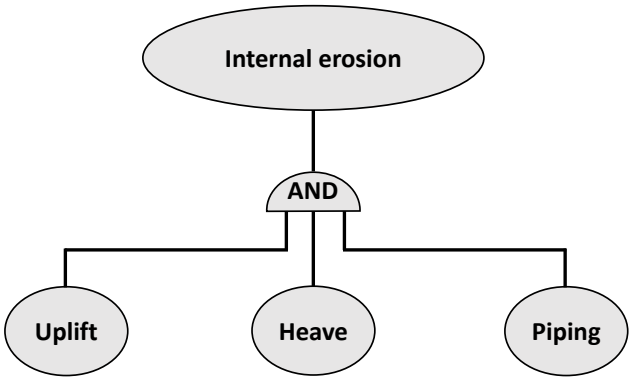

Figure 2.10: Fault tree of the failure mechanism internal erosion.

tion is presented and explained in more detail below. The parameters of these three limit state functions are graphically represented in Figure 2.11 and presented in more detail in Table 2.3. The stochastic variables of the limit state functions are the load (h_w) due to inherent uncertainty, the geotechnical parameters (γ_{sat}, k, D, d, k_h, L_f and d_{70}), the phreatic level (h_p), and the model parameters (m_u, m_p and i_c) due to epistemic uncertainty. The parameters of these stochastic variables are case dependent, except for the model parameters for which their parameters are provided by the WBI2017. The distributions of all stochastic variables are based on Schweckendiek et al., 2014 and VNK reports Vergouwe, 2016.

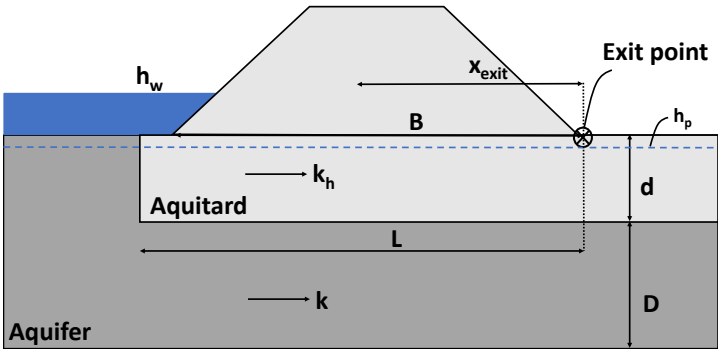

Figure 2.11: Graphical representation of the parameters for the failure mechanism internal erosion.

Table 2.3: Parameters needed for the computation of the internal erosion failure probability.

Variable	Symbol	Type	Distribution
70%-fractile of grain size distribution [m]	d_{70}	Strength	Log-normal
Aquifer thickness [m]	D	Load	Log-normal
Aquitard thickness [m]	d	Strength	Log-normal
Bedding angle [rad]	θ	Strength	Deterministic
Critical heave gradient [-]	i_c	Strength	Log-normal
Drag coefficient [-]	η	Strength	Deterministic
Hydraulic conductivity aquifer [m/s]	k	Load	Log-normal
Hydraulic conductivity aquitard [m/s]	k_h	Strength	Log-normal
Kinematic viscosity of water [m^2/s]	ν	Strength	Deterministic
Length of the effective foreshore [m]	L_f	Strength	Log-normal
Model factor piping [-]	m_p	Strength	Log-normal
Model factor uplift [-]	m_u	Strength	Log-normal
Phreatic level [m]	h_p	Strength	Normal
Reference value of d70 [m]	d_{70m}	Strength	Deterministic
Saturated volumetric weight of sand [kN/m^3]	γ_{sat}	Strength	Normal
Saturated volumetric weight of water [kN/mş]	γ_w	Strength	Deterministic
Volumetric weight of sand grains [kN/m^3]	γ_s	Strength	Deterministic
Water level [m]	h_w	Load	Gumbel or empirical
Width of the dike [m]	B	Strength	Deterministic

Limit state function of uplift

The uplift sub-mechanism occurs when the hydraulic head in the aquifer exceeds the weight of the aquitard at a certain location, which creates a breach. The limit state function for this sub-failure mechanism is based on the vertical equilibrium of the forces acting on the aquitard (see Equation 2.10). It is the difference between the critical head difference, multiplied with a model factor, and the actual head difference.

$$Z_u = m_u \times \Delta\phi_{c,u} - \Delta\phi, \tag{2.10}$$

where:

- Z_u [m]: limit state function for uplift.
- m_u [-]: uplift model factor addressing the uncertainty in the critical head difference [-].
- $\Delta\phi_{c,u}$ [m]: critical local head difference.
- $\Delta\phi$ [m]: actual local head difference [m].

The critical head difference, which is the strength of this sub-mechanism, is based on the local weight of the blanket layer at the breach and can be found with Equation (2.11).

$$\Delta\phi_{c,u} = d\frac{\gamma_{sat} - \gamma_w}{\gamma_w}, \tag{2.11}$$

where:

- d [m]: local thickness of the blanket layer.
- γ_{sat} [kN/m^3]: saturated volumetric weight of the blanket.
- γ_w [kN/m^3]: saturated volumetric weight of water.

The actual head difference is the load of the sub-mechanism, it is the difference between the piezometric head at the exit point and the water level at the riverside, see Equation (2.12).

$$\Delta\phi = \phi_{exit} - h_w, \tag{2.12}$$

where:

- ϕ_{exit} [m]: piezometric head at the exit point.
- h_w [m]: river water level.

The piezometric head (Equation (2.13)) depends on the exit point: the further it is from the toe of the dike, the more the pressure dissipates and, thus, the lower its value. This effect is taken into account with the damping factor (λ), see Equation (2.14).

$$\phi_{exit} = h_p + \lambda(h_w - h_p), \tag{2.13}$$

where:

- h_p [m]: hinterland phreatic level.
- λ [-]: damping factor.

The damping factor is lower the further away it is from the toe of the dike. It depends on the length, hydraulic conductivity, and the average thickness of the aquifer, as well as the width of the dike and the location of the breach, plus, if relevant, on the length of the foreshore.

$$\lambda = \frac{\lambda_h}{L_f + B + \lambda_h} \exp\left(\frac{\frac{B}{2} - x_{exit}}{\lambda_h}\right) \tag{2.14}$$

$$\lambda_h = \sqrt{\frac{kDd}{k_h}}, \tag{2.15}$$

where:

- x_{exit} [m]: distance of the exit point from the center of the levee footprint.
- B [m]: width of the levee.
- L_f [m]: length of the effective foreshore.
- k [m/s]: hydraulic conductivity of the aquifer.
- D [m]: aquifer thickness.
- λ_h [-]: leakage factor.
- k_h [m/s]: hydraulic conductivity of the aquitard.

Limit state function of heave

The second sub-mechanism depends on the vertical groundwater velocity in the breached aquitard. If it exceeds a critical value (the critical heave gradient), grains of sand are washed through the breach, and heave failure happens. Therefore, the limit state function is the difference between the critical heave gradient and the actual exit gradient (see Equation (2.16)).

$$Z_h = i_c - i, \tag{2.16}$$

where:

- Z_h [-]: limit state function of heave.
- i: exit gradient [-].
- i_c: critical heave gradient [-].

The exit gradient (Equation (2.17)) is the load of this sub-mechanism and is based on the piezometric head (presented above, see Equation (2.13)), the phreatic level, and the blanket thickness. The thicker the blanket, the lower the exit gradient, and the fewer chances of heave occurring. The critical heave gradient is the strength of this sub-mechanism and is a stochastic variable following a log-normal distribution. Its parameters are suggested by the WBI2017.

$$i = \frac{\phi_{exit} - h_p}{d}. \tag{2.17}$$

Limit state function of piping

Finally, the last sub-mechanism occurs when water flows under the dike, creating a pipe that washes away the sand in the aquifer under the dike and, eventually, the dike itself. This process starts at the breaching point and occurs when the critical head difference, averaged over the length of the dike, is breached. The limit state function is the difference between this critical head difference (multiplied by a factor) and the actual head difference (see Equation (2.18)).

$$Z_p = m_p H_{c,p} - (h_w - h_p - 0.3d), \tag{2.18}$$

where:

- Z_p [-]: limit state function of piping.
- m_p [-]: model uncertainty factor.
- $H_{c,p}$ [m]: critical head difference.

The critical head difference (Equation (2.19)) is the strength of the sub-mechanism and is based on the seepage length, the average thickness of the blanket layer, and the size of the sand grains. The actual head difference is the load of the sub-mechanism and is the water level, minus the phreatic level, minus 0.3 times the average blanket thickness.

$$H_{c,p} = F_1 F_2 F_3 L, \tag{2.19}$$

$$F_1 = \eta \left(\frac{\gamma_s}{\gamma_w} - 1 \right) \tan\theta, \tag{2.20}$$

$$F_2 = \frac{d_{70m}}{\sqrt[3]{\frac{\nu k L}{g}}} \left(\frac{d_{70}}{d_{70m}} \right)^{0.4}, \tag{2.21}$$

$$F_3 = 0.91 \left(\frac{D}{L} \right)^{\frac{0.28}{\left(\frac{D}{L}\right)^{2.8}} + 0.04}, \tag{2.22}$$

where:

- L: seepage length [m].
- γ_s: Volumetric weight of sand grains [kN/m^3].
- θ: bedding angle [deg].
- η: drag coefficient [-].
- ν: kinematic viscosity of water [m^2/s].
- d_{70}: 70%-fractile of the grain size distribution [m].
- d_{70m}: reference value of d70 [m].
- g: gravitational constant [m/s^2].

2.3. Role of vegetation in the current safety assessment

In the guidelines of the WBI2017, the only vegetation type considered in the computation of the failure probability is grass on the inner and/or outer slope, which is used as a revetment. This type of vegetation on the slope of dikes has been intensively studied and quantified for its positive effect of erosion resistance by increasing cohesion and, thus, the dike strength (Stuip et al., 1999; van Hasselt and van Everdingen, 1998). Therefore, only this type of herbaceous vegetation on slopes is considered when computing the failure probability of, for example, erosion of the outer slope and overtopping/overflow (*Schematiseringshandleiding grasbekleding*, 2019). A scheme of how a dike's cross-section is simplified when designing and assessing a dike is shown in Figure 2.12, where the location of the only vegetation type considered is presented.

Other well known effects are monitored regularly rather than taken into account in the computation of the failure probability, due to the lack of knowledge. A few examples of guidelines that can be followed to monitor types of vegetation are listed below.

- For vegetation on the floodplains along rivers: a guideline is available through a website containing a vegetation map ("*Vegetatie legger*" in Dutch) ("Vegetatielegger", 2020). On this website, the types of vegetation that are allowed to grow and their locations to not impede the water flow are presented. This website is based on research such as the report called Flow resistance of vegetation in floodplains ("*Stromingsweerstand vegetatie in uiterwaarden*" in Dutch) (van Velzen et al., 2003), which provides how the effect of 30 different types of vegetation on the floodplain can be taken into account in models such as *WAQUA* (software that computes river water levels) to compute the increased water level due to their presence (*Users Guide WAQUA: General Information*, 2016). This was done by translating the vegetation's structure type into roughness parameters such as the Chezy and/or Nikuradse k-value.

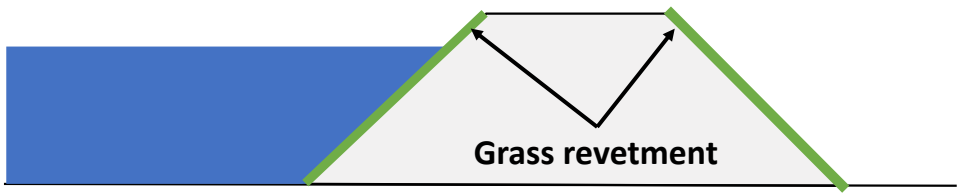

Figure 2.12: Schematization of a river dike cross-section and location of the only vegetation taken into account during its assessment.

- For large woody vegetation near dikes: In the WBI2017 there is a section for not water retaining objects ("*Niet waterkerende objecten (NWO)*" in Dutch) and under that section, there is a sub-section for vegetation ("*Begroeiing (NWObo)*" in Dutch). This guideline is for large vegetation more than 5 m in height and with a diameter of more than 0.15 m. The height, diameter, skewness, and location of the vegetation are evaluated, and it is determined whether the vegetation can remain or not (Rijkswaterstaat, 2017a). If the outcome is that the large vegetation cannot stay, a document called "*BomenT fase*" shows more steps that can be followed to assess the effect of the woody vegetation near or on the dike (van Houwelingen, 2012).

Thus, the increase in water level due to vegetation along rivers and the presence of large vegetation near or on dikes are both currently considered indirectly in the assessment. Including the effects of vegetation directly in the computation of the failure probability would provide a better overview of their impact.

3

Including effects of vegetation in the Dutch safety assessment

This chapter presents the five different vegetation effects on the load and strength of the failure mechanisms considered in this study. Four effects impact overtopping/overflow and two internal erosion, one effect (increase in water level) affects both failure mechanisms. The first two sections explain the effects, one section per failure mechanism, and the last section describes how each was modeled to be taken into account in the safety assessment.

As a reminder, the types of vegetation considered in this study are: woody vegetation (e.g. trees and bushes), reed beds (reeds are tall, grass-like plants of wetlands) and scrubs (which are low woody plants), and herbaceous vegetation (low vegetation), see Figure 3.1.

(a) (b) (c)

Figure 3.1: Types of vegetation taken into account in this study: (a) Willows, thus woody vegetation, (b) reed, (c) grass, thus herbaceous vegetation. These images are taken from the report "Flow resistance of vegetation in floodplains" (van Velzen et al., 2003).

3.1. Vegetation effects considered for overtopping/overflow

An overview of the types and locations of vegetation considered in this study to influence the failure mechanism overtopping/overflow are presented in Figure 3.2. In this figure, the parameters affected by these vegetation types are also presented. A summary of the four main effects caused by the different vegetation types and their locations is presented in Table 3.1, as

well as the corresponding parameter of the limit state function affected. The following sections briefly describe the causes and consequences of these vegetation effects.

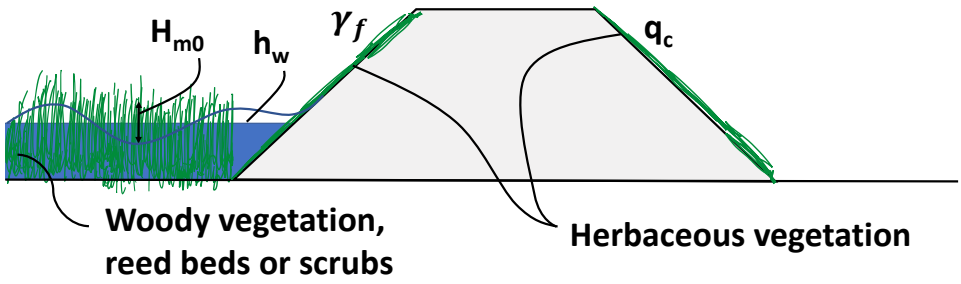

Figure 3.2: Location of different types of vegetation considered in the computation of the failure probability of overtopping/overflow.

Table 3.1: Characteristic of the vegetation that have an effect on the failure mechanism overtopping/overflow.

Effect	Type	Location	Parameter affected
Increase in water level (negative effect)	Woody vegetation and/or reed beds and scrubs	Floodplain / foreshore	Water level (h_w)
Increased erosion resistance (positive effect)	Herbaceous vegetation	Inner slope	Critical discharge (q_c)
Wave height reduction (positive effect)	Woody vegetation and/or reed beds and scrubs	Foreshore	Significant wave height (H_{m0})
Increased roughness (positive effect)	Herbaceous vegetation	Outer slope	Roughness factor (γ_f)

3.1.1. Increase in water level

This effect is caused by extra woody vegetation and/or reed beds and scrubs added along the river, on the floodplain or, to a lesser extent, on the foreshore of the dike, see Figure 3.3. The vegetation currently present on the floodplains, and/or foreshore is already taken into account, and, therefore, does not lead to an increase in water level. The increase in water level mainly depends on the structure (height, diameter, leaves, etc.) and density (amount vegetation per square meter) of the extra vegetation (Järvelä, 2002a, 2002b; Vastila and Jarvela, 2014), as well as on the average flow velocity and the water depth (Fathi-Maghadam and Kouwen, 1997; Ston and Shen, 2002). In general, the higher the flow velocity, the higher the increase in water level and vice versa. The water depth also plays a role, as when the vegetation starts getting submerged, its effect decreases. Several studies aimed at modeling this effect by incorporating

the vegetation roughness using the Chezy, Manning, or Darcy Weisbach parameters (Wu et al., 1999), depending on the vegetation type. For example, at four meters depth, it is advised to used a chezy coefficient of 10.75 for reed beds, 11.25 for willows, and 41 for grasslands (van Velzen et al., 2003). The Chezy coefficient is a function of the Reynolds Number and the relative roughness of a channel. The lower its value the higher the roughness.

It is expected that higher water levels lead to higher overtopping/overflow failure probabilities. For overtopping, this can be understood physically, since a higher water level leads to the water being closer to the crest of the dike and, thus, for a given wave height, there are more chances that water would flow over the dike. It can also be explained mathematically by observing the equations for overtopping, (see Equations (2.6) and (2.7)), in which the water level is implicitly found in the freeboard and the wave height. For overflow, the same effect applies: The higher the water level, the higher the probability of failure by overflow (see Equation (2.6)). Physically this means that the water levels are higher above the crest and, thus, a larger amount of water flows over, which increases the chances of failure.

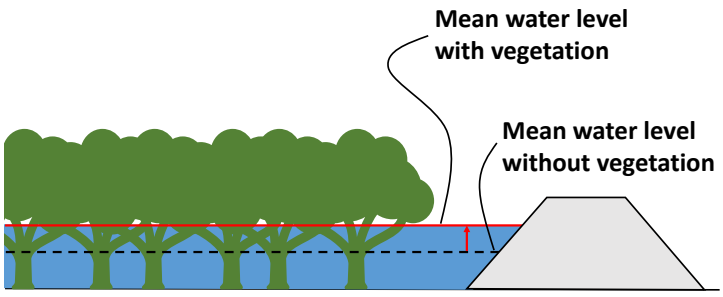

Figure 3.3: Woody vegetation, reed beds and scrubs on the floodplains or foreshore of dikes can lead to an increase in water level.

3.1.2. Increase in erosion resistance of the inner slope

The increase in erosion resistance due to herbaceous vegetation on the inner slope of the dike is caused by its biomass above and below ground (Vannoppen et al., 2016). The biomass above ground of the vegetation leads to an increase in surface roughness, which reduces the flow velocities and, therefore, also the flow shear stresses on the slope. The biomass below ground, composed mainly of roots, can reduce erosion thanks to its potential of increasing the soil shear strength, i.e. the soil becomes more cohesive (De Baets et al., 2008). The characteristics leading to a reduction of erosion are mainly the root density, root length density, and mean root diameter. This effect also depends on the type of soil and the flow velocity, according to some experimental studies (De Baets et al., 2006; De Baets et al., 2007; Vannoppen et al., 2016). For herbaceous vegetation, Berendse et al., 2015 found that the higher the diversity of the herbaceous vegetation, the higher the erosion resistance. This effect has been thoroughly studied in the Netherlands and, therefore, several guidelines exist on how to take it into account in the assessment of dikes (Stuip et al., 1999; van der Meer et al., 2012; van Hasselt and van Everdingen, 1998).

In general, this effect influences the amount of water allowed to flow over the dike before failure

and, thus, the critical discharge parameter of the limit state function. Thus, it is expected to have a strong impact on the failure probability because the critical discharge is one of the two main parameters of the limit state function, the other one being the actual overtopping discharge, see Equation (2.4). The higher the critical discharge value, the lower the failure probability and vice versa. This can also be understood physically, since an increase in critical discharge leads to more water being allowed to flow over the dike and, thus, providing a lower failure probability.

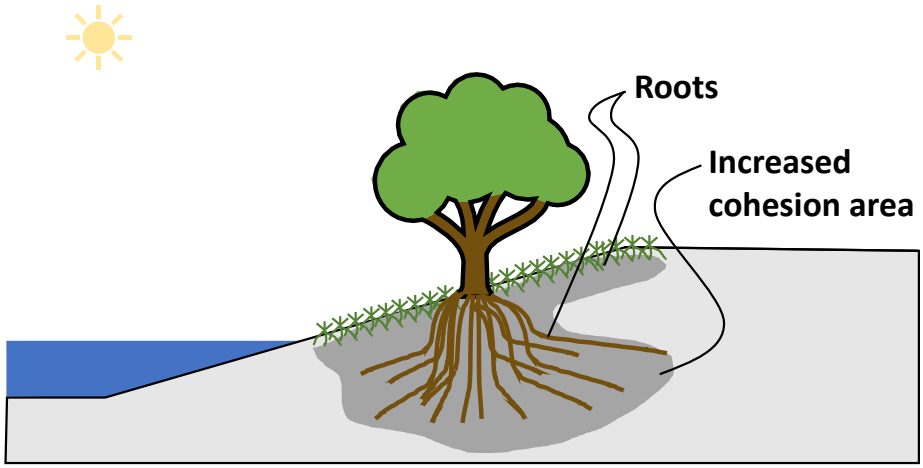

Figure 3.4: Illustration of an increased cohesion zone leading to more erosion resistance due to the roots of vegetation.

3.1.3. Reduction in wave height

The reduction in the incoming wave height due to woody vegetation or reed beds and scrubs on the foreshore is caused by the increase in roughness created by these vegetation types, which dissipates the wave energy (Klein Breteler et al., 2016). This effect mainly depends on the averaged diameter of the trunk, its height, and the density of vegetation (amount of vegetation per square meter). Another important parameter is the width of the vegetation zone in front of the dike (de Vries et al., 2015; Klein Breteler et al., 2016). Furthermore, this effect also depends on the flow velocity and the initial wave height (Verheij and Sprengers, 2012). The higher the initial wave height, the stronger the reduction that can be achieved. This effect has also been studied intensively in the past few years and several formulas have been created to model and predict the wave height reduction (Losada et al., 2016; Stuip et al., 1999; Suzuki, 2011; Verheij, 1995). Additionally, practical studies, such as those by Fort Steurgat and by Tiel-Waardenburg (de Vries and Dekker, 2009; Smale and Borsboom, 2016; Venema et al., 2014a, 2014b), have also been performed.

Overall, this effect is expected to lower the failure probability of overtopping. Overflow, on the other hand, is not affected by this parameter as it is not impacted by waves, as shown in Equation (2.6).

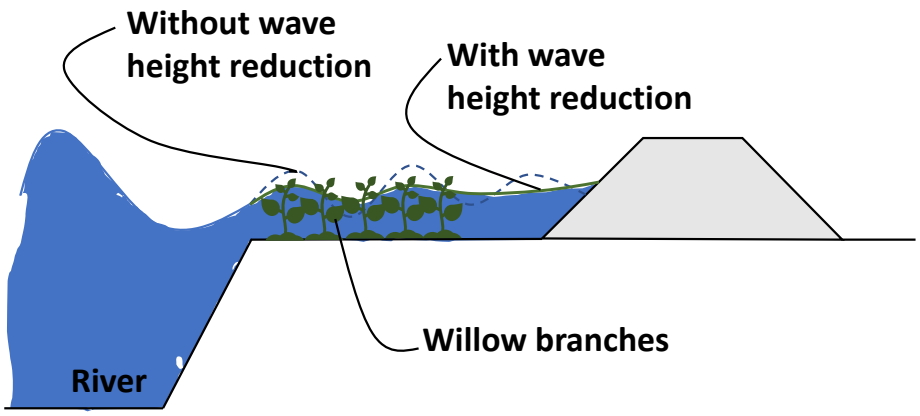

Figure 3.5: Illustration of wave height reduction due to vegetation located on the foreshore.

3.1.4. Increase in roughness of the outer slope

The increase in roughness on the outer slope caused by herbaceous vegetation mostly depends on its height and density (Vannoppen et al., 2016) and the water level. In case the herbaceous vegetation is submerged, its effect is reduced (Fathi-Maghadam and Kouwen, 1997; Ston and Shen, 2002).

This phenomenon influences the roughness factor (γ_f) of the overtopping failure mechanism. Lowering this factor increases the roughness and leads to a lower failure probability. This impact is also dependent on the initial wave height, and stronger effects are expected for higher wave heights. Mathematically, the lower γ_f, the lower the overtopping discharge. Overflow is not affected by γ_f, because when it occurs, any herbaceous vegetation on the outer slope is already completely submerged.

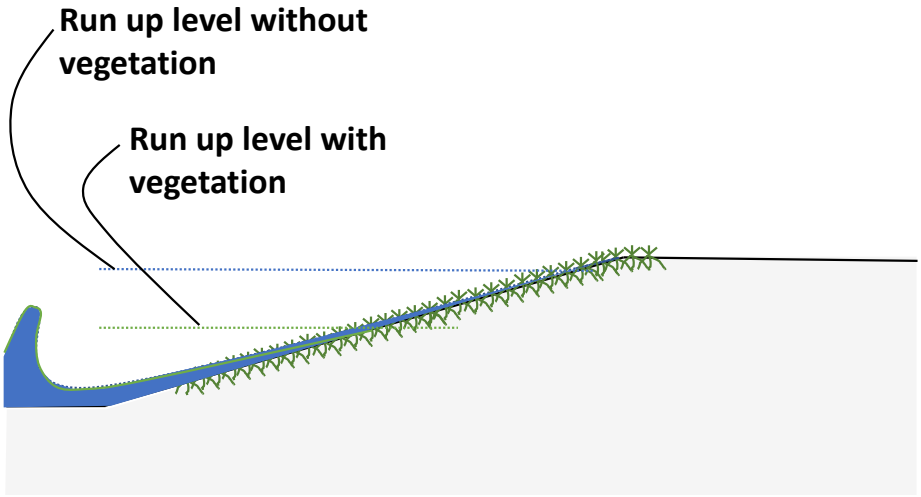

Figure 3.6: Illustration of an increased roughness on the outer slope of a dike.

3.2. Vegetation effects considered for internal erosion

An overview of the two vegetation types and locations considered in this study for the internal erosion failure mechanism is found in Figure 3.7, where the parameters affected are also presented. A more detailed summary is presented in Table 3.2.

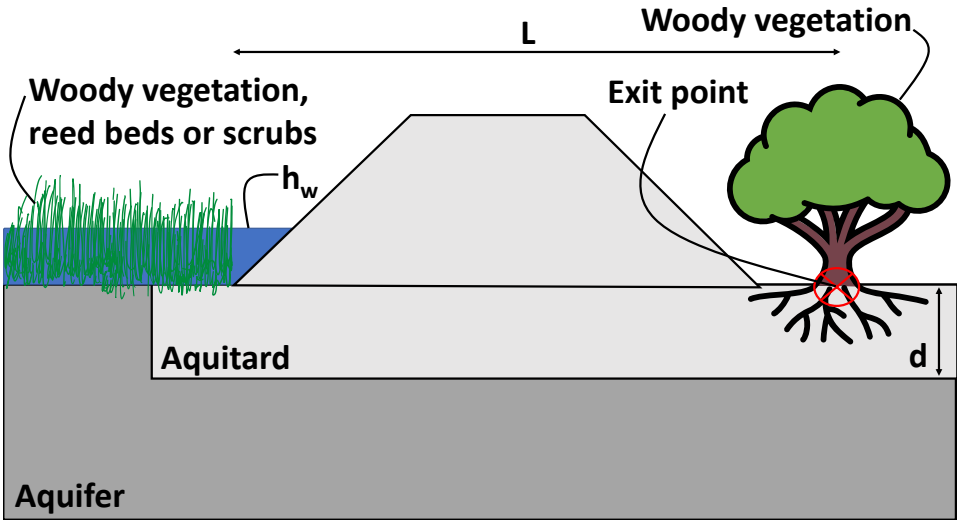

Figure 3.7: Location of different types of vegetation considered in the computation of the failure probability of internal erosion.

Table 3.2: Characteristics of the vegetation that have an effect on the failure mechanism internal erosion.

Effect	Type	Location	Parameters affected
Increase in water level	Woody vegetation and/or reed beds and scrubs	Floodplain / foreshore	Water level (h_w)
Tree toppling over	Woody vegetation and/or reed beds and scrubs	Hinterland	Exit point location (x_{exit}), seepage length (L) and blanket thickness (d)

3.2.1. Increase in water level

The characteristics of extra vegetation leading to an increase in water level were already described in Section 3.1.1. The important aspect of an increase in water level for internal erosion is that the head difference across the dike increases, which influences all its three submechanisms negatively since this leads to higher pressure on the impermeable layer. Mathematically, this effect is observed in the piezometric head, which increases with increasing water level. For uplift, a higher water level leads to a higher actual head difference and, thus, a lower safety factor. In the heave process, a higher piezometric head leads to a higher actual exit gradient and, hence, more chances of failure. Finally, for piping, the actual average head difference increases with the water level, leading to the same conclusion as for the overtopping/overflow failure mechanism. Therefore, for internal erosion, as for overtopping and overflow, an increase in water level leads to an increase in the failure probability.

3.2.2. Tree toppling over

Large woody vegetation, i.e. trees, on the hinterland can fall over due to high water levels and wind speeds (Roth et al., 2017). The effect of a tree toppling over on internal erosion depends mainly on the root ball size, its location, and the dike material. The characteristics of the roots of a tree depend on the tree species, its age, the soil texture, its compaction, and the water access (Zanetti et al., 2009).

Trees that may topple over close to the toe of the dike at the hinterland, can increase the risk of internal erosion due to the divot it creates (Lanzafame and Sitar, 2018). This phenomenon has two main impacts (see Figure 3.8): a local reduction of the blanket thickness, which creates a weak spot for uplift and heave; and an increase in seepage from the riverside to the land side of the dike through this divot. However, a falling tree can easily be detected allowing for a quick intervention (Roth et al., 2017).

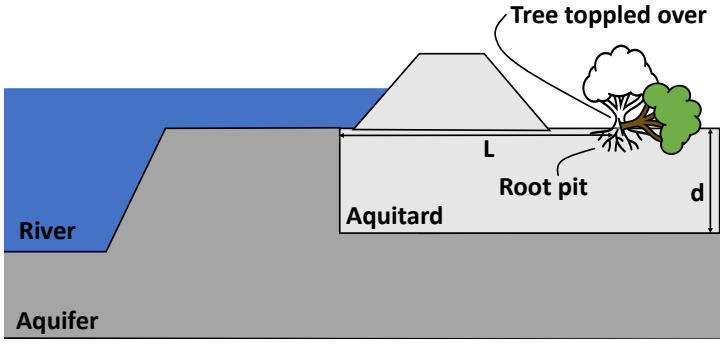

Figure 3.8: Illustration of the effect of a tree falling over on internal erosion. The blanket thickness is locally decreased and the exit point is changed depending on the location of the tree.

3.3. Modeling vegetation effects in the Z-functions

As it was explained in the sections above, the presence of certain types of vegetation at certain locations can influence certain parameters that condition the limit state functions (of different failure mechanisms) and, hence, the failure probability of dikes.

In a general form, these dependencies can be expressed using generic functions, such as f and g. The limit state function of a failure mechanism can be expressed as a function f of a set of n different parameters ($\alpha_1, \ldots, \alpha_n$, contained in $\boldsymbol{\alpha}$), such as the water level or the wave height.

$$\mathrm{Z} = f(\boldsymbol{\alpha}). \tag{3.1}$$

As aforementioned, some of these α_i (with $i \in [1, \ldots, n]$) parameters are conditioned by the presence of certain vegetation types in certain locations and can be, therefore, expressed as a function g_i of the vegetation:

$$\alpha_i = g_i(\mathrm{veg}). \tag{3.2}$$

Applying substitution, the influence of vegetation in the failure probability of dikes can be estimated by introducing Equation (3.2) in Equation (3.1) obtaining:

$$Z = f(\boldsymbol{\alpha}) = f(g_1(\text{veg}), \ldots, g_n(\text{veg})), \tag{3.3}$$

where veg stands for the characteristics of vegetation influencing the parameters $\boldsymbol{\alpha}$. Including the effects of vegetation through this method leads to no change in the validity of the limit state function, which is also an assumption made.

The current study uses this approach to include the effects of vegetation in the computation of the failure probability, by determining the $\boldsymbol{\alpha}$ parameters for overtopping/overflow and internal erosion that are affected by vegetation and by assuming their g_i functions to find the failure probabilities. These g_i functions are not yet known due to a lack of empirical data, in the current study, realistic assumptions were employed. However, these g_i functions are important for the process of including vegetation in the assessment method of dikes, therefore, it is highly recommended to study these phenomena more intensely in the future. To this date, this approach has never been applied due to a lack of knowledge regarding:

- The parameters of the relevant limit state functions influenced by vegetation effects (the $\boldsymbol{\alpha}$, finding those was the focus of this study).
- The quantitative translation of the vegetation effects into those parameters (the g functions which were assumed throughout this study).

An illustrative example of this approach regards the limit state function for overtopping/overflow, which is a function of the water level, see Equation (3.4).

$$Z_{OT/OF} = f(h_w) \tag{3.4}$$

where:

- $Z_{OT/OF}$ [l/(s m)]: limit state function of overtopping.
- f: (generic) function of the limit state.
- h_w [m]: water level.

In Chapter 3 it was discussed that, at the same time, the water level depends on the presence of extra vegetation on the floodplain or foreshore and its type. This influence can be modeled following a generic function g, see Equation (3.5).

$$h_w = g(h_{veg}, \phi_{veg}, D_{veg}, d_w, u) \tag{3.5}$$

where:

- g: function of the water level.
- h_{veg} [m]: average vegetation height.
- ϕ_{veg} [m]: average diameter of vegetation.
- D_{veg} [vegetation/m^2]: density of vegetation.
- d_w [m]: water depth.
- u [m/s]: flow velocity.

Following the same reasoning as in Equation (3.3), we obtain.

$$Z_{OT/OF} = f[g(h_{veg}, \phi_{veg}, D_{veg}, d_w, u)] \tag{3.6}$$

From the limit state functions of overtopping/overflow and internal erosion presented in Chapter 2 and the vegetation effects presented in the sections above, the parameters of each failure mechanism influenced by vegetation were determined. A summary of these parameters (or $\boldsymbol{\alpha}$) is presented in Table 3.3.

Table 3.3: Summary of the modeling of the vegetation effects in the framework. A distribution type of "Not applicable" means that it is a function of other variables.

Effect of vegetation	Parameter influenced ($\boldsymbol{\alpha_i}$)	Distribution	Modification (g)
Increase in water level	Water level (h_w)	Gumbel	Increased by a constant value
Erosion resistance	Critical discharge (q_c)	Log-normal	Mean value was changed by a factor
Wave height reduction	Wave height (H_{m0})	Not applicable	Multiplied by a coefficient
Roughness outer slope	Roughness factor (γ_f)	Deterministic	Provided a new lower value
Trees on the hinterland	Local blanket thickness (d)	Log-normal	Subtracted by a constant value
	Seepage length (L)	Not applicable	Increased by a constant value
	Location of the exit point (x_{exit})	Not applicable	Increased by a constant value

In the long term, the aim is to determine all the parameters affected by vegetation, depending on its type and location, for most, if not all, failure mechanisms and determine to what extent they are affected by vegetation. This way, an extra step could be added in the assessment of dikes to take the effect of vegetation into account (see Figure 3.9). In this extra step, all vegetation types located near or on the dike are quantified, to know the magnitude of their effect, i.e. how much a strength or load parameter would change. The rest of the assessment is unchanged and the same limit state is used to compute the failure probability.

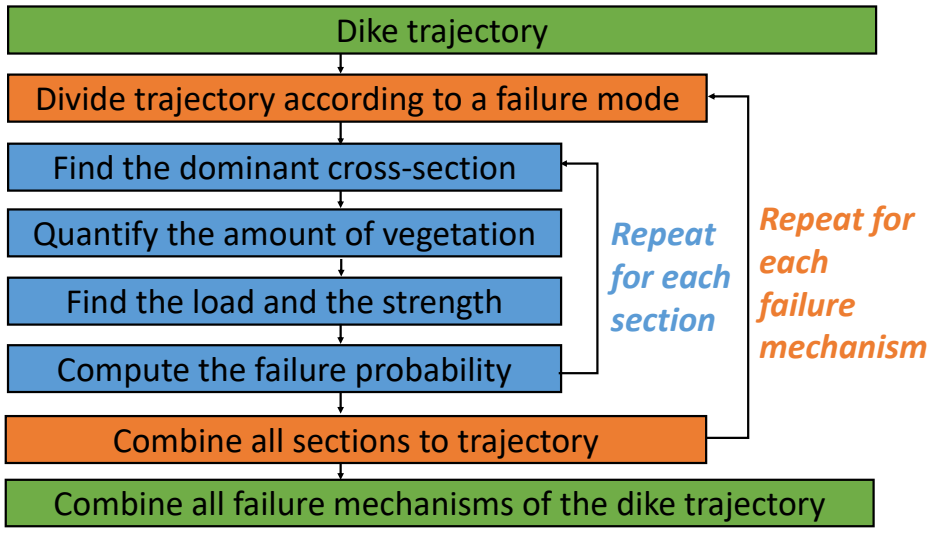

Figure 3.9: Extra step in the schematization of the assessment method for computing the failure probability of a dike segment considering multiple failure mechanism to include the effect of vegetation.

3.3.1. Increase in water level

The parameter influenced by this effect is the water level. To model this effect, a constant was added to this parameter:

$$h_{w,\,veg} = h_w + C_{hw} \tag{3.7}$$

where:

- $h_{w,\,veg}$ [m]: water level increase by the presence of vegetation on the floodplain or foreshore.
- C_{hw} [m]: constant vegetation parameter for added to model the effect of vegetation.

The value of C_{hw} depends on the type of extra vegetation added to the floodplain or foreshore, however, the relationship between the two is unknown. Therefore, the choice of C_{hw} is based on a study of the Rhine river, where it was found that the effect of vegetation succession plans along the river's floodplains could lead up to 0.6 m of increased water level (Makaske et al., 2011). The amount of the vegetation in the succession plans is unknown. Thus, to model the effect of extra woody vegetation and/or reeds beds and scrubs added to the foreshore of a dike, it was decided to use a conservative increase in water level of up to 0.1 m. Thus, this effect was modeled by adding a constant, which took a value up to 0.1 m, to the stochastic parameter of the water level. By using the same limit state function and reliability method, the failure probability with the increase in water level was computed.

3.3.2. Erosion resistance

The parameter influenced by this effect is the critical discharge. To model this effect, the mean of the stochastic parameter was modified:

$$\mu_{qc,\,veg} = \mu_{qc}\, C_{qc} \tag{3.8}$$

where:

- $\mu_{\text{qc, veg}}$ [l/(s m)]: mean critical discharge including a change in vegetation type/quality on the inner slope.
- μ_{qc} [l/(s m)]: mean critical discharge.
- C_{qc} [m]: constant vegetation parameter for decreasing or increasing the mean critical discharge by a percentage.

The coefficient C_{qc} depends on the root strength of the vegetation present on the inner slope. No studies were found that provided a link between C_{qc} and the root of vegetation. Most studies focused on the strength of roots (how they get detached from the soil due to a peak flow velocity) rather than the amount of water (in l/(s m)) that can flow over a slope, with a vegetated revetment, before reaching 20 cm of erosion. Therefore, to quantify this effect, C_{qc} was chosen to take the values of 0.8 and 1.2 to model an above– and below–average grass quality, respectively. Two sets of parameters corresponding to wave heights below 1 m proposed by the WBI2017 for the critical discharge were used in this study, one for good grass and one for worse grass quality (which is chosen as reference) were used. The former has a mean discharge of 225 l/(s m) and a standard deviation of 250 l/(s m) and the latter a mean of 100 l/(s m) and a standard deviation of 120 l/(s m). The standard deviations and the log-normal distribution of both grass qualities were kept unchanged.

3.3.3. Wave height reduction

The parameter influenced by this effect is the wave height. To model this effect, the parameter was multiplied by a constant called the wave coefficient (WC), which has a value lower than one:

$$H_{\text{m0, veg}} = H_{\text{m0}}\,\text{WC} \tag{3.9}$$

where:

- $H_{\text{m0, veg}}$ [m]: wave height at the toe of the dike reduced by vegetation.
- WC [-]: constant vegetation parameter for wave height coefficient.

The choice of the quantification of this effect was based on the studies at Fort Steurgat and Tiel Waardenburg. The former had a 60% wave reduction with a 40 m wide zone of willow trees (Venema et al., 2014b). The latter calculated a maximum of 31% wave height reduction with a 60 m wide zone of willow trees and only 11% with the same zone width but with scrubs instead of willows (Smale and Borsboom, 2016). Therefore, it was decided to model the wave reduction of the case studies by taking a wave coefficient between 0.2 and 1, modeling 80% to 0% wave height reduction, respectively.

3.3.4. Roughness outer slope

The parameter influenced by this effect is the deterministic roughness factor. To model this effect, the value of this parameter was decreased by multiplying it by a factor:

$$\gamma_{\text{f, veg}} = \gamma_{\text{f}}\,C_{\gamma f} \tag{3.10}$$

where:

- $\gamma_{\text{f, veg}}$ [-]: influence factor for roughness adjusted by vegetation.
- $C_{\gamma f}$ [-]: constant vegetation parameter for adjusting the roughness factor.

Klein Breteler et al., 2016 showed that up to 0.61 m crest height reduction could be achieved by reducing the roughness factor to a value of 0.8. Therefore, to quantify this effect, the roughness factor was reduced to a value between 0.8 and 1, $C_{\gamma f}$ took values between 0 and 0.2.

3.3.5. Trees on the hinterland

Trees on the hinterland do not cause harm to the dike unless they topple over. If this occurs, three parameters are influenced: the local blanket thickness (d), the seepage length (L), and the location of the exit point (x_{exit}). These are all parameters of the internal erosion failure mechanism and, therefore, they affect the three limit state functions of the sub-mechanisms: uplift, heave, and piping. To model this effect, the local blanket thickness was reduced by a constant (see Equation (3.11)). The seepage length and the location of the exit point were changed according to the location of the woody vegetation (see Equations (3.12) and (3.13) respectively).

$$\mu_{\text{d, veg}} = \mu_{\text{d}} C_d \tag{3.11}$$

$$L_{\text{veg}} = L + loc \tag{3.12}$$

$$x_{\text{exit, veg}} = x_{\text{exit}} + loc \tag{3.13}$$

where:

- $\mu_{\text{d, veg}}$ [m]: local mean value of the blanket thickness at the location where the tree as toppled over.
- C_d [m]: constant vegetation parameter for mean length of the root ball.
- L_{veg} [m]: seepage length when the exit point is at the tree's location.
- $x_{\text{exit, veg}}$ [m]: distance between the center of the dike and the exit point which is at the tree's location.
- loc [m]: constant vegetation parameter for the location of the tree, it is the distance between the toe of the dike and the new exit point.

The reduction in local blanket thickness depends on the size of the vegetation's root-ball. However this effect is local, and the parameter for the blanket thickness (d) in the three limit state functions sometimes refers to the average thickness rather than the local one. In the sub-mechanisms of uplift and heave, it refers to the local thickness because the events happening have a very characteristic local nature, at the crack/sand boil. For piping, it refers to the global one, i.e the erosion channel should occur throughout the dike's width. Consequently, a change in local blanket thickness only affects the first two sub-mechanisms: uplift and heave. Due to a lack of literature, it was assumed that the length of the root ball has a maximum value of 50% of the initial blanket layer thickness.

The changes in seepage length and the location of the exit point depend on the location of the tree, i.e. the new exit point. These changes affect all three sub-mechanisms but in different ways. For uplift and heave, it is the piezometric head at the exit point (ϕ_{exit}) that is influenced. Its value decreases due to a lower damping factor (λ) which is caused by the increase in x_{exit} (see Equation (2.13) and 2.14). For piping, the change in exit point influences the seepage length. To study changes in x_{exit} and seepage length, trees up to five meters away from the toe of the dike were modeled, i.e. loc takes values between 0 and 5.

3.3.6. Modeling vegetation effects - Summary

As a summary, this study looked at the effects of five vegetation effects, which in total influence seven different parameters, two of which are modified in the same way. Therefore, six different constant vegetation parameters (C_{hw}, C_{qc}, WC, $C_{\gamma f}$, C_d and loc) are needed to model these effects. Their values depend on the types of vegetation present on the dike's cross-section.

4

Method

4.1. Theory

The method to include vegetation effects in the computation of the failure probability considering overtopping/overflow and/or internal erosion, presented in Section 3.3, was used to create a framework. This framework was constructed to determine if a certain combination of vegetation effects would result in an overall positive, negative, or negligible effect (in case positive and negative effects compensate each other). This study models the framework with Bayesian Belief Networks (BBNs), which are acyclic graphical probabilistic models that provide a visual representation of dependencies between a set of continuous or discrete variables (Neapolitan, 2004). Their ability to combine information in a very clear and graphical way is the main advantage of using them to understand the impact of different vegetation scenarios on the failure probability.

For example, imagine that a water authority needs to assess a dike to ensure its compatibility with the safety standards. Let's consider that the cross-section under study is very vulnerable to overtopping/overflow. The water authority may wonder whether the dike's cross-section potentially benefits from existing willow trees on its foreshore to reduce wave heights at its toe. From an approximate study, it is assumed that the current willows could reduce the wave height by 40%. The water authority responsible also wants to know whether it is beneficial to increase the willow plantation zone to achieve 60% wave reduction. Furthermore, on the inner slope, a grass revetment is used for erosion protection. The grass revetment is still in good shape, but the water authority wonders what the impact on the failure probability would be in case the quality of the grass degrades. Furthermore, the water authority wonders what would happen if both hypothetical scenarios (wave height reduction and grass quality) were combined. To help the water authority understand the impact of all the vegetation scenarios, both individually and simultaneously, it would be beneficial to construct a BBN.

BBNs consist of nodes and directed arcs, where nodes represent the random variables (X_1, X_2, ..., X_n), and arcs provide information about the dependencies between these random variables. In this example, there are three random variables, i.e. three nodes: the amount of wave height reduction (Wave reduction), the grass quality (Erosion resistance), and the probability of having overtopping/overflow (Overtopping/overflow), see Figure 4.1.

BBNs have three types of nodes: parent nodes, child nodes, and root nodes. Parent nodes have outgoing arcs and child nodes are those which the arcs are pointing towards. Hence if two nodes, X_i and X_j, are connected by an arc with the arc pointing towards X_j, then X_i is called parent node and X_j a child node. The nodes at the "top" of the BBN are the root nodes and have no parents. In the example, Wave reduction and Erosion resistance are both root nodes and parents nodes of Overtopping/overflow, the child node, see Figure 4.1.

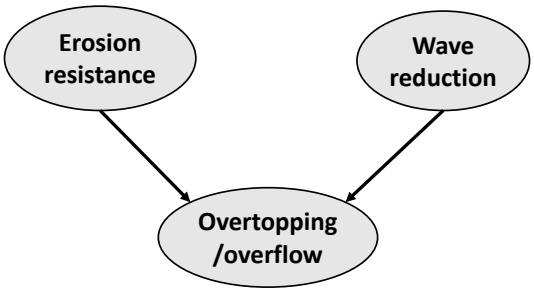

Figure 4.1: Example of a BBN, Wave reduction and Erosion resistance are both root nodes and parents nodes of Overtopping/overflow, the child node.

The type of nodes depends on the direction of the arcs, which are placed according to the dependencies between variables. Child nodes depend on their parent nodes. If two nodes X_i and X_j, are connected by an arc, with the arc pointing towards X_j, then X_i is directly influencing X_j, i.e. both nodes are dependent. Similarly, if X_i and X_j are not connected by any arc, then they are conditionally independent. Consequently, all root nodes are independent of each other. This graphical representation with nodes and arcs make BBNs attractive because it is visually possible to determine which nodes are dependent on each other and which ones are not. Using slightly more elaborate techniques, such as d-separation (Pearl, 1995), it is even possible to visually identify conditional inter-dependencies.

As mentioned above, every node in a BBN is a random variable, therefore, it carries information, which can be continuous or discrete. The type of information conditions whether the BBN is continuous, discrete, or mixed when nodes are respectively only continuous, only discrete, or both types of random variables. Working with continuous BBNs is more strenuous since it requires more computational effort. In this study, discrete BBNs are used.

In discrete BBNs, the information carried by each node is called states. In the example of Figure 4.1, the Wave reduction node has three states: 0%, 40% and 60%, representing 0%, 40% and 60% wave reductions, respectively. The node Erosion resistance has two states: $good$ or bad, representing good and bad grass quality respectively. The node Overtopping/overflow has two states: failure or no failure. Each state in a node has a certain probability of occurrence, which is represented, for root nodes, in marginal probability tables, and for child nodes, in conditional probability tables, i.e. their states depend on the states of their parents. The potential of BBNs lays in those conditional probability tables, which are the key to computing the probability of any type of scenario.

To illustrate this, the example mentioned above was given assumed probabilities. The marginal

distributions of the root nodes were considered uniform, see Table 4.1 and 4.2, and the conditional probability table of the child node was filled with exaggerated fictional probabilities for illustration purposes, see Table 4.3.

Table 4.1: Marginal probability table of Wave reduction, where the first row gives the different states the node has and the row below their respective probabilities.

Wave reduction	$WC0$	$WC40$	$WC60$
P(Wave reduction) [-]	0.333	0.333	0.333

Table 4.2: Marginal probability table of Erosion resistance, where the first row gives the different states the node has and the row below their respective probabilities.

Erosion resistance	$Good$	Bad
P(Erosion resistance) [-]	0.5	0.5

Table 4.3: Conditional probability table of Overtopping/overflow with fictional values.

Wave reduction	Erosion resistance	$Failure$	$Nofailure$
$WC0$	$Good$	0.02	0.98
$WC0$	Bad	0.05	0.95
$WC40$	$Good$	0.002	0.998
$WC40$	Bad	0.005	0.995
$WC60$	$Good$	0.0002	0.9998
$WC60$	Bad	0.0005	0.9995

Using the marginal and conditional probability tables of a BBN and some basic probabilistic knowledge (Dekking et al., 2005), any scenario can be computed. The probabilities of scenarios in a BBN can be determined using Eq. (4.1).

$$\mathrm{P(X)} = \sum_{i=1}^{n} \mathrm{P(X}|X_{\mathrm{pa}(i)})\mathrm{P}(X_{\mathrm{pa}(i)}), \tag{4.1}$$

where:

- P(X): probability of X.
- $\mathrm{P(X}|\mathrm{X}_{\mathrm{pa}(i)})$: probability of X given its parents.
- $\mathrm{P}(\mathrm{X}_{\mathrm{pa}(i)})$: probability of the parents of X.

These calculations can be automated and (almost) instantaneous if the BBN is modeled in a software such as *Netica* (*NETICA*, 2010), which also has the advantage of providing a pleasant visualization of the problem. To model a BBN in *Netica*, the nodes, their states, and the arcs have to be implemented, together with their respective marginal or conditional probability tables. Once modeled, *Netica* provides visually the state of each node and their respective

marginal probabilities in percentage, see Figure 4.2. The marginal probability of having overtopping/overflow failure is thus 1.29%. The model can then be used to compute any conditional probabilities. Figure 4.3 shows the probabilities of the BBN given a 40% wave reduction and good grass quality, it can be observed that the failure probability then becomes 0.20%. Whereas Figure 4.4 presents the probabilities of the BBN given a 60% wave height reduction and no choice in grass quality, the failure probability is then even lower 0.035%.

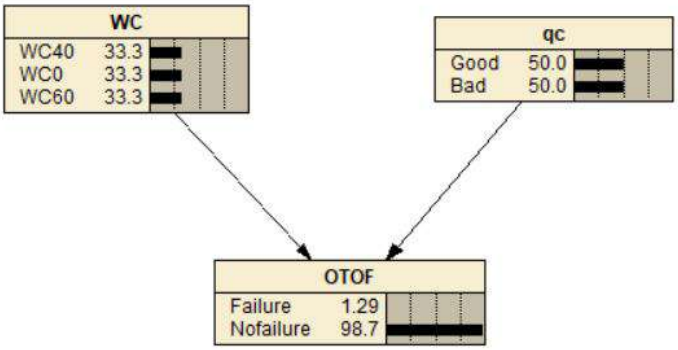

Figure 4.2: BBN example in *Netica* with fictional values. The software automatically computes and visually provides the marginal probability tables of each node.

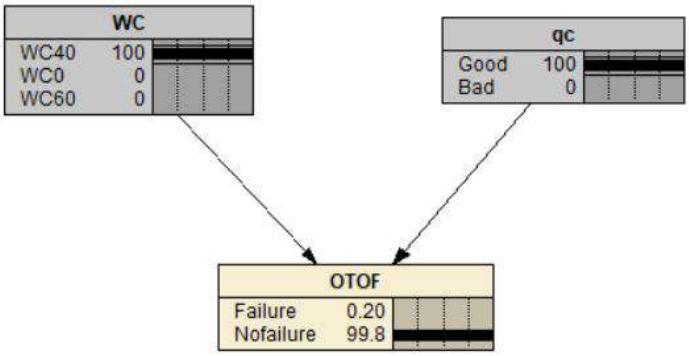

Figure 4.3: BBN example in *Netica* with fictional values conditionalized on a wave height reduction of 40% and good grass quality. The software automatically computes and visually provides the relevant probabilities of each states per node.

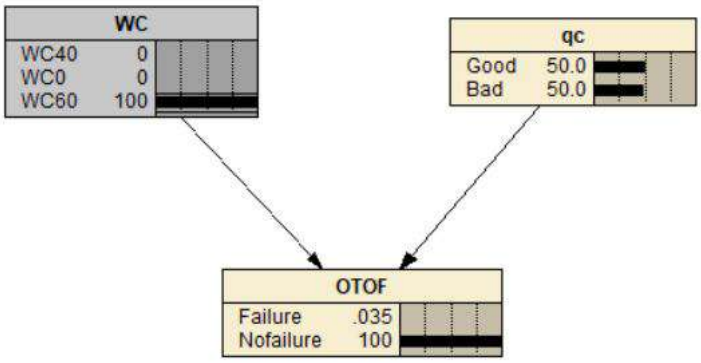

Figure 4.4: BBN example in *Netica* with fictional values conditionalized on a wave height reduction of 60%. The software automatically computes and visually provides the relevant probabilities of each states per node.

Hence, from this BBN, the water authority in the example can make more informed decisions about whether or not to add vegetation, what quantity and where. From the BBN in the example, it is possible to conclude that by achieving a 60% wave reduction, a failure probability 100 times lower would be obtained, and that a variation between good and bad grass quality only increases the failure probability 2.5 times, see Table 4.3. Thus, based on these outcomes, the water authority would benefit from increasing the vegetation on the foreshore to achieve the aforementioned 60% wave reduction whereas the quality of the grass on the inner slope, on the other hand, would not be an important concern.

Besides computing joint and marginal probabilities, BBNs can also be used for the consideration of inference, i.e. finding the likelihood of a cause given an event. For example, given a failure scenario, they can determine the likelihood of having a certain wave height reduction and grass quality, see Figure 4.5. From this figure, it can be concluded that the most likely cause of failure is the scenario with no wave reduction and bad grass quality. Similarly, the same can be done for a scenario without failure, see Figure 4.6. These examples show the potential of this framework because it can instantaneously compute multiple failure probabilities with different vegetation scenarios.

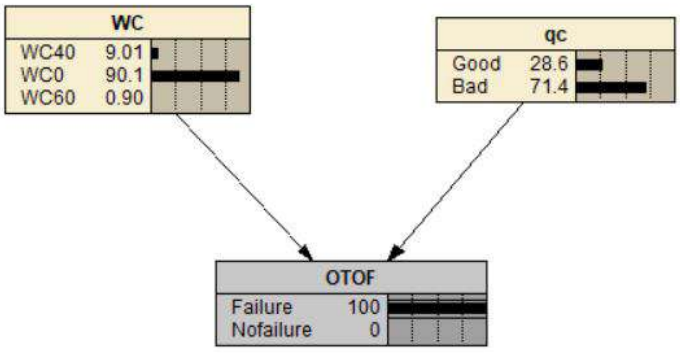

Figure 4.5: BBN example in *Netica* with fictional values conditionalized on $Failure$. The software automatically computes inference and visually provides the relevant probabilities of each states per node.

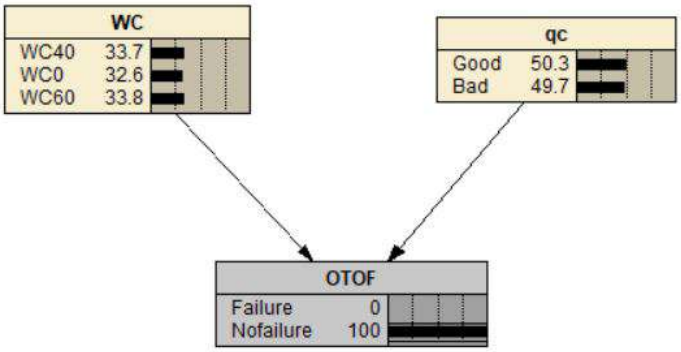

Figure 4.6: BBN example in *Netica* with fictional values conditionalized on $Nofailure$. The software automatically computes inference and visually provides the relevant probabilities of each states per node.

However, these outcomes are based on unrealistic fictional values selected solely for illustration purposes. In reality the differences between the failure probabilities of different vegetation scenarios will not be so different, and, as such, the decision-making process will be less obvious. To use this method in practice, the values of the conditional probability table (shown in Table 4.3) of overtopping/overflow cannot be fabricated but should be computed based on the characteristics of the cross-section under study and the modified limit state function (f) of the failure mechanism under study, see Table 4.4. The modified limit state function refers to the method explained in Section 3.3, in which the parameters influenced by vegetation are modified accordingly and the same limit state function is used to compute the failure probability.

Table 4.4: Equations of the conditional probability table of Overtopping/overflow which can be computed with a reliability method such as MC simulations, f represents the limit state function of overtopping/overflow.

Wave reduction	Erosion resistance	Failure	No failure
$WC0$	$Good$	$P_{f,WC0,good} = f(H_{m0} * 1, \mu_{qc} = 225, \sigma_{qc} = 250)$	1 - $P_{f,WC0,good}$
$WC0$	Bad	$P_{f,WC0,bad} = f(H_{m0} * 1, \mu_{qc} = 100, \sigma_{qc} = 120)$	1 - $P_{f,WC0,bad}$
$WC40$	$Good$	$P_{f,WC40,good} = f(H_{m0} * 0.6, \mu_{qc} = 225, \sigma_{qc} = 250)$	1 - $P_{f,WC40,good}$
$WC40$	Bad	$P_{f,WC40,bad} = f(H_{m0} * 0.6, \mu_{qc} = 100, \sigma_{qc} = 120)$	1 - $P_{f,WC40,bad}$
$WC60$	$Good$	$P_{f,WC60,good} = f(H_{m0} * 0.4, \mu_{qc} = 225, \sigma_{qc} = 250)$	1 - $P_{f,WC60,good}$
$WC60$	Bad	$P_{f,WC60,bad} = f(H_{m0} * 0.4, \mu_{qc} = 100, \sigma_{qc} = 120)$	1 - $P_{f,WC60,bad}$

Using the data of Case study 1 at Culemborg (see Chapter 5), the conditional probability table represented above could be filled and implemented again in *Netica*, see Figure 4.7. Again, the same conditionalisation on the wave height reduction (see Figure 4.8) and the grass quality (see Figure 4.9) were made. Conversely, this time the impact of the wave height reduction is close to non-existent and the grass quality has a larger impact. Therefore, the water authority

would do best by not adding more vegetation on the foreshore but devote the efforts to maintain regularly the vegetation on the inner slope.

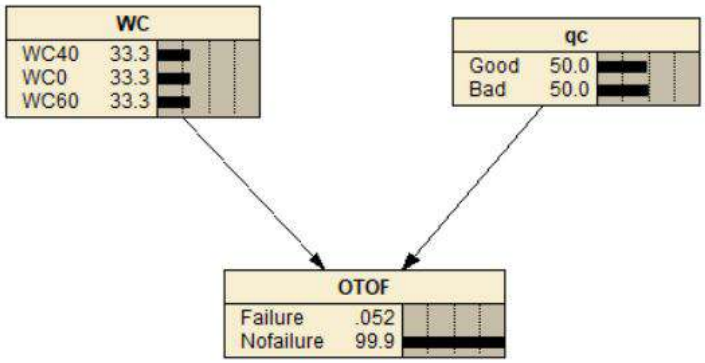

Figure 4.7: BBN example in *Netica* with real values taken from case study 1 at Culemborg. The software automatically computes and visually provides the marginal probability tables of each node.

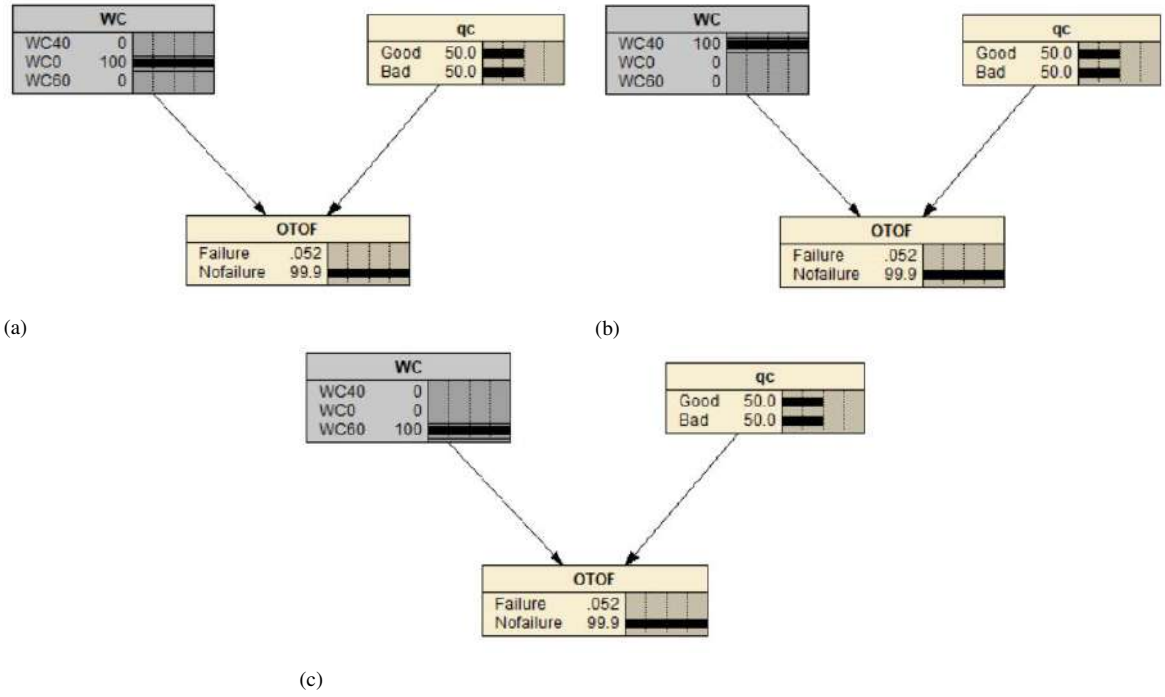

Figure 4.8: BBN example in *Netica* with real values made from the data of case study 1 at Culemborg conditionalized on different amounts of wave height reduction: (a) 0%, (b) 40% and (c) 60%.

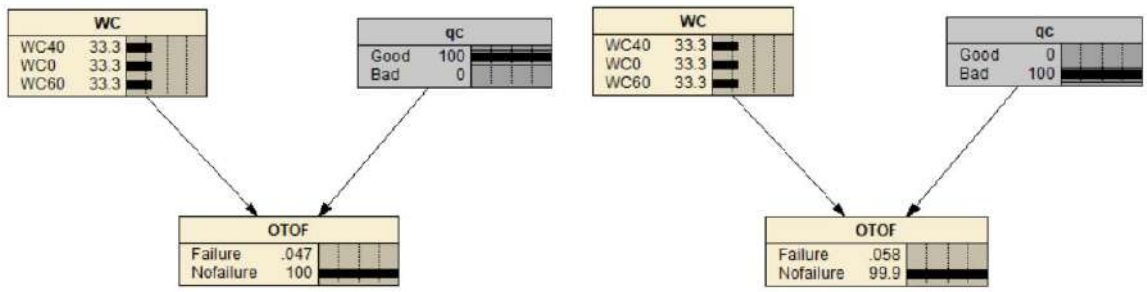

(a) (b)

Figure 4.9: BBN example in *Netica* with real values made from the data of case study 1 at Culemborg conditionalized on different grass quality: (a) good and (b) bad.

It is easy to realize that filling these tables row by row can become very tedious as the conditional probability tables become longer, because a reliability method needs to be conducted for each row. This work can be automated using the same software program *Netica* presented above, or *Pomegranate*, which is a *Python* software package. For these programs to compute the conditional probability table automatically, a file needs to be provided with a large amount of data from which the probabilities can be calculated, i.e. by counting the frequency of occurrence. Due to the lack of experimental data, this file can be constructed using Monte Carlo simulations and the limit state functions modified accordingly (see Section 3.3). Table 4.5 provides an example of such a file customized to the water authority problem presented previously. The values of the first and second columns (Wave reduction and erosion resistance) are generated randomly. The last column (Overtopping/overflow) generates a $Failure$ if its limit state function, considering the two previous columns, provides a negative value and $Nofailure$ otherwise. Using this type of data file, the conditional probability table of the child node can be computed with equations, such as Equation 4.2, which provides a conditional probability as shown in Table 4.6.

Table 4.5: Example of a matrix that can be used by *Netica* or *Pomegranate* to compute the conditional probability tables of a BBN. No failure indicates a positive Z-function for overtopping/overflow and failure indicates a positive one.

Wave reduction	Erosion resistance	Overtopping/overflow
0%	Good	No failure
0%	Good	Failure
40%	Bad	No failure
60%	Bad	No failure
...	...	...

$$P_f|WC60, good = \frac{N_f|WC60, good}{N_{WC60,good}} \tag{4.2}$$

where:

- $P_f|WC60, good$ [-]: Failure probability given 60% wave reduction and good grass quality.

- $N_f|WC60, good$ [-]: Number of failures given 60% wave reduction and good grass quality.
- $N_{WC60,good}$ [-]: Number of cases with 60% wave reduction and good grass quality.

Table 4.6: Conditional probability table of Overtopping/overflow in the BBN example based on a file data created with MC simulations and the limit state function of overtopping/overflow modified to fit the vegetation effects under study.

Wave reduction	Erosion resistance	$Failure$	$Nofailure$
$WC0$	$Good$	$\frac{N_{f\|WC0,good}}{N_{WC0,good}}$	1 - $\frac{N_{f\|WC0,good}}{N_{WC0,good}}$
$WC0$	Bad	$\frac{N_{f\|WC0,bad}}{N_{WC0,bad}}$	1 - $\frac{N_{f\|WC0,good}}{N_{WC0,good}}$
$WC40$	$Good$	$\frac{N_{f\|WC40,good}}{N_{WC40,good}}$	1 - $\frac{N_{f\|WC0,good}}{N_{WC0,good}}$
$WC40$	Bad	$\frac{N_{f\|WC40,bad}}{N_{WC40,bad}}$	1 - $\frac{N_{f\|WC0,good}}{N_{WC0,good}}$
$WC60$	$Good$	$\frac{N_{f\|WC60,good}}{N_{WC60,good}}$	1 - $\frac{N_{f\|WC0,good}}{N_{WC0,good}}$
$WC60$	Bad	$\frac{N_{f\|WC60,bad}}{N_{WC60,bad}}$	1 - $\frac{N_{f\|WC0,good}}{N_{WC0,good}}$

The accuracy of the model when it computes the conditional probability tables with a file is based on the length of the file, i.e. the number of simulations made. The number of simulations needed for good accuracy of the model is based on the two following points:

1. The failure probability of the failure mechanism under study: The result of a MC simulation can vary given its stochastic nature and, therefore, to achieve convergence and the correct failure probability, a large number of simulations (N) is required. To know when convergence is reached, the Coefficient Of Variation (V) can be computed. Assuming that the number of failures in a given MC follows a binomial distribution (failure or no failure), the coefficient of variation of the probability of failure can be estimated as:

$$V_{P_f} = \frac{\sigma_{P_f}}{P_f} \approx \sqrt{\frac{P_f}{NP_f^2}} = \frac{1}{\sqrt{NP_f}}, \tag{4.3}$$

   where:
   - V_{P_f}: coefficient of variation of the probability of failure.
   - σ_{P_f}: standard deviation of the probability of failure.
   - P_f: probability of failure.
   - N: number of simulations.

   The number of simulations needed can then be found by assuming a commonly used value of V_{P_f} of 0.05, as it leads to an acceptable variation in results of the MC simulation. From Eq. (4.3), it is clear that the lower the probability of failure (P_f) desired, the more simulations are required, see Equation (4.4).

$$N = \frac{1}{0.05^2\, P_f}. \tag{4.4}$$

2. The number of parent nodes and the number of states a node has: As an estimate, the number of simulations needed according to the failure probability mentioned above

needs to be multiplied by the number of states each parent node has. For the example given above, the lowest failure probability was 0.0002, thus, with a coefficient of variation of 0.05, this leads to 2 million samples needed. The example has two parent nodes, one with three states and one with two. Thus, for an accurate model, 12 million samples would be required.

To evaluate the validity of the marginal probabilities of the child node and, thus, the probability of failure, the same MC simulations can be used. Overall, it can be concluded that, when the conditional probability tables are computed with a file, the number of samples is essential to obtain accurate results and that this amount is case dependent.

By constructing the BBN as presented with the example, the variables of the limit state functions are hidden in the conditional probability tables. It was chosen not to model them as root nodes to avoid having a mixed BBN with continuous and discrete nodes. This was also decided because most software packages consider discrete BBNs, therefore, the variables of the limit state functions would need to be discretized, which is very time consuming and leads to inaccuracy. Hence, the conditional probability tables are case dependent and have to be constructed for each case study and cannot be used in general.

The main advantages of BBNs are, firstly, their ability to describe visually the different types of dependencies in a model (see Table 4.7). Secondly, the model can be easily and rapidly conditionalized to compute the probabilities of a wide variety of complex scenarios. Therefore, there is no need to compute a new simulation every time a different vegetation scenario is considered. Finally, BBNs provide high flexibility, as they can be easily modified and extended if needed. These three advantages are the main reasons why BBNs were selected to model the effects of vegetation on dikes in the current study.

A downside of this way of using BBNs is that its conditional probabilities need to be constructed from a file for each case study. It is easy to see that the construction of the file can become very time consuming if tens of millions of samples need to be simulated. However, this is a one-time-only expense, i.e. once the file is created, no long computations are needed anymore and any scenario can be computed in a matter of a few milliseconds. This is, thus, a fair price to pay for the advantages provided by BBNs. Another important aspect of BBNs is that they are sensitive to the graphic structure given, i.e. a different structure would provide different results. Thus, an accurate structure is important to obtain the right results, since wrong independence assumptions can lead to a wrong model, e.g. if two nodes are assumed to be independent when in reality they are not.

Table 4.7: Advantages and disadvantages of a BBN analysis.

Advantages	Disadvantages
• Easy computation for variables with any distribution. • Graphical representation. • Capacity to combine many different scenarios easily and clearly. • Can easily compute conditional probabilities.	• Depending on the number of nodes and states used, it can require a high computation time. • Sensitive to a different structure.

Many software packages exist to model BBNs, such as *UNINET* ("Uninet", n.d.), *NETICA* (*NETICA*, 2010), etc. To model the BBN used for the framework in this study, it was chosen to use *Pomegranate* instead of *Netica*, which was used for the example, because it is open-access and because it is coded in *Python*, making it easier to process the results. These advantages compensate for the few negative sides of Pomegranate, such as its lack of graphical interface.

4.2. Modeling with Pomegranate

Pomegranate (Schreiber, 2018) is a *Python* package that works, as of now, only with discrete BBNs. It allows for a great degree of flexibility, i.e. it can be used in different cases, regardless of whether the conditional probabilities and the structure of the model are known or not, see Table 4.8. In this study, the structure of the BBN is known but the conditional probabilities are not. As mentioned above, Pomegranate can construct the probability tables using a file containing a large amount of data by counting the frequency of occurrence of scenarios given to its parents.

This process of constructing the conditional probability tables is the most time consuming, but it is also the most important as it will influence the degree of accuracy of the model. The larger the amount of data, the more accurate the model will be. The computations were conducted using a Windows computer with an Intel® Core™ i7 processor with 16 GB RAM and a clock speed of 5 GHz.

Table 4.8: Advantages and disadvantages of Pomegranate.

Advantages	Disadvantages
• Easy processing results. • Open access. • In theory, it can construct as many nodes and arcs in a BBN as needed. There is no limit on the size of the BBN. • Very flexible, can be used even if the conditional probabilities and the structure of the model are unknown.	• No graphical interface. • Although this was not a problem in this study, Pomegranate has limited memory. Thus, a limitation to the size of the file and the number of parent nodes and states exists.

4.3. The framework

4.3.1. Constructing the framework

The framework modeled in this study is an extension of the example presented above, see Figure 4.1. The extension included an addition of root nodes to represent all six vegetation parameters presented in Section 3.3. Each root node contained five to six states and was uniformly distributed. Another child node was added to represent the internal erosion failure mechanism. Each vegetation node, i.e. root node, has an arc pointed towards the failure mechanism it influences. Finally, the last node to compute the total failure probability considering both failure mechanisms was added, see Figure 4.10.

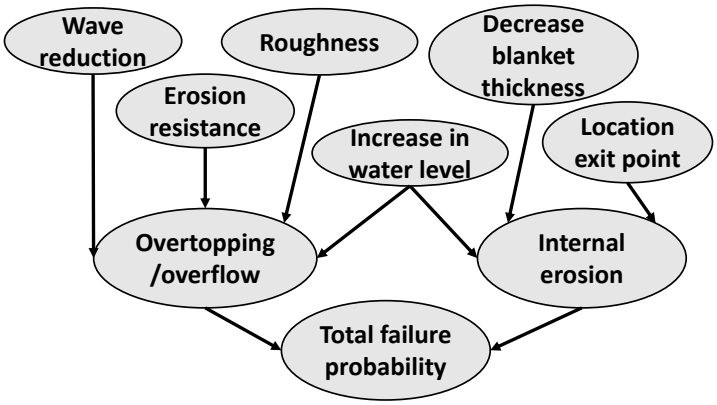

Figure 4.10: BBN considering both failure mechanisms and vegetation effects.

With this extension, three conditional probability tables were needed, instead of one, for each child node. To compute them, a file containing data about all three child nodes could be used by Pomegranate to compute those tables. The states of overtopping/overflow node and internal erosion node could be computed as previously mentioned with their respective limit state functions and the relevant g functions of Section 3.3. The state of the last node (Total failure probability) could be computed depending on the outcome of the two previous nodes. If at least one results to failure, the last node will have failure too.

This extensive addition of nodes considerably increased the computational time required for creating the file needed to calibrate the model. Therefore, it is important to first study the effects separately just using MC simulations to know whether an effect is important to add for the specific case study or not. This way, marginal effects are not added to the framework, which reduces computational time considerably. When the failure probabilities of certain failure modes are very low, the file will need to contain even more samples. Therefore, especially for these cases, it is important to not add unnecessary nodes and/or states.

This framework could be further extended in the future to consider additional vegetation effects and failure mechanisms. All that is needed is a study to find the $\boldsymbol{\alpha}$ parameters and g functions, see Section 3.3. An example of such an extension is found in Figure 4.11, where VE stands for Vegetation Effects and FM for Failure Mechanism.

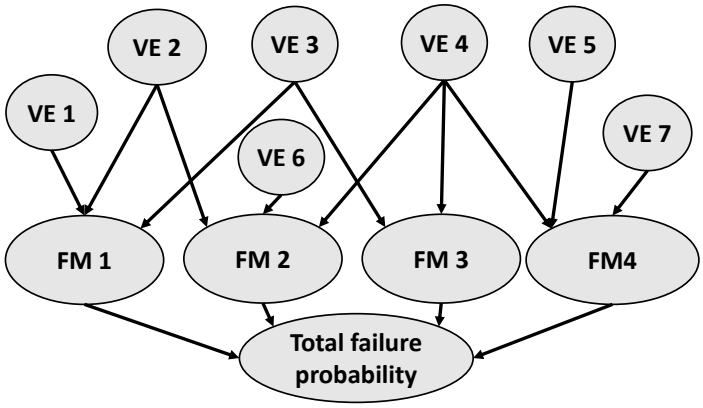

Figure 4.11: Graphical representation of the framework. In this example, seven Vegetation Effects (VE) are studied, together with four Failure Mechanisms (FM).

The advantages and disadvantages of the framework are listed in Table 4.9.

Table 4.9: Advantages and disadvantages of the framework.

Advantages	Disadvantages
• Can combine a lot of different vegetation effects and understand their combined effects. • Can be extended. • Can be used to do inferences, i.e. find the most likely cause of an event.	• Depending on the number of parent nodes, their state and the failure probability, its calibration can be time-consuming. However, this is a one-time cost. • Requires the knowledge of the quantification of vegetation effects which is usually not known. • No dependence between stochastic variables, and vegetation effects are not time-dependent. However, this can still be added if needed.

4.3.2. Analysing the results

Before creating the framework for each case study, a MC simulation was conducted for each individual effect as suggested above, i.e. to eliminate the marginal effects, reducing the computational time for calibrating the framework. These MC simulations were analyzed by creating graphs with the normalized failure probability and/or the normalized reliability index (also known as the beta value, which is based on the inverse standard normal cumulative density function, see Equations (4.5)) on the y-axis, and on the x-axis, different value of each vegetation parameters. Equations (4.6), and (4.7) present the computations for the normalized failure probability and normalized reliability index, respectively. From these graphs, the effects that are marginal, i.e. those with a constant horizontal line, could be determined.

$$\beta = \Phi^{-1}\left(1 - \mathrm{P}_f\right), \tag{4.5}$$

$$\mathrm{P}_{f\,\mathrm{normalized}} = \frac{\mathrm{P}_{f\,\mathrm{veg}}}{\mathrm{P}_{f\,\mathrm{no\ veg}}}, \tag{4.6}$$

$$\beta_{\mathrm{normalized}} = \frac{\Phi^{-1}\left(1 - \mathrm{P}_{f\,\mathrm{veg}}\right)}{\Phi^{-1}\left(1 - \mathrm{P}_{f\,\mathrm{no\ veg}}\right)}, \tag{4.7}$$

where:

- $\mathrm{P}_{f\,\mathrm{normalized}}$ [-]: normalized conditional failure probability.
- $\mathrm{P}_{f\,\mathrm{no\ veg}}$ [-]: failure probability conditioned on the scenario without vegetation.
- $\mathrm{P}_{f\,\mathrm{veg}}$ [-]: failure probability conditioned on a scenario with vegetation.
- $\beta_{\mathrm{normalized}}$ [-]: normalized beta value.
- Φ^{-1} [-]: Inverse of the standard normal distribution.

It was decided to normalize the failure probability (see Equation (4.6)) and the beta value (see Equation (4.7)) to observe the changes more clearly, because some failure probabilities can be very low. The normalization was done with respect to the failure probability of the scenario without vegetation. This allows for an easy determination of whether the total effect of vegetation is positive (normalized failure probability is lower than one and normalized beta value is higher than one), or negative (normalized failure probability is higher than one and normalized beta value is lower than one). For this study, the scenario without vegetation has the following vegetation parameters:

- C_{hw} = 0 m
- C_{qc} = 1
- WC = 1.
- $C_{\gamma f}$ = 0.
- C_d = 0 m.
- loc = 0 m.

In case a vegetation effect only takes place when a certain event occurs, such as the reduction in blanket thickness effect in case a tree topples over, the probability of that event occurring (in this example a tree toppling over) also needs to be taken into account. The normalized failure probability can then be computed with Equation 4.8. In this study, the probability that a tree topples over was assumed to be 1%. This value can be considered as overly conservative. A tree toppling over is a rare event. The first reason is that it will first break before being pulled out of the ground. Furthermore, for it to occur it requires a combination of high wind speeds and water levels. Whereas according to the empirical wind speed from station Deelen, reaching wind speeds above 40 m/s (approximately representing an average storm) has a probability of $10^{-}7$, thus much less than 1%. Therefore, the probability of occurrence of high water levels and wind speeds alone are low and if considering both at the same time the probability will be even lower, because both variables are considered independent in upper-river areas. Lastly, if a tree does topple over, it will most likely be noticed and therefore its effect will probably not be felt.

$$P_{f\,\text{normalized}} = \frac{P_{f\,\text{veg,tree}}\,P(\text{tree}) + P_{f\,\text{veg}}\,(1 - P(\text{tree}))}{P_{f\,\text{no veg}}}, \tag{4.8}$$

where:

- $P_{f\,\text{veg,tree}}$ [-]: failure probability conditioned on a scenario with vegetation if a tree topples over.
- P(tree) [-]: probability that a tree topples over, assumed to be 1%.

The results of the framework were analyzed using heat maps, which are colorful graphics that allow for three-dimensional visualization of data, which have two axes (horizontal and vertical) indicating the independent variables and the values of a third variable depicted as colored cells. In this study, the x and y-axes represent different vegetation parameters and the color shows for the normalized failure probability or normalized beta value, same as mentioned above (see Equations (4.6) to (4.8)). The following color coding should be employed to read the heat maps:

- If the color ranges from yellow/green, it indicates that the quantity of effect corresponding to the vegetation types and locations under study is positive, i.e. the normalized failure probability is lower than 1 and the normalized beta value is higher than 1.
- If the color ranges from orange/red, it indicates that the quantity of effect corresponding to the vegetation types and locations under study is negative, i.e. the normalized failure probability is higher than 1 and the normalized beta value is lower than 1.
- If the normalized failure probability or beta value is one, no change in failure probability is observed between the vegetated scenario and the none vegetated scenario.

4.4. Assumptions made in this thesis

Perhaps the largest assumption made in this study is, as mentioned above, the quantification of vegetation effects. Due to the lack of knowledge and data for the case studies, the density of each vegetation type near and on the dike cross-sections per case study was not known. Therefore, for example, the wave reduction achieved with the current vegetation state on the foreshore of each case study is unknown. An assumption had to be made for the amount of each vegetation effect.

A second assumption is that the limit state functions for overtopping/overflow and internal erosion are still valid with vegetation present. These functions are empirical formulae calibrated according to experimental set-ups that often do not contain vegetation. Thus, the calibration factors could be different when vegetation is present. Due to the relatively low accuracy of these formulae (over time many different values were used (van der Meer et al., 2018)), the presence of vegetation is not expected to influence these factors to a large extent. Furthermore, these calibration factors do not have the highest impact on the failure probability and, therefore, this assumption is considered acceptable, especially because this study only considers differences in terms of the order of magnitude for a first approximation of vegetation effects.

A third assumption is that all stochastic variables are independent. This assumption is usually made when assessing dikes according to the WBI due to the high complexity of computations when considering interdependency. In reality, stochastic variables are not always independent and several correlations can be found. For overtopping/overflow this assumption is not odd since the stochastic variables are wind, water level, bottom level, and critical discharge. The last one is independent as it is mostly based on the quality of the grass on the inner slope of the dike. The bottom level can also be considered independent as water levels and the wind do not influence this parameter. Lastly, only the water level and the wind could be considered as somehow dependent since one affects the other, but especially in river areas, where wind speeds are not very high, these effects can be considered independent. For internal erosion, more correlations can be found, especially geotechnical parameters influence each other a lot. However, the magnitudes of these correlations are very hard to quantify, and therefore, this was a necessary assumption. However, in the future, these dependencies can easily be taken into account by mapping the corresponding stochastic variables as root nodes in the BBN and adding their dependencies with arcs.

Another assumption made is that the effect of vegetation is not time-dependent, which is of course not the case as vegetation can vary considerably over time, e.g. it can break, decay, grow, etc. However, because the assessment of the current state of vegetation is under study and not during the lifetime of the dike this assumption is acceptable. In future studies, this time

dependence can be taken into account by using dynamic BBNs.

Throughout this study, failure is defined as the moment the limit state function is negative, however, this does not always correspond to total failure. Looking beyond the limit state functions, vegetation can act as a buffer or enhance failure, e.g. if there are already holes. This is considered as out of the scope of the present study.

No 3D effects were considered, therefore the cross-sectional flow of water is not taken into account. It was found in a study (Smale and Borsboom, 2016) that the current of water can reduce wave heights, but this was not considered here. The guidelines of the Dutch assessment methods were followed together with all its assumptions.

5

Case studies

Three case studies were chosen to demonstrate the use of the framework, all located in the upper-river areas of the Netherlands, their location can be found in Figure 5.1. The parameters were found from varying sources, they were not all provided by the water authorities responsible, and therefore, some assumptions were made which could mean that the computed failure probabilities might differ from reality. The case studies are for demonstration purposes, thus, the assumptions made are deemed reasonable.

Figure 5.1: Location of all case studies: Culemborg (in green), Grebbedijk (in red) and Duursche Waarden (in purple).

5.1. Common parameters for all case studies

5.1.1. Parameters for Z-function of overtopping/overflow

Following the guidelines of the WBI, all upper-river dikes are subject to the same wind condition coming from the wind station of Deleen, thus, all three case studies are subject to the same wind data that is managed by the Royal Netherlands Meteorological Institute ("Koninklijk Nederlands Meteorologisch Instituut" (KNMI) in Dutch). The empirical wind speeds per wind direction together with their probability of occurrence were extracted from the WBI *"Hydra-NL"*, and are based on the winter hourly maximum wind speed extracted up to the year 1951. This data includes statistical uncertainties. The empirical data was fitted to a Weibull distribution with parameters (u and k) for each wind direction and are summarized in Table 5.1 along with the probability of occurrence. An example of such a fit is provided in Figure 5.2, for wind direction WNW, which is 292.5 ° N.

Table 5.1: Wind direction, Weibull parameters (u and k) and probability of occurence for each wind direction.

Wind direction	u	k	Occurrence [%]
22.5 [NNE]	7.78	2.46	3.0
45 [NE]	7.87	2.57	4.0
67.5 [ENE]	7.84	2.40	5.9
90 [E]	6.63	2.06	6.1
112.5 [ESE]	5.02	1.73	5.3
135 [SE]	6.33	1.96	6.5
157.5 [SSE]	7.52	2.27	6.2
180 [S]	8.79	2.42	7.7
202.5 [SSW]	9.70	2.41	12.3
225 [SW]	10.05	2.25	13.6
247.5 [WSW]	10.48	2.10	11.3
270 [W]	9.63	1.83	6.0
292.5 [WNW]	9.16	1.82	4.1
315 [NW]	7.99	1.60	3.2
337.5 [NNW]	6.17	1.51	2.7
0 [N]	0.83	881	2.1

As described in Appendix C, only the dominant wind directions was used for the computation of the failure probability per case study to reduce computational time. These were 270°N for Culemborg, 247.5°N for Grebbedijk, and 225°N for the Duursche Waarden.

Another variable in common for all three case studies is the critical discharge because all case studies have wave heights lower than 1 m and it was assumed that their grass quality is similar, although this is not necessarily the case. The parameters used in this study for the critical discharge are found in Table 5.2.

Table 5.2: Parameters of the critical discharge used as reference in this study.

Variable	Symbol	Distribution	Parameters
Critical discharge [l/(s m)]	q_c	Log-normal	$\mu = 100, \sigma = 120$

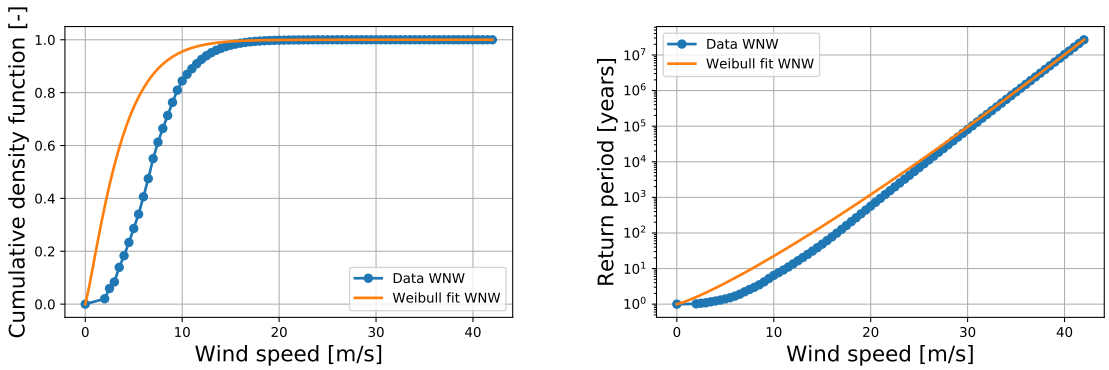

(a) (b)

Figure 5.2: Cumulative density function (a) and return period (b) of wind speed NWN fitted to the Weibull distribution.

5.1.2. Parameters for Z-function of internal erosion

For internal erosion, a few parameters are similar for all three case studies. Those are mainly model parameters such as the critical heave gradient, the model factor of uplift, etc., it also includes characteristics of water such as the kinematic viscosity. These parameters together with their distribution and value are found in Table 5.3.

Table 5.3: Parameters of the internal erosion variables that are taken as similar for all case studies.

Variable	Symbol	Distribution	Parameters
Bedding angle [rad]	θ	Deterministic	37
Critical heave gradient [-]	i_c	Log-normal	$\mu = 0.5, \sigma = 0.1$
Drag coefficient [-]	n	Deterministic	0.25
Hydraulic conductivity aquitard [m/s]	k_h	Log-normal	$\mu = 10^{-6}, \sigma = 5\,10^{-7}$
Kinematic viscosity of water [m^2/s]	ν	Deterministic	$1.33\,10^{-6}$
Model factor addressing the uncertainty in the critical head difference	m_u	Log-normal	$\mu = 1, \sigma = 0.1$
Model factor addressing the uncertainty in piping [-]	m_p	Log-normal	$\mu = 1, \sigma = 0.12$
Reference value of d70 [m]	$d70_m$	Deterministic	$2.08\,10^{-4}$
Volumetric weight of sand grains [kN/m^3]	γ_s	Deterministic	26.5
Volumetric weight of water [kN/m^3]	γ_w	Deterministic	10

5.2. Case study 1: Culemborg

The first case study, henceforth referred to as Culemborg, is dike trajectory 43-1, which is managed by the Water Board of Rivierenland and is located in the province of Gelderland along the river Lek. The water safety portal (in Dutch: "*Waterveiligheidsportaal*") website, which gives an overview of all the primary dikes in the Netherlands ("Vegetatiemonitor", n.d.), provides the safety standards for all primary dikes. For this case study, its required and maximum safety

standards are $1/30,000$ and $1/10,000$ respectively. The trajectory begins at the Amsterdam-Rijnkanaal and extends up to Fort Everdingen, reaching a length of 15.86 km. For this study, the section of interest goes from dike post BF095.50 to BF098.30 and is 280 m in length (see Figure 5.3).

Figure 5.3: Location of the section of interest in the dike segment Culemborg, screenshot from "*Hydra-nl*" of dike trajectory 43-1.

The same water levels were used for both failure mechanisms as it does not vary much along the section of interest. These were also extracted from the same software "*Hydra-nl*". Using the Testmodus functions, the empirical data could be extracted. The parameters set to find the data were:

- A trapezium representation of the peak water level with as minimum 750 m^3 and maximum 25,000 m^3.
- A maximum water velocity of 50 m/s.
- Includes model uncertainties suggested by the WBI2017.
- Prediction for the year 2050 with climate change of the KNMI scenario W.

The empirical data was fitted to a Gumbel distribution based on its mean and the standard deviation, which gave an overestimation of the water levels and thus the failure probability. However, this overestimation was needed in order to find a failure probability for overtopping/overflow, which was otherwise too small to be computed. This also reduced the computational time considerably, therefore, this assumption is considered acceptable as this study only looks at relative changes rather than assessing the dike section. The parameters of the Gumbel distribution used are 0.54 for the scale parameter and 4.3 for the location parameter. A representation of the fit is found in Figure 5.4. This figure shows that the fit gives indeed an overestimation of the water levels, for a water level of 7 m, the return period is approximately 5×10^2 according to the empirical data and approximately 10^2 according to the fitted Gumbel distribution. This explains why an overestimation of the failure probability is expected. As can be seen from the figure, the fit gets worse for higher water levels with a low probability of occurrence.

5.2.1. Parameters overtopping/overflow

The failure probability of overtopping/overflow for the section of interest is equal to the failure probability of the dominant cross-section, i.e. the one with the lowest crest height. To find it, a cross-section was extracted every 100 m of the section from ("*Actueel Hoogtebestand Nederland*" ("Actueel Hoogtebestand Netherland", n.d.)), which contains the elevation data of

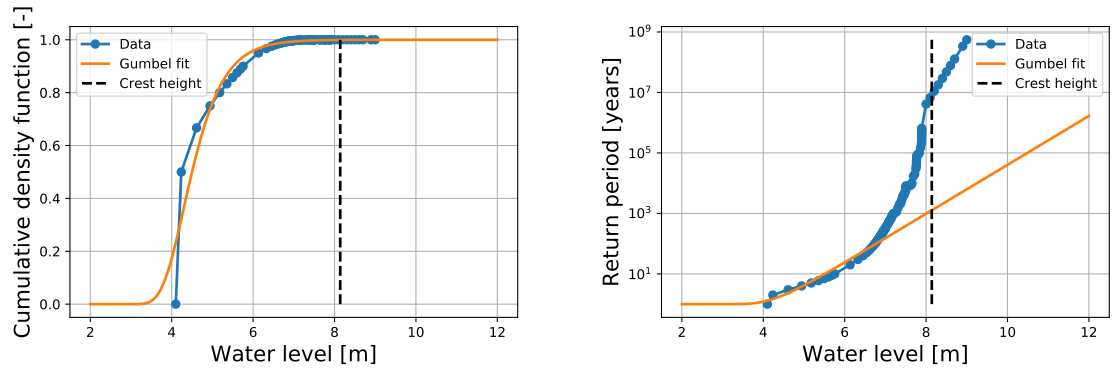

(a) (b)

Figure 5.4: Cumulative density function (a) and return period (b) of the water level in the section of interest of Culemborg.

the whole of the Netherlands. Once found, the geometric parameters for this case study could be found, see Table 5.4.

Table 5.4: Geometrical parameters of overtopping/overflow for the dominant cross-section of the Culemborg.

Variable	Symbol	Distribution	Parameters
Angle normal to dike [°N]	β	Deterministic	9
Bottom level [m+NAP]	h_b	Normal	$\mu = 2.35, \sigma = 0.3$
Crest height [m+NAP]	h_c	Deterministic	8.14
Outer slope [-]	α	Deterministic	1/3.1

Another case dependent parameter needed is the fetch of the dominant cross-section, which was extracted from "*Hydra-nl*", see Table 5.5.

To know if the dominant cross-section satisfies the safety standards, the computed failure probability needs to be lower than 2.4e-05, which is the required overtopping/overflow failure probability for a cross-section of this case study according to its safety standards, computed from Equation (2.2). The reliability index for this required failure probability is 4.06, found with Equation (4.5).

5.2.2. Parameters internal erosion

The failure probability of internal erosion for the section of interest is equal to the failure probability of the dominant cross-section,i.e. the one with the smallest dike width. To find it, a cross-section was extracted every 100 m of this section from "*AHN*" ("Actueel Hoogtebestand Netherland", n.d.). Once found, the geometric parameters for this case study could be found, see Table 5.6.

The geotechnical parameters were found from data provided by the water authority responsible and can be found in Table 5.7.

The computed failure probability of the dominant cross-section satisfies the safety standards, if its value is lower than 4.94e-07, which is the required internal erosion failure probability for a cross-section of this case study according to its safety standards, computed from Equation

Table 5.5: Fetch Culemborg for each wind direction.

Wind direction	F [m]
22.5 [NNE]	1196
45 [NE]	1564
67.5 [ENE]	1740
90 [E]	1496
112.5 [ESE]	811
135 [SE]	369
157.5 [SSE]	120
180 [S]	60
202.5 [SSW]	60
225 [SW]	88
247.5 [WSW]	375
270 [W]	1001
292.5 [WNW]	1424
315 [NW]	1542
337.5 [NNW]	1287
0 [N]	881

Table 5.6: Geometrical parameters of internal erosion corresponding to the dominant cross-section of Culemborg.

Variable	Symbol	Distribution	Parameters
Length of the effective foreshore [m]	L_f	Normal	$\mu = 20, \sigma = 2$
Width of the dike [m]	B	Deterministic	40

(2.2). The reliability index for this required failure probability is 4.89, found with Equation (4.5).

5.3. Case study 2: Grebbedijk

The second case study, referred to as the Grebbedijk, is dike trajectory 45-1, located in the province of Utrecht, it runs along the Neder-Rijn. Its safety standards, required and maximum, are $1/100,000$ and $1/30,0000$ respectively. It is managed by the water board Vallei en Veluwe, and it starts at Wageningen and ends near Heimerstein, reaching a length of approximately 5.35 km. The dike section of interest for the Grebbedijk is GR043-054, which is between the dike post 44 to 52, located at the end of the trajectory by Heimerstein (see Figure 5.5).

For this case study the same water levels were used for both failure mechanisms. The same software "*Hydra-nl*" was used to find the empirical data for the water level using the same settings as for Culemborg. The mean and the standard deviation of this empirical water level data were fitted to a Gumbel distribution, which is again expected to give a conservative estimate of the failure probability, its scale and location parameters are 0.63 and 8.44 respectively. The fit is presented in Figure 5.6.

Table 5.7: Geo-technical parameters for internal erosion corresponding to the dominant cross-section of Culemborg.

Variable	Symbol	Distribution	Parameters
70%-fractile of grain size distribution [m]	d70	Log-normal	$\mu = 2.8\,10^{-4}, \sigma = 4.2\,10^{-5}$
Aquifer thickness [m]	D	Log-normal	$\mu = 25, \sigma = 5$
Blanket thickness at the exit point (Lognormal) [m]	d	Log-normal	$\mu = 4.45, \sigma = 1.335$
Hinder land phreatic level [m+NAP]	h_p	Normal	$\mu = 3.5, \sigma = 0.1$
Hydraulic conductivity of the aquifer [m/s]	k	Log-normal	$\mu = 7.52\,10^{-4}, \sigma = 3.76\,10^{-4}$
Saturated volumetric weight of the blanket [kN/m^3]	γ_{sat}	Normal	$\mu = 14.45, \sigma = 0.7225$

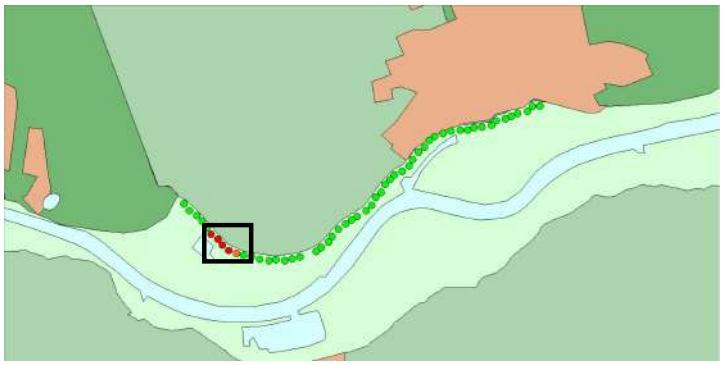

Figure 5.5: Location of the section of interest in the dike segment Grebbedijk, screenshot from "*Hydra-nl*" of dike trajectory 45-1.

5.3.1. Parameters overtopping/overflow

The geometrical parameters for the dominant cross-section of Grebbedijk's section of interest were found in the same way as for Culemborg and are found in Table 5.8. The fetch was extracted from "*Hydra-nl*" and is presented in Table 5.9.

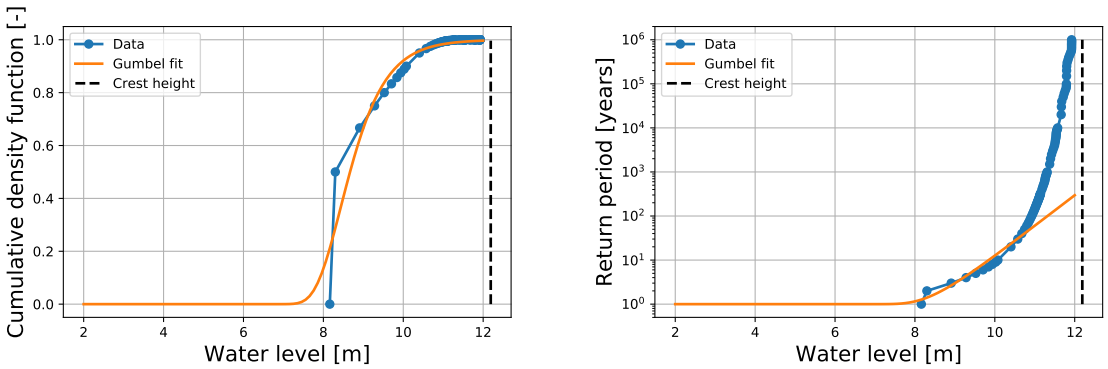

(a) (b)

Figure 5.6: Cumulative density function (a) and return period (b) of the water level in the section of interest of Grebbedijk.

Table 5.8: Geometrical parameters of overtopping/overflow for the dominant cross-section of the Grebbedijk.

Variable	Symbol	Distribution	Parameters
Angle normal to dike [°N]	β	Deterministic	208
Bottom level [m+NAP]	h_b	Normal	$\mu = 6.93, \sigma = 0.3$
Crest height [m+NAP]	h_c	Deterministic	12.19
Outer slope [-]	α	Deterministic	1/2.7

Table 5.9: Fetch Grebbedijk for each wind direction.

Wind direction	F [m]
22.5 [NNE]	71
45 [NE]	76
67.5 [ENE]	378
90 [E]	866
112.5 [ESE]	1310
135 [SE]	1553
157.5 [SSE]	1416
180 [S]	1210
202.5 [SSW]	1132
225 [SW]	1203
247.5 [WSW]	1387
270 [W]	1369
292.5 [WNW]	1127
315 [NW]	727
337.5 [NNW]	323
0 [N]	143

The computed failure probability of the dominant cross-section satisfies the safety standards, if its value is lower than 8e-06, which is the required overtopping/overflow failure probability for a cross-section of this case study according to its safety standards, computed from Equation

(2.2). The reliability index for this required failure probability is 4.31, found with Equation (4.5).

5.3.2. Parameters internal erosion

The geometrical parameters for the dominant cross-section of Grebbedijk's section of interest were found in the same way as for Culemborg and are found in Table 5.10. The geotechnical parameters were extracted from assessment reports of the water authority responsible and are found in Table 5.11.

Table 5.10: Geometrical parameters of internal erosion corresponding to the dominant cross-section of Grebbedijk.

Variable	Symbol	Distribution	Parameters
Length of the effective foreshore [m]	L_f	Normal	$\mu = 5, \sigma = 0.2$
Width of the dike [m]	B	Deterministic	29.5

Table 5.11: Geo-technical parameters of internal erosion corresponding to the dominant cross-section of Grebbedijk.

Variable	Symbol	Distribution	Parameters
70%-fractile of grain size distribution [m]	d70	Log-normal	$\mu = 3.07\,10^{-4}, \sigma = 4.61\,10^{-5}$
Aquifer thickness [m]	D	Log-normal	$\mu = 30, \sigma = 6$
Blanket thickness at the exit point (Lognormal) [m]	d	Log-normal	$\mu = 2, \sigma = 0.6$
Hinder land phreatic level [m+NAP]	h_p	Normal	$\mu = 7, \sigma = 0.1$
Hydraulic conductivity of the aquifer [m/s]	k	Log-normal	$\mu = 5.89\,10^{-4}, \sigma = 2.95\,10^{-4}$
Saturated volumetric weight of the blanket [kN/m^3]	γ_{sat}	Normal	$\mu = 17.6, \sigma = 0.88$

The computed failure probability of the dominant cross-section satisfies the safety standards, if its value is lower than 4.69e-07, which is the required internal erosion failure probability for a cross-section of this case study according to its safety standards, computed from Equation (2.2). The reliability index for this required failure probability is 4.90, found with Equation (4.5).

5.4. Case study 3: Duursche Waarden

Finally, the last case study, the Duursche Waarden, is dike trajectory 53-2, which is managed by the water authority Waterschap Drents Overijsselse Delta. Its safety standards, required and maximum, are $1/10,000$ and $1/3,000$ respectivel. It is situated in the province of Overijssel, along the Ijssel river, starting above Molenbelt and ending near Zwolle with a total length of approximately 28.9 km. Finally, for the Duursche Waarden, the dike section of interest is

between the 26.1 km and 27.5 km of the trajectory, in front of a protected nature area called the Duursche Waarden, which is part of Natura 2000 (*Beheerplan Natura 2000 Rijntakken (038)*, 2018) (see Figure 5.7).

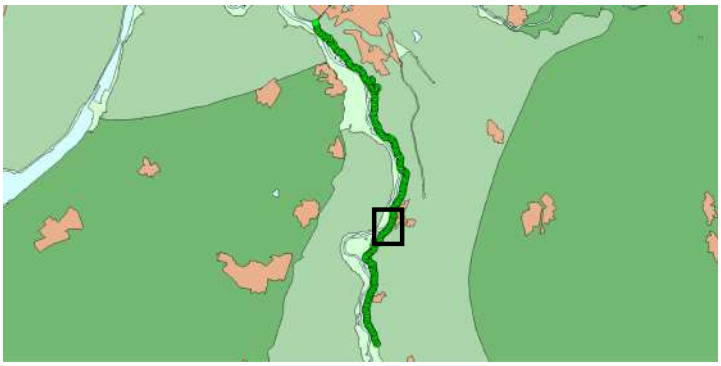

Figure 5.7: Location of the section of interest in the dike segment Duursche Waarden, screenshot from "*Hydra-nl*" of dike trajectory 53-2.

For this case study the same water levels were used for both failure mechanisms. The same software "*Hydra-nl*" was used to find the empirical data for the water level using the same settings as for Culemborg. The mean and the standard deviation of this empirical water level data were fitted to a Gumbel distribution, which is again expected to give a conservative estimate of the failure probability, its scale and location parameters are 0.3 and 3.9 respectively. The fit is presented in Figure 5.8.

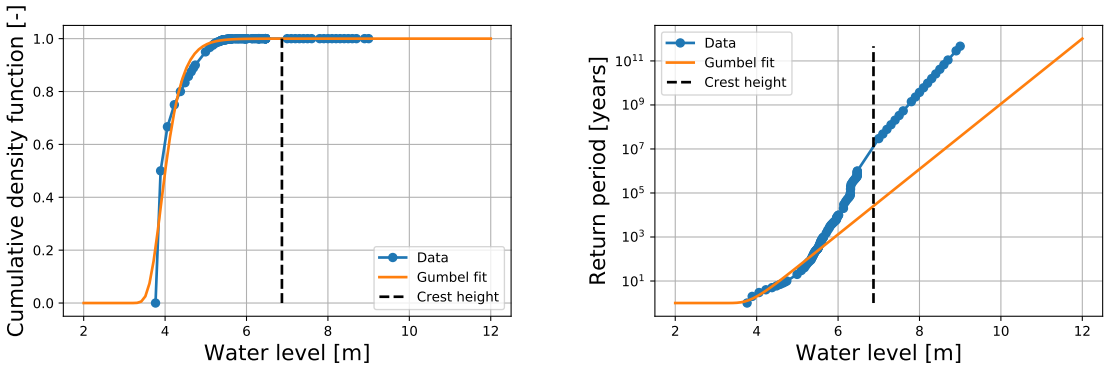

(a) (b)

Figure 5.8: Cumulative density function (a) and return period (b) of the water level in the section of interest of Duursche Waarden.

5.4.1. Parameters overtopping/overflow

The geometrical parameters for the dominant cross-section of Duursche Waarden's section of interest were found in the same way as for Culemborg and are found in Table 5.12. The fetch was extracted from "*Hydra-nl*" and is presented in Table 5.13.

Table 5.12: Geometrical parameters of overtopping/overflow for the dominant cross-section of the Duursche Waarden.

Variable	Symbol	Distribution	Parameters
Angle normal to dike [°N]	β	Deterministic	296
Bottom level [m+NAP]	h_b	Normal	$\mu = 2.21, \sigma = 0.3$
Crest height [m+NAP]	h_c	Deterministic	6.87
Outer slope [-]	α	Deterministic	1/2.8

Table 5.13: Fetch Duursche Waarden for each wind direction.

Wind direction	F [m]
22.5 [NNE]	1186
45 [NE]	511
67.5 [ENE]	139
90 [E]	66
112.5 [ESE]	52
135 [SE]	54
157.5 [SSE]	75
180 [S]	525
202.5 [SSW]	911
225 [SW]	1115
247.5 [WSW]	1089
270 [W]	728
292.5 [WNW]	657
315 [NW]	1106
337.5 [NNW]	1488
0 [N]	1512

The computed failure probability of the dominant cross-section satisfies the safety standards, if its value is lower than 8e-05, which is the required overtopping/overflow failure probability for a cross-section of this case study according to its safety standards, computed from Equation (2.2). The reliability index for this required failure probability is 3.77, found with Equation (4.5).

5.4.2. Parameters internal erosion

The geometrical parameters for the dominant cross-section of Grebbedijk's section of interest were found in the same way as for Culemborg and are found in Table 5.14. The geotechnical parameters were extracted from assessment reports of the water authority responsible and are found in Table 5.15.

Table 5.14: Geometrical parameters of internal erosion corresponding to the dominant cross-section of Duursche Waarden.

Variable	Symbol	Distribution	Parameters
Length of the effective foreshore [m]	L_f	Normal	$\mu = 20, \sigma = 2$
Width of the dike [m]	B	Deterministic	44

Table 5.15: Geo-technical parameters of internal erosion corresponding to the dominant cross-section of Duursche Waarden.

Variable	Symbol	Distribution	Parameters
70%-fractile of grain size distribution [m]	d70	Log-normal	$\mu = 3.53\,10^{-4}, \sigma = 5.3\,10^{-5}$
Aquifer thickness [m]	D	Log-normal	$\mu = 30, \sigma = 6$
Blanket thickness at the exit point (Lognormal) [m]	d	Log-normal	$\mu = 2.5, \sigma = 0.75$
Hinder land phreatic level [m+NAP]	h_p	Normal	$\mu = 1.5, \sigma = 0.1$
Hydraulic conductivity of the aquifer [m/s]	k	Log-normal	$\mu = 2.89\,10^{-4}, \sigma = 1.45\,10^{-4}$
Saturated volumetric weight of the blanket [kN/m^3]	γ_{sat}	Normal	$\mu = 16, \sigma = 0.8$

The computed failure probability of the dominant cross-section satisfies the safety standards, if its value is lower than 9.12e-07, which is the required internal erosion failure probability for a cross-section of this case study according to its safety standards, computed from Equation (2.2). The reliability index for this required failure probability is 4.77, found with Equation (4.5).

5.5. Vegetation on the section of the case studies

5.5.1. Allowed vegetation

The vegetation on the dike trajectories was found with the tool "*Vegetatielegger*" in the website "*Vegetatiemonitor2.0*" ("Vegetatiemonitor", n.d.), which is a map showing the vegetation allowed on the floodplains of major Dutch Rivers. This type of vegetation does not impede water flow in the river. It was created by Rijkswaterstaat and Deltares. The "*vegetatielegger*" divides vegetation into different classes:

- "*Gras en akker*": homogeneous grassland and meadow, represented in light green.
- "*Riet en ruigte*": homogeneous reed bed and brushwood, represented in purple.
- "*Bos*": homogeneous forest, represented in dark green.
- "*Struweel*": homogeneous bush, represented in orange.
- "*Mengklasse 90/10*": mixture 90/10, consists of grassland and meadow, reed bed and brushwood, bushes and/or forest. These areas are naturally grazed grasslands with a maximum of 10% bush, forest, and/or reed bed/brushwood. These areas are represented in the lightest yellow.

- "*Mengklasse 70/30*": mixture 70/30, consists of grassland and meadow, reed bed and brushwood, bushes and/or forest. These areas are naturally grazed grasslands with more than 40% grass and meadow and a maximum of 30% bush and/or forest. These areas are represented in the medium yellow.
- "*Mengklasse 50/50*": mixture 50/50, consists of grassland and meadow, reed bed and brushwood, bushes and/or forest. These areas are naturally grazed grasslands with more than 20% grass and meadow and a maximum of 50% bush and/or forest. These areas are represented in the darkest yellow.

Culemborg

Figure 5.9, shows the vegetation allowed on the dike section at Culemborg according to the Dutch norm. Two vegetation types can be found: Grassland/meadows and reed bed/brushwood. The vegetation in front of the dike does not look dense enough and wide enough to reduce the wave height or to affect the water levels locally. The outer and inner slopes are both covered with a grass revetment and there is a road on the crest of the dike.

Figure 5.9: Vegetation allowed near the dike trajectory by the Culemborg according to the "*vegetatielegger*".

Grebbedijk

The Grebbedijk contains on its floodplain mainly the mixture class 70/30 (see Figure 5.10). Furthermore, the dike revetment is covered with grass. There is a Natura 2000 area on the floodplain, which could act as a source for wave height reduction.

Figure 5.10: Vegetation allowed near the dike trajectory by the Grebbedijk according to the "*vegetatielegger*".

Duursche Waarden

The section by the Duursche Waarden has many classes of vegetation on its floodplain (see Figure 5.11), which are: forest, reed bed/brushwood, and all three mixture classes. Also, here wave reduction due to vegetation is expected. The revetment is here again made of grass.

5.5.2. Current vegetation

Now the current vegetation according to google street map was assessed.

Figure 5.11: Vegetation allowed near the dike trajectory by the Duursche Waarden according to the "*vegetatielegger*".

Culemborg

In the dike section of Culemborg, a relatively wide floodplain with low vegetation can be observed, see Figure 5.12(b). Mostly grass and reeds are present. There are some trees scattered on the hinterland very close to the toe, see Figure 5.12(a). There does not seem to be much vegetation on the floodplain to reduce the wave height, but for the location on the picture it seems enough space to potentially add some vegetation that could. Furthermore, there are many houses very close to the toe of the dike.

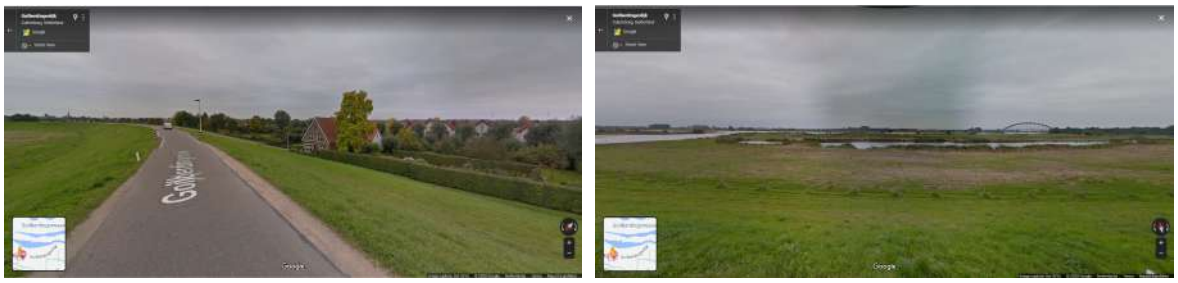

(a) (b)

Figure 5.12: Vegetation seen from googlemaps street view on the floodplain and the hinterland of the Culemborg case study.

Grebbedijk

For the Grebbedijk, quite some vegetation on the hinterland and floodplains could be observed, see Figure 5.13. These vegetations are scattered across the floodplain and in the hinterland, where some areas are densely populated with trees. The floodplain seems wider than for Culemborg.

(a) (b)

Figure 5.13: Vegetation seen from googlemaps street view on the floodplain and the hinterland of the Grebbedijk case study.

Duursche Waarden

The dike section of the Duursche Waarden, see Figure 5.14, is similar to the Grebbedijk. The floodplains seem even larger and more densely populated with trees and other large vegetation.

(a) (b)

Figure 5.14: Vegetation seen from googlemaps street view on the floodplain and the hinterland of the Duursche Waarden case study.

Officially, considering the safety assessment, all three case studies should have as only vegetation type: grass on their inner and outer slopes. However, it can be seen that this is not the case. Even though none of the three case studies officially account for vegetation near or on their dikes, except for grass on both slopes, all do have vegetation. Some of which could potentially influence the failure probability. Notably, if large and dense vegetation is present on some part of the foreshore, as was observed for the Grebbedijk and the Duursche Waarden, vegetation is expected to have an impact on the failure probability. How much different quantities of vegetation effects, depending on the types, densities, and locations of vegetation, could affect these case studies is explained in more detail in Chapter 6.

6

Results and discussions

As was suggested in Chapter 4, a study of the individual effects was first made for each failure mechanism considering all three case studies, see Section 6.1. This allowed to filter out the marginal effects in order to reduce the computational time of the BBN. Once the results were known, the most relevant vegetation parameters were used to create the framework for each case study. The results of the BBN for Duursche Waarden are presented in Section 6.2; results for the other case studies are included in Appendices G and H.

6.1. Individual effects on a failure mechanism

To find the dominant vegetation effects of each case study for both failure mechanisms individually a MC analysis is conducted. The results are normalized based on the failure probability and beta value without vegetation, see Equations (4.6) and (4.7) respectively. Two graphs are presented for each vegetation effect (Figure 6.1 to 6.4), the left one shows the normalized probability on the y-axis, while the right one presents the normalized beta value. The x-axes of both graphs represent a vegetation parameter. The changes in beta value are usually less significant than the changes in failure probability. Therefore, the y-axes of both graphs have different scales. A detailed analysis of the scenario without vegetation for all case studies can be found in Appendix D.

6.1.1. Overtopping/overflow

As mentioned in Chapter 3, four of the five vegetation effects had an impact on the failure mechanism overtopping/overflow. Each effect has an impact on one parameter. Therefore, to quantify each effect on the failure probability, these parameters were modified individually according to their respective g functions and vegetation parameter as presented in Section 3.3. To simulate different quantities of vegetation, five or six values were chosen for each vegetation parameter.

The overtopping/overflow failure probabilities are based on the load due to wind waves, the parameters of which were found with the equations of Young and Verhagen (1996) (Young and Verhagen, 1996), see Appendix B. Due to the limited fetch at the cross-section of interest for all case studies considering the dominant wind direction, the mean wave heights are very low, all below 0.1 m, see Table 6.1.

Table 6.1: Mean and maximum wave height for all case studies at the dominant wind direction.

	Culemborg	Grebbedijk	Duursche Waarden
Dominant wind direction [°N]	270	247.5	225
Mean wave height [m]	8.6×10^{-2}	9.0×10^{-2}	7.2×10^{-2}
Maximum wave height [m]	8.4×10^{-1}	8.8×10^{-1}	9.4×10^{-1}

The required failure probabilities for overtopping/overflow (considering a cross-section as explained in Chapter 5) can be found in Table 6.2 together with the actual failure probability and beta value without vegetation. It can be deduced that none of the case studies satisfies the requirements, i.e. all actual failure probabilities without vegetation are much higher than the required ones. Due to the large difference between the two, it is expected that even the most positive vegetation effects cannot make the case studies satisfy their safety standards. These high failure probabilities are partly due to the conservative Gumbel parameters used of the water levels during the computations. Nevertheless, it is still relevant to study the magnitude of each vegetation effect.

Table 6.2: Failure probability (P_f) and beta value (β) for overtopping/overflow without considering vegetation effects for each case study, and required failure probability (P_{req}) and beta value (β_{req}) for overtopping/overflow considering one cross-section.

	Culemborg	Grebbedijk	Duursche Waarden
P_f	6.1×10^{-4}	1.9×10^{-3}	2.56×10^{-5}
β	3.23	2.89	4.04
P_{req} [-]	2.4×10^{-5}	8×10^{-6}	8×10^{-5}
β_{req} [-]	4.06	4.31	3.775

The first vegetation effect studied is an increase in water level due to extra woody vegetation, reed bed, and/or scrubs added to the already existing vegetation on the floodplain or foreshore of the dike. This effect influences the water level parameter and was modeled by increasing it by a constant value of up to 0.1 m, see Equation (3.7). The results are shown in Figure 6.1, where it can be observed that a change of 0.1 m has a strong negative impact on the failure probability. The case study the most affected by this increase is the Duursche Waarden, its failure probability increases by approximately 50% reaching a value of 3.79×10^{-5} and its beta value is reduced by 2% to a value of 3.96.

The second effect considers a change in erosion resistance due to herbaceous vegetation on the inner slope of the dike. This effect influences the critical discharge parameter and was modeled by increasing or decreasing the mean value by 20%, see Equation (3.8). Two sets of parameters suggested by the WBI2017 were used. The first set corresponds to worse grass quality (with a mean of 100 l/(s m) and a standard deviation of 120 l/(s m)), it was used as a reference. The second set corresponds to good grass quality (with a mean of 225 l/(s m) and a standard deviation of 250 l/(s m)). Figure 6.2 shows that all three case studies react strongly and similarly to a change in mean critical discharge. Having a good grass quality instead of a worse one, leads to approximately 28% lower failure probability for the Duursche Waarden, with a value of 1.90×10^{-5}. For this case study, with worse grass quality, increasing and decreasing its mean value by 20% leads to 5% lower and 10% higher failure probability, values of 2.43×10^{-5} and 2.83×10^{-5}, respectively. With good grass quality it leads to 14%

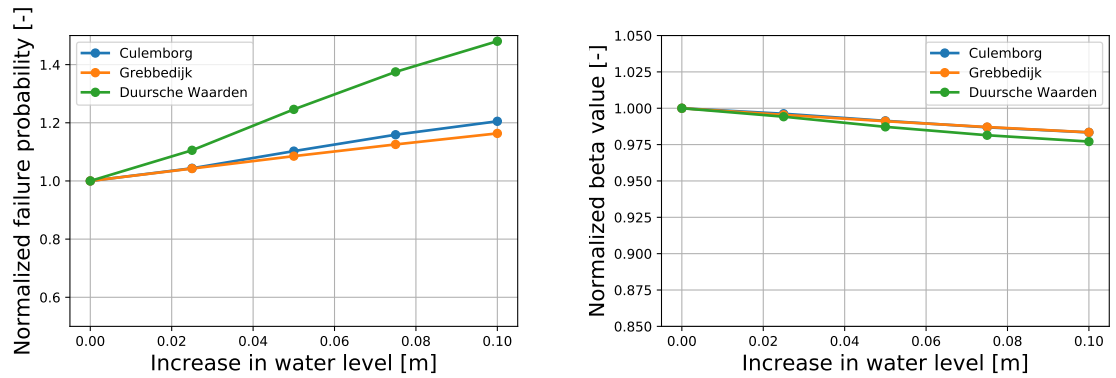

(a) (b)

Figure 6.1: Quantitative effect of the water level on the overtopping/overflow failure probability for all case studies. It can be observed that a slight increase in this parameter leads to high changes in failure probability and beta value.

lower and 4.2% higher failure probability, values of 1.82×10^{-5} and 2.17×10^{-5} respectively. The changes in beta values concerning the first set of parameters roughly varies from -0.5% to 2%.

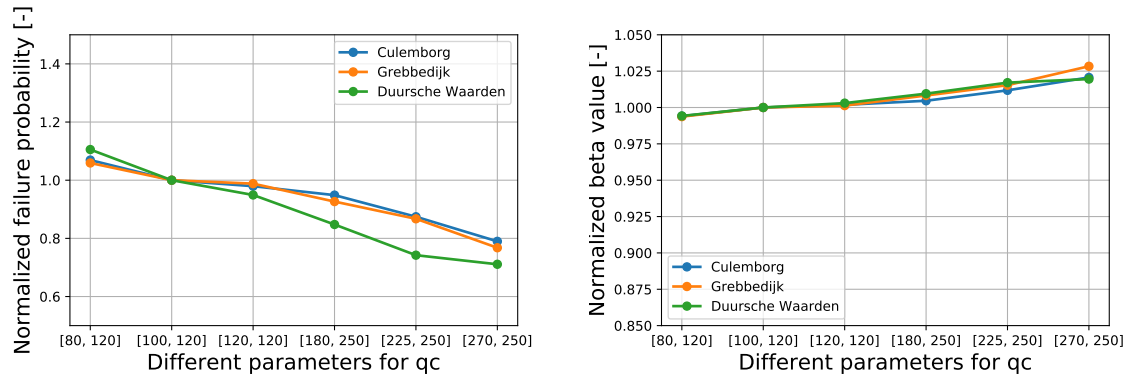

(a) (b)

Figure 6.2: Quantitative effect of the critical discharge on the overtopping/overflow failure probability for all case studies. It can be observed that a slight increase in this parameter leads to high changes in failure probability and beta value.

The third effect accounts for a decrease in wave height due to woody vegetation, reed beds, and/or scrubs on the foreshore of the dike's dominant cross-section (see Figure 6.3). This has an impact on the wave height parameter computed with the Young and Verhagen equations (Young and Verhagen, 1996), which was modeled by reducing the calculated wave height parameter, see Equation (3.9). Reductions up to 80% were simulated which decreased the failure probability by roughly 1% for the Duursche Waarden, and even less for the two other case studies. No changes in beta values were observed. This marginal effect (usually known to be efficient) is not efficient here due to the extremely low initial wave heights in each case study, which causes all three systems to be overflow dominant.

The last effect studied for overtopping/overflow is a change in roughness of the outer slope due to the presence of herbaceous vegetation. This effect had an impact on the roughness factor

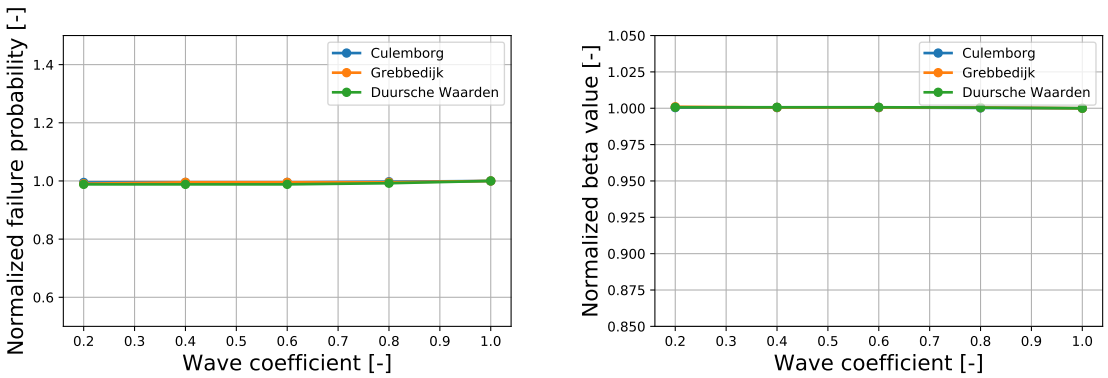

(a) (b)

Figure 6.3: Quantitative effect of the wave height on the overtopping/overflow failure probability for all case studies. It can be observed that an increase in this parameter leads to very marginal changes in failure probability and beta value.

which was modified to a lower value (up to 0.8) to simulate an increase in roughness, see Equation (3.10). The results in Figure 6.4 show no impact due to a change in roughness factor. This is again due to the very low initial wave heights that make the three case studies overflow dominant, i.e. failure is predominantly due to overflow, therefore, the roughness of the outer slope is not relevant as it is submerged.

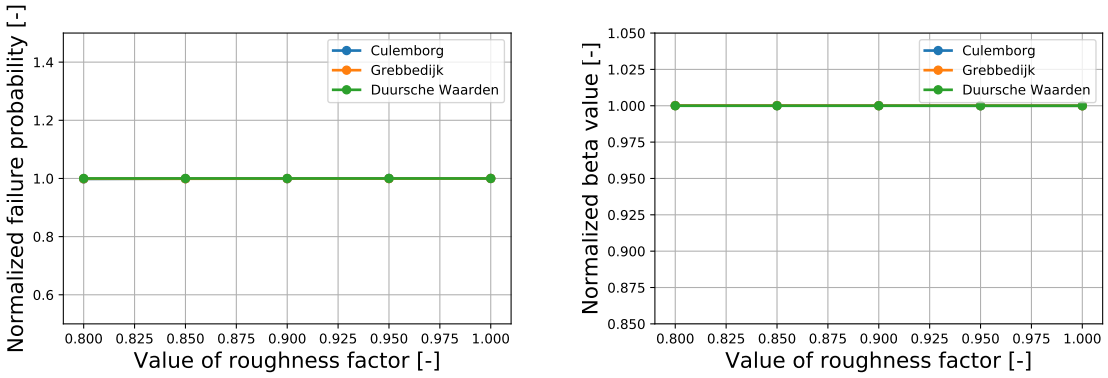

(a) (b)

Figure 6.4: Quantitative effect the roughness factor on the overtopping/overflow failure probability for all case studies. It can be observed that an increase in this parameter does not lead to changes in failure probability and beta value.

From these graphs, it can be concluded that:

- Any changes in the water level and the critical discharge can lead to significant changes in the failure probability of overtopping/overflow. For the Duursche Waarden, an increase in failure probability of up to 50% was observed with a 0.1 m increase in water level, and a reduction of about 28% was estimated with better grass quality. Therefore, any vegetation leading to changes in those two parameters should be considered with care in the assessment process.
- In comparison, the changes regarding the wave height are marginal, so only small variations are expected when accounting for them in the assessment of overtopping/overflow for these particular case studies.

- Lastly, the roughness factor in the outer slope has an even more negligible contribution and was, therefore, ignored in the creation of the framework for this study.

A more detailed sensitivity analysis of these parameters on overtopping/overflow can be found in Appendix E.

6.1.2. Internal erosion

Two of the five effects of vegetation had an impact on the failure mechanism of internal erosion. The first, increase in water level, influences one parameter. The second one, the effect of a tree toppling over on the hinterland, has an impact on three parameters of the limit state functions of the three sub-mechanisms. Therefore, to quantify both effects on the failure probability, these parameters were modified individually according to their respective g function(s) and vegetation parameter(s) as presented in Section 3.3. To simulate different types and quantities of vegetation, five different values were chosen for each of the vegetation parameters.

Results are presented in terms of normalized failure probability and beta value with respect to the case without vegetation. For internal erosion, the failure probability and beta value without vegetation for all case studies can be found in Table 6.3. From Chapter 5, the required failure probabilities for internal erosion considering a cross-section were added to the table. It can be deduced that none of the case studies satisfies the requirements, i.e. all computed failure probabilities without vegetation are much higher. Here again the most positive effects of vegetation cannot make the cross-sections of each case study satisfy their safety standards. It is, however, still relevant to study how each is affected by vegetation.

Table 6.3: Failure probability (P_f) and beta value (β) for internal erosion without considering vegetation effects for each case study, and required failure probability (P_{req}) and beta value (β_{req}) for overtopping/overflow considering one cross-section.

	Culemborg	Grebbedijk	Duursche Waarden
P_f	3.27×10^{-3}	1.76×10^{-1}	2.24×10^{-3}
β	2.72	0.93	2.83
P_{req} [-]	4.94×10^{-7}	4.69×10^{-7}	9.12×10^{-7}
β_{req} [-]	4.89	4.90	4.77

The increase in water level due to extra woody vegetation, reed bed, and/or scrubs added to the already existing vegetation on the floodplain or foreshore of the dike influences the water level parameter and was modeled by increasing it by a constant of up to 0.1 m, as in the previous section see Equation (3.7). The results are shown in Figure 6.5, where it is observed that the Duursche Waarden is the most affected when looking at the normalized failure probability and that Grebbedijk is the most affected when looking at the normalized beta value. This higher change in the beta value for Grebbedijk is due to its initial relatively high failure probability without vegetation, which means that any small changes leads to high changes in beta value compared to the Duursche Waarden which has an approximately one hundred times lower initial failure probability without vegetation. Considering the Duursche Waarden, a constant increase in water level of 0.1 m has a strong negative impact on the failure probability of internal erosion which now increases by approximately 40%, reaching a value of 3.26×10^{-3}. The beta value also decreases by approximately 4% for this case study, reaching a value of 2.72. For the Grebbedijk, a constant increase of 0.1 m leads to a failure probability of 2.02×10^{-1}, only

approximately 15% higher than the initial case without an increase and a beta value of 0.83, which is approximately 10% lower than the case without vegetation.

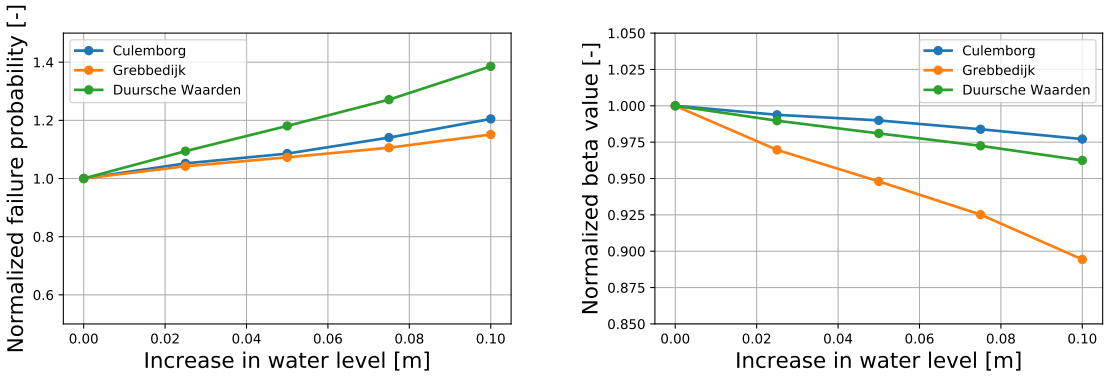

(a) (b)

Figure 6.5: Quantitative effect of the water level on the internal erosion failure probability for all case studies. It can be observed that a slight increase in this parameter leads to high changes in failure probability and beta value.

The second effect only occurs on the condition that a tree topples over on the hinterland. Therefore, the probability that a tree topples over needs to be taken into account as explained in Section 4.3.2, see Equation (4.8). It was assumed that a tree toppling over has a probability of occurrence of 1%. This effect was modeled using the vegetation parameters loc (location of the exit point) and C_d (local blanket thickness).

The change in location of the exit point influences the piezometric head at the exit point and the seepage length, see Equations (3.13) and (3.12) respectively. The corresponding results due to these two changes are shown in Figure 6.6, where it is observed that no changes in failure probability and beta value occur. The same study was made increasing the probability of a tree toppling to a value of 5%, similar results were found.

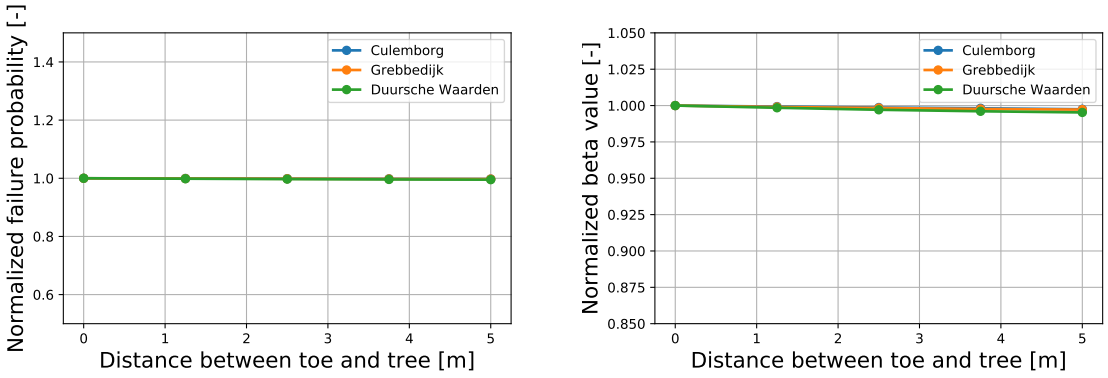

(a) (b)

Figure 6.6: Quantitative effect of the location of the exit point on the internal erosion failure probability for all case studies now including the probability of a tree toppling over. It can be observed that an increase in the distance between toe and tree has no effect on the normalized failure probability and beta value.

The effect of a local decrease in blanket thickness was modeled by decreasing its original thickness by a percentage, see Equation (3.11). The results are presented in Figure 6.7, which again shows a negligible change. This is due to the same reason mentioned above, i.e. there

is a low probability of a tree toppling over. It can also be explained because internal erosion, as mentioned in Chapter 2, is a fully dependent system, i.e. the failure probability is equal to the sub-mechanism with the lowest value. In this case, the dominant sub-mechanism is piping, which is the only one not affected by a local decrease in blanket thickness. Thus, mathematically, if the dominant sub-mechanism is not impacted by the effect, the whole failure mechanism internal erosion is not impacted.

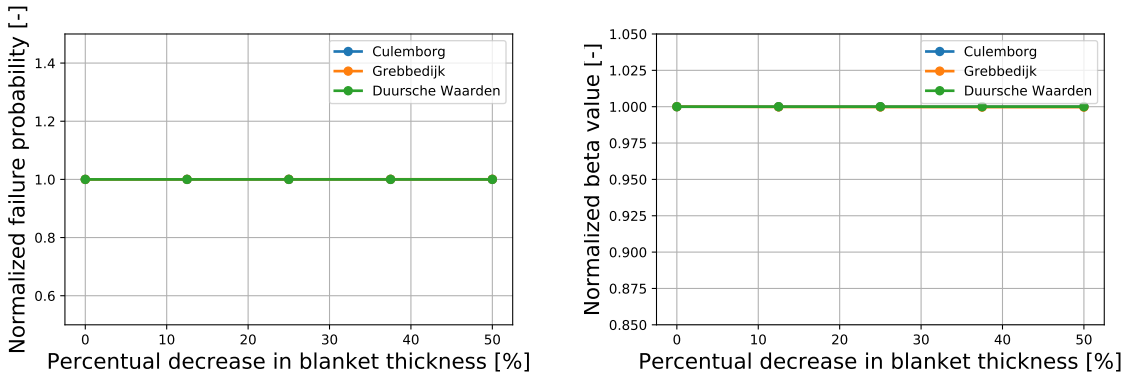

(a) (b)

Figure 6.7: Quantitative effect of the decrease in local blanket thickness on the internal erosion failure probability for all case studies. It can be observed that a decrease in this parameter leads to no changes in failure probability and beta value.

From these results, it can be concluded that:

- The increase in water level is the only effect that has a high impact on the failure probability of internal erosion.
- The effects of a tree toppling over are marginal. For a change in exit point location (loc), this is due to the low probability that a tree topples over. For the local decrease in local blanket thickness (C_d) the effect is marginal also because it does not affect the piping sub-mechanism, i.e. if the system is piping dominant it does not have an impact on the failure probability of internal erosion. Therefore, in the construction of the framework, the parameter of decrease in local blanket thickness was disregarded.

A more detailed sensitivity analysis of these parameters on internal erosion can be found in Appendix F.

6.2. Results of the framework Duursche Waarden

This section presents the results of the framework corresponding to the Duursche Waarden case study. The results of the other two case studies (Culemborg and Grebbedijk) are gathered in Appendices G and H for brevity reasons. The Duursche Waarden was selected as a representative example due to the stronger influence of the vegetation effects, whereas the two other case studies showed similar but milder reactions.

The framework created for the case study the Duursche Waarden has four root nodes, each representing a different vegetation parameter. Figure 6.8 shows its graphical representation. The vegetation parameters representing an increase in roughness of the outer slope ($C_{\gamma f}$) and for a local decrease in blanket thickness (C_d) were not considered to due to their marginal

effects as found in Section 6.1. For an explanation of its construction and structure, see Chapter 4.

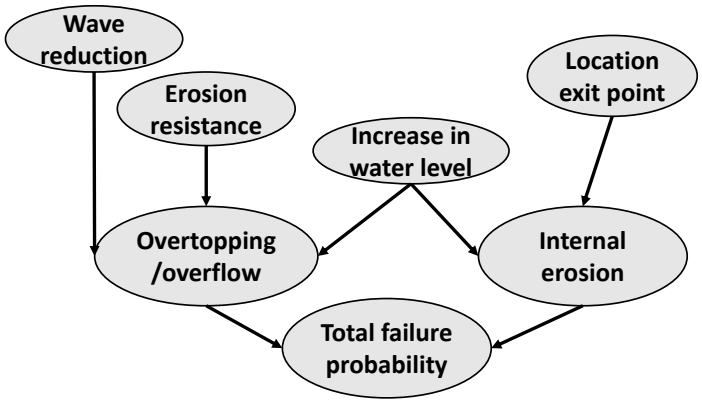

Figure 6.8: BBN considering both failure mechanisms and vegetation effects constructed for the Duursche Waarden case study.

The framework was used to analyse the impact of combined vegetation effects on the failure probability. Heat maps are used to present the results, the x and y axes represent a different vegetation parameter whereas the color depicts the normalized failure probability (left graphs) and the normalized beta value (right graphs), see Section 4.3.2. The normalization is now conducted with respect to the total failure probability of the Duursche Waarden's cross-section of interest without vegetation, which was estimated to be 2.42×10^{-3}. The beta values are normalized by the total beta value without vegetation which is approximately 2.82 for this case study. The internal erosion failure mechanism is dominant in this case study, i.e. its failure probability is approximately one hundred times higher than the one for overtopping/overflow.

Figure 6.9 shows the impact on the total failure probability of both an increase in water level and a change in mean critical discharge. From this figure, it can be observed that the increase in water level is the dominant effect. An increase in water levels of 0.1 m can lead to up to 38% increase in the total failure probability (value of 3.3×10^{-3}) and 3.7% decrease in beta values (reaching 2.71), i.e. slightly lower values than when considering only internal erosion and much lower than when only overtopping/overflow was considered. The effect of a change in mean critical discharge is no longer as relevant as when it was considered for only overtopping/overflow (see Section 6.1.1), i.e. changes of up to 0.4% in failure probability can be observed and only 0.1% for changes in beta values.

Looking at the effects of wave height reduction and increase in water level (see Figure 6.10) it is observed that the increase in water level is the dominant effect with the wave coefficient showing no impact on the total failure probability or total beta value.

When comparing the change in exit point location and the increase in water level (see Figure 6.11), it is noticed that the increase in water level has again a dominant impact on the total failure probability and the beta value.

Considering only the change in exit point in Figure 6.11, it is observed that the failure probability for an exit point located 5 m away from the toe is always marginally lower than when located at the toe of the dike. This suggests that a tree toppling over has a positive impact on the failure probability. However, this cannot be true as a tree toppling over does not increase

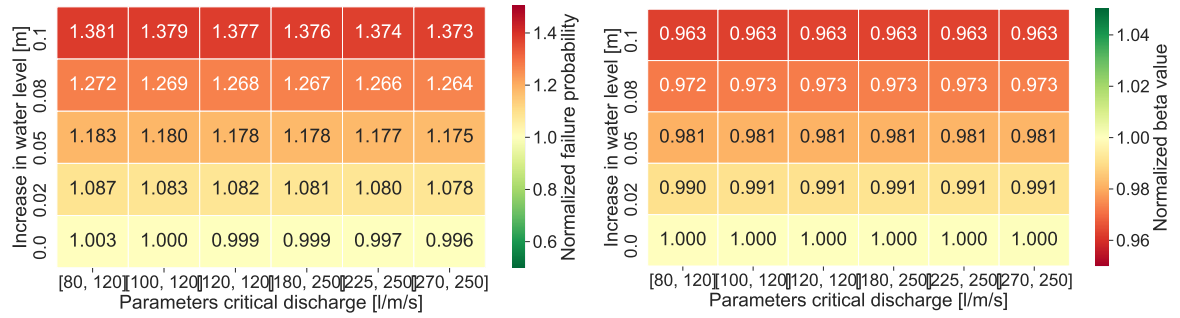

(a) (b)

Figure 6.9: Quantitative effect of the increase in water level and change in mean critical discharge on the total failure probability (a) and normalized beta value (b) for the Duursche Waarden. It can be observed that an increase in water level is the dominant effect when considering both failure mechanisms.

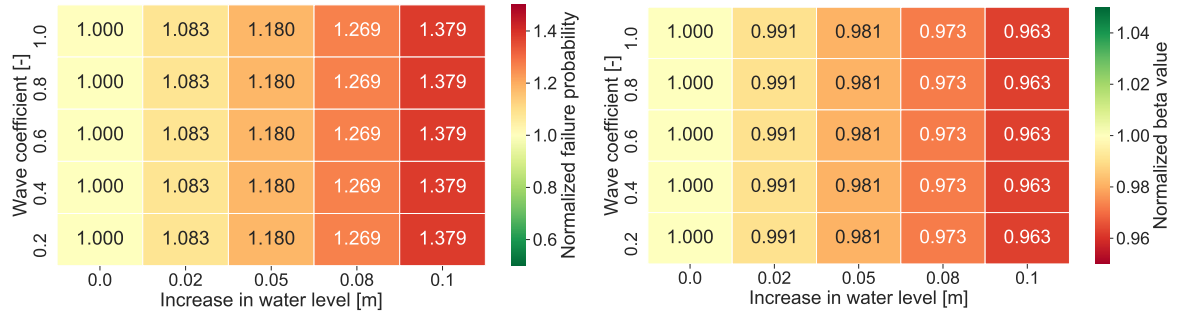

(a) (b)

Figure 6.10: Quantitative effect of the decrease in wave height and increase in water level on the total failure probability (a) and normalized beta value (b) for the Duursche Waarden. It can be observed that an increase in water level is the dominant effect and that the decrease in wave height has no impact when considering both failure mechanisms.

the strength or decrease the load of the dike. This phenomena can be explained because the location of the exit point for the reference scenario (without vegetation) is located at the toe of the dike. Therefore, any tree toppling over further away creates an exit point more distant to the toe, i.e. it has a positive impact on the failure probability and beta value. As such, it should be concluded that any tree located further away then the original exit point without vegetation should not be considered.

In this case study the exit point location without vegetation is at the toe of the dike. Therefore, all trees toppling over further away from the toe have a positive impact on the failure probability and should be, therefore, ignored. Hence, all graphs showing the impact of change in exit point (combined with the wave reduction or changes in mean critical discharge) are discarded as similar conclusions can be drawn.

The last heat map shows the combined effect of wave reduction effect and a change in mean critical discharge. Here again, it can be seen that the wave reduction effect has no impact on the total failure probability. The change in mean critical discharge shows again marginal effects up to 4% decrease in failure probability (value of 2.41×10^{-3}) but this time no changes in beta value. The lower impact of changes in beta value for different mean critical discharges compared to changes in water levels in Figure 6.9 is because water levels can increase the

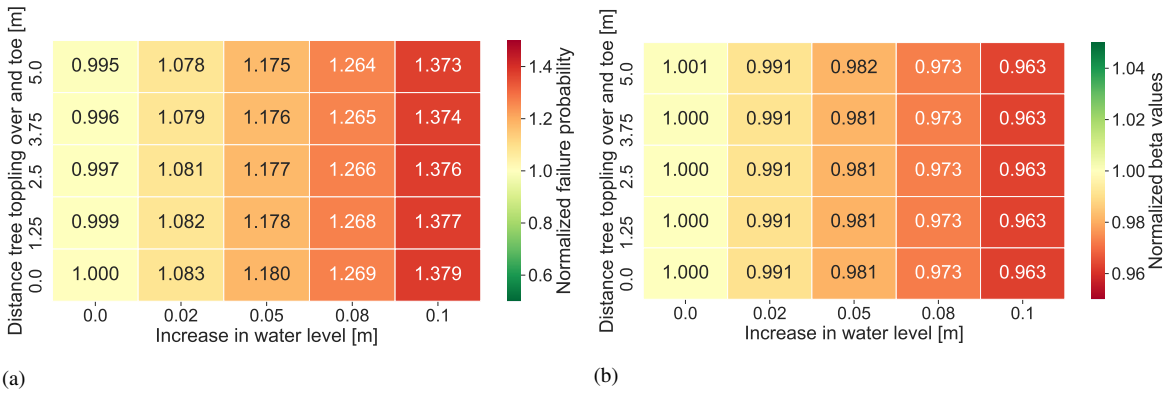

Figure 6.11: Quantitative effect of the change in exit point location and increase in water level on the total failure probability (a) and normalized beta value (b) for the Duursche Waarden. It can be observed that an increase in water level is the dominant effect and that the change in exit point location has a marginal impact when considering both failure mechanisms.

importance of the critical discharge whereas WC has no impact.

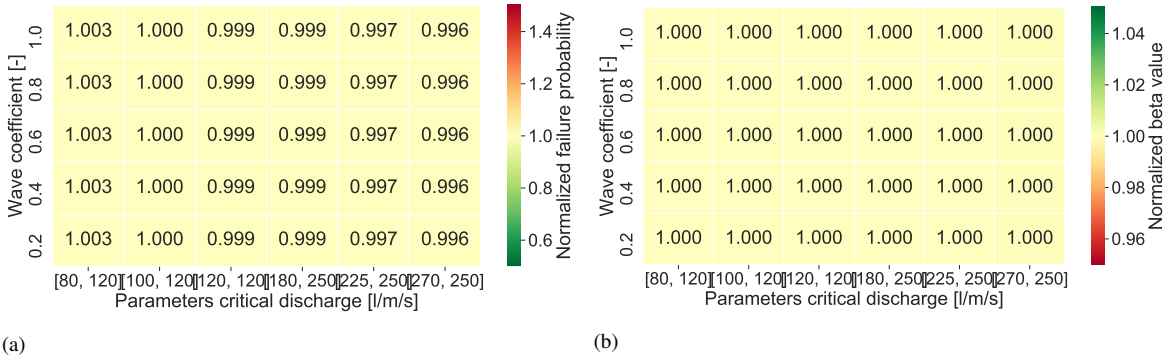

Figure 6.12: Quantitative effect of the reduction of wave height and the change in mean critical discharge on the total failure probability (a) and normalized beta value (b) for the Duursche Waarden. It can be observed that a reduction in wave height as no effect and that a change in mean critical discharge has a marginal impact when considering both failure mechanisms.

From the heat maps it can be concluded that:

- When considering the total failure probability only the water level is left with having a high impact.
- The effect of a tree toppling over and the change in mean critical discharge have a similar marginal magnitude of impact. However, the effect of a tree toppling over should not be considered if it shows a positive effect.
- The wave height reduction which already had a low impact when considering only overtopping/overflow has no impact on the total failure probability.

The change in mean critical discharge and water level were dominant effects when considering only overtopping/overflow, therefore, it is interesting to analyze their combined effect normalized now on the failure probability of overtopping/overflow without vegetation instead of the total one, which showed that the change in mean critical discharge had no impact. Figure 6.13 shows that when considering only overtopping/overflow both effects have a similar but opposite impact which means that they can compensate each other.

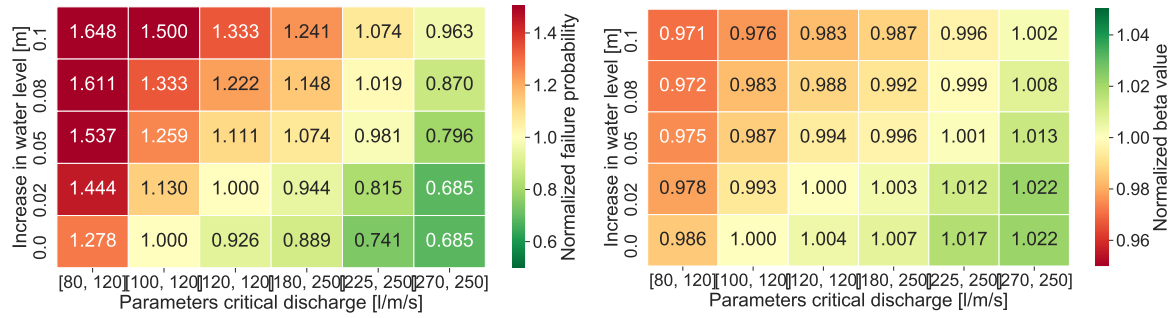

(a) (b)

Figure 6.13: Quantitative effect of the increase in water level and the change in mean critical discharge on the overtopping/overflow failure probability (a) and normalized beta value (b) for the Duursche Waarden. It can be observed that an increase in water level and that a change in mean critical discharge can compensate each other.

It is interesting to use the framework to further study those two effects. Inference is used for this purpose, where the marginal distributions of both root nodes: "increase in water level" and "erosion resistance" are analysed given different types of failures: overtopping/overflow, internal erosion, and both. Initially, the marginal distributions are uniformly distributed. The results are presented in Figure 6.14, where the y-axis denotes the probability density function and the x-axis the increase in water level and the change in mean critical discharge for the graph on the left and right, respectively. It can be observed that the increase in water level is affected by both failure mechanisms individually and combined, i.e. given failure its marginal distribution changes. The overtopping/overflow failure mechanism has the largest influence on this parameter. The total failure probability has a similar behavior as when only considering internal erosion, which confirms that it is the dominant failure mechanism. When considering different parameters for the critical discharge, it can be concluded that only the failure mechanism of overtopping/overflow impacts by this effect, i.e. the marginal distribution is altered given this type of failure.

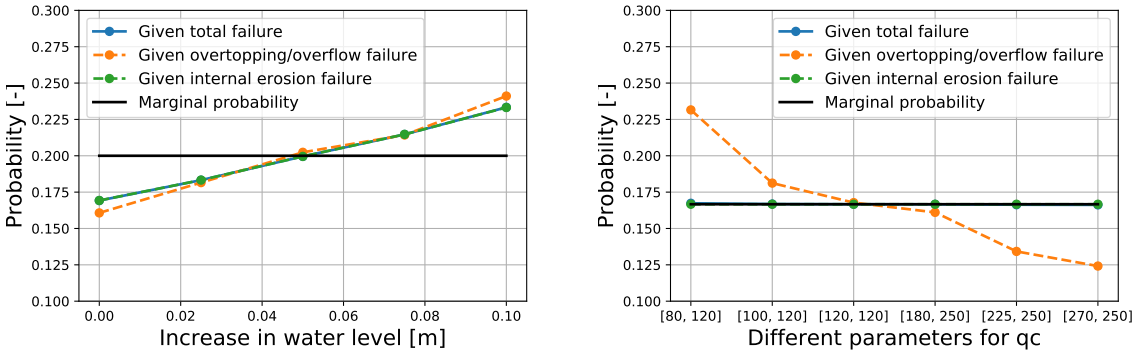

(a) (b)

Figure 6.14: Marginal distribution of the increase in water level (a) and the change in mean critical discharge (b) conditionalized on different failure types.

It can be concluded that the positive effects of vegetation on overtopping/overflow are not visible when considering the total failure probability due to the dominance of the internal erosion failure mechanism. However, for case studies with overtopping/overflow as dominant

failure mechanism, it is expected that the effects impacting this mechanism would be more dominant on the total failure probability. Case studies with higher wave heights would also show very different results, the reduction in wave height and change in roughness factor would have a higher impact.

The results of the three case studies showed similar trends due to their similar characteristics, which are typical for upper-river dikes in the Netherlands (high design water levels, low wave heights, piping dominant, etc.). As such, conclusions made about what are the dominant vegetation effects could be summarised in a road-map (see Figure 6.15), which can be used only for upper river dikes. This road-map can be eventually extended to more general applications after tailoring the values with relevant case studies. By applying this road-map, depending on which failure mechanism is dominant, and some characteristics of the case study, the dominant vegetation parameter(s) that are required to creating the framework for quantifying the vegetation effects on the total failure probability are determined. Thus, this road-map offers the most significant vegetation effects of a case study that would need to be considered when constructing its framework, i.e. the locations and types of vegetation that are most likely to cause a strong impact on the dike.

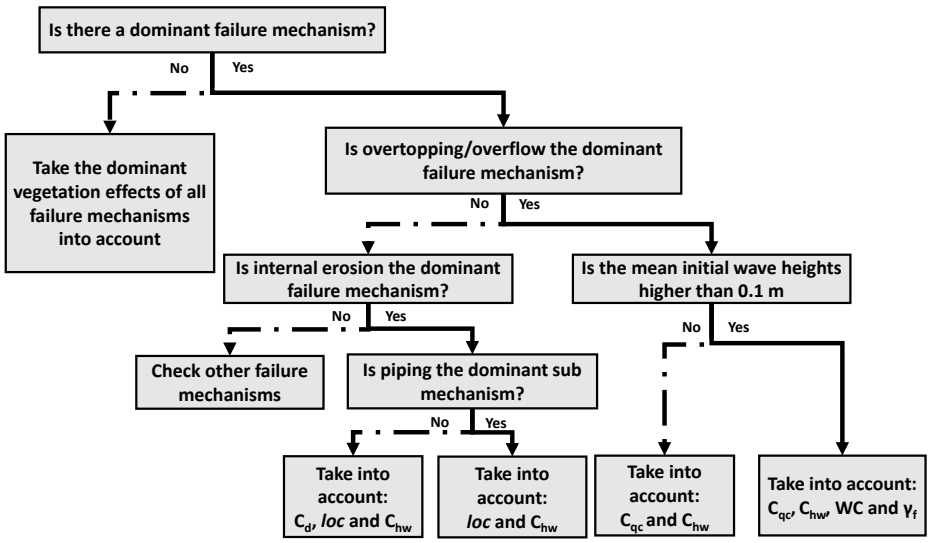

Figure 6.15: Road-map for deciding which vegetation parameters to take into account in the creation of the framework for quantifying vegetation effects on the failure probability of dikes in the upper river areas in the Netherlands.

To determine whether the total effect(s) of the dominant vegetation parameter(s), found using the road-map above in Figure 6.15, is (are) positive, negative, or neutral, two other road-maps were created. If loc is a dominant parameters see Figure 6.16. If the effects of both C_{hw} and C_{qc} combined are dominant, see Figure 6.17, which is specific for the Duursche Waarden case study.

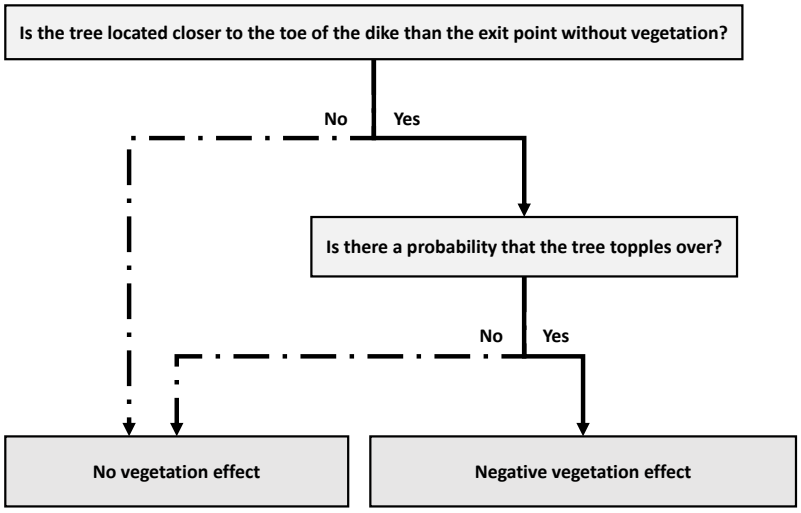

Figure 6.16: Road-map to decide when to take the change in location effect, due to a tree toppling over on the hinterland, into account in the framework.

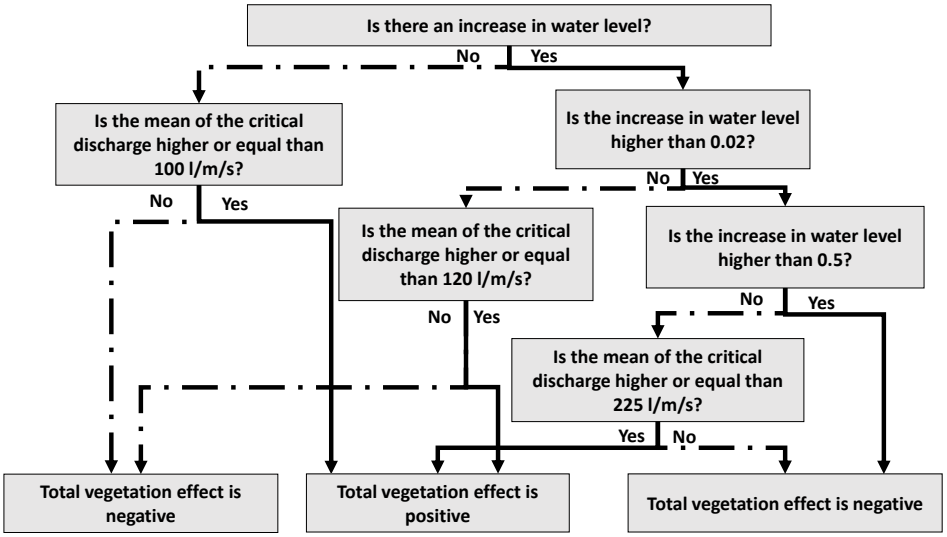

Figure 6.17: Road-map to help decide how much increase in water level a dike can withstand according to its mean critical discharge, this is specific to the Duursche Waarden case study.

6.3. Discussions

6.3.1. Overtopping/overflow

Considering only the failure mechanism overtopping/overflow:

- A high increase in water level (above 0.1 m) has a high impact on the failure probability and should, therefore, be handled with care.
- Herbaceous vegetation with high root strength should be placed on the inner slope since they have a strong impact on the failure probability and their positive effect can compensate for an increase in water level due to vegetation on the floodplains at the riverside.
- Vegetation can also be placed on the foreshore, as it will have no negative impact on the failure probability. The magnitude of this effect depends on the initial wave height.

In case the wave initial height is very low this effect will be marginal. The presence of this vegetation can slightly increase the water level. It is therefore advised to check this, however, this increase is expected to be negligible.

- The impact of herbaceous vegetation on the outer slope depends in the same way on the initial wave height. If the initial wave height is low, and therefore, the dike is overflow dominant, the vegetation will have no impact on the failure probability. However, this effect has no negative impact so vegetation can still be placed for aesthetic purposes or the benefit of another failure mechanism, such as erosion of the outer slope.

6.3.2. Internal erosion

Considering only the failure mechanism internal erosion:

- An increase in water level has a strong impact on this failure mechanism.
- Trees on the hinterland have no impact on the failure probability due to their assumed 1% probability of toppling over occurrence. Its impact is also marginal because the exit point location without vegetation is usually taken as the toe of the outer slope, i.e. the new exit point at the tree location is always further way than the case without vegetation. Thus, the occurrence of piping is always more likely in a situation without a tree. This means that if taken into account, its effect on the total failure probability, if the system is piping dominant, will be positive. This is not correct since the impact of a tree toppling over cannot be positive. Therefore, any positive effect due to a tree located at a further away exit point should be ignored as it does not reduce the probability of another sand boil occurring somewhere else. However, if the tree is located closer its negative effect should be taken into account in the computations of the failure probability.

6.3.3. Both failure mechanisms

Considering both failure mechanisms overtopping/overflow and internal erosion:

- The high dominance of the internal erosion failure mechanism, due to its 100 times higher failure probability, causes any positive vegetation effect on overtopping/overflow to be no longer noticeable when considering the total failure probability. It can be concluded that the effects of vegetation are the most effective/significant when they affect the dominant failure mechanism, as expected.
- The increase in water level harms both failure mechanisms. However, its effect is quantitatively higher for overtopping/overflow than for internal erosion. This is because a few centimeters increase in the water level can lead to much more water going over the dike, whereas it leads to marginal changes in the piezometric head. Considering the effect on the total failure probability, because internal erosion is dominant, its effect is also quantitatively less than for only overtopping/overflow.

6.3.4. Other failure mechanisms

The types of vegetation studied here could also have an impact on other failure mechanisms not considered yet. For example, the vegetation on the outer slope was found to not affect the failure mechanism overtopping/overflow but it will most likely have an impact on the failure mechanism erosion of the outer slope. Thus, it is still difficult to obtain a general idea of the actual impact of vegetation on the total failure probability without considering all the failure mechanisms simultaneously.

6.3.5. Discussion about the framework

Some remarks about the framework are listed below:

- The framework was mainly employed to quickly analyze a large number of different vegetation scenarios. This way, the computation of the graphs and heat maps was performed almost instantaneously. In general, once the input matrix is created, generating the BBN and computing different failure probabilities only takes a matter of a few milliseconds, showing the potential of this framework.
- The BBN can also be used for inference purposes, i.e. computing the probability density function of a vegetation parameter given a failure scenario. This was performed for the increase in water level and the change in mean critical discharge. By doing this, the most probable parameters given failure can be computed.
- BBNs are powerful tools that can compute several different types of calculations (not all utilized in this study). The uniform distributions of the vegetation root nodes were assumed due to a lack of field data and, because the BBNs were only used for conditionalization purposes, this was deemed as a good assumption. However, if the amount of vegetation along the dike trajectory is known, a more accurate distribution can be made for each root node to model the exact amount of vegetation for dike under study. Another advantage of BBNs is their ability to adjust their calculations to field observations. If field experiments were made, this method can be used to adjust the BBNs' conditional probability tables, which were based on the assumption that the limit state functions would not change because of the presence of vegetation.
- Furthermore, the current BBN was only used for one cross-section but can be enhanced to consider the full extent of a dike's trajectory.
- The calibration process needed to compute the conditional probability tables can be time-consuming, especially if the failure probabilities are very low, due to the requirement of the coefficient of variation having a maximum value of 0.05. For the Duursche Waarden, due to a low failure probability in the order of 10^{-5}, the computation of both mechanisms lasted for approximately 11 hours. However, for higher failure probabilities, such as the case of the Grebbedijk in the order of 10^{-3}, the calibration process took roughly 5 hours.
- Computational time of the input matrix was considerably reduced by not including the roughness factor and the decrease in blanket thickness. Further analyses can also reduce the computational time by reducing the number of different states for each vegetation parameter. To have the lowest computational time just two states can be used: one representing the case without vegetation and one with the desired vegetation conditions.
- The potential of this framework was not fully exploited yet, since it can be further extended to better describe the reality of the dike under study. Creating this framework requires a certain familiarity with the field of full probabilistic analysis, but, once created, it can be easily used and understood by everybody.

6.3.6. Practical considerations

Overall, the relevance of the impact of vegetation on a dike strongly depends on the initial failure probability without vegetation. The effects of vegetation are the most relevant in case the actual failure probability of the dike is in the same order as its requirement. In that case, a 30% decrease can represent a remarkable difference and be crucial for compliance with its safety requirement, reaching the optimal economical benefit of vegetation.

All case studies considered in this thesis, on the other hand, do not comply with their safety requirements, i.e. the failure probabilities estimated were higher than the required ones. Therefore, considering the safety standards, any potential vegetation effect would be negligible in comparison with the considerably higher failure probability because the cross-sections of the three dikes need to be strengthened, nevertheless.

All these discussions show that the effects of vegetation can be very powerful if a dike has a failure probability around its safety standard. Vegetation cannot compensate for a truly underdesigned dike (e.g. with a failure probability 100 times higher than its safety standard).

6.3.7. Vegetation parameters

The results obtained in this thesis should be used with care, they are meant to give an idea of the order of magnitude of an effect, and as such, to understand what the dominant effects are. The results also provide knowledge about when one effect becomes dominant over another. This helps to further understand the impact of certain types of vegetation at certain locations, and to encourage further research on this topic.

Therefore, the results obtained from the case studies are based on virtual values of the vegetation parameters, which were mostly overly-conservative. An increase in water level of 0.1 m requires a high amount of vegetation added to the already existing one, which is very unlikely to happen. It is important to understand that all the existing vegetation does not lead to an increase in water level as its effect was already considered in the computation of the water levels. The exact amount of extra vegetation needed to achieve this 0.1 m increase in water level is unknown and expected to be very large. Such an increase is more likely to be caused by climate change (increase in peak river discharge due to more frequent rainfall) or due to the lack of space (narrow floodplains due to urbanization that do not provide enough space for the water to pass). The changes in mean critical discharge are also extreme cases, which might explain their relatively high impact. The wave height reductions used are more realistic. The roughness factor reduced to 0.8 is also unlikely to occur, however it was chosen to be overly conservative to confirm that it would not have a relevant impact. Finally, the reduction in blanket thickness was also extreme to understand whether it would eventually have an impact.

7

Conclusions and recommendations

7.1. Conclusions

This thesis dealt with the topic of implementing quantified effects of vegetation in the assessment method of Dutch river dikes, i.e. in the calculation of their failure probability. Nowadays, dikes are becoming increasingly important in river areas because climate change is causing more frequent and more extreme rainfalls. The continuous rise in population and economic value of these areas only worsens the issue. Especially in countries with low ground levels, such as the Netherlands, the risk of river flooding is significantly increasing. Therefore, there is a need for strengthening the current dike systems. Traditionally, this would mean increasing their height, but this is a very expensive process. Moreover, it may not always be possible to increase the height because of the lack of space.

An innovative solution to this problem is called Nature-based (NB) flood defences, which combine dikes with some natural elements. The most common NB dikes include vegetation, such as salt marshes or willows, on their foreshore to reduce the wave height at the toe of the dikes. Recent studies have shown potential positive effects of other types of vegetation placed on other locations as well, such as herbaceous vegetation on the slopes which could increase the soil cohesion and, thus, reduce erosion and increase slope stability. However, most water authorities remain reluctant to add vegetation on dikes due to the potential adverse effects some vegetation can have, which is also location dependent. For example, large vegetation located on the floodplain or the foreshore can increase water levels or the presence of large vegetation can increase seepage if not well maintained, due to dead roots or if it topples over.

The overall influence of vegetation, i.e. considering both positive and/or negative effects, is still difficult to predict due to the lack of guidelines on how to consider such effects in the safety assessment of dikes. This hinders the implementation of NB flood defences.

This study aimed at filling this knowledge gap by creating an innovative framework to determine the overall impact of five different effects of vegetation on the total failure probability considering two failure mechanisms: overtopping/overflow and internal erosion. By employing the framework on three case studies, all located in the upper river areas of the Netherlands, some general conclusions could be deducted regarding where vegetation is the most beneficial considering these types of dikes. This framework allows to eventually include quantified

vegetation effects in the assessment process of dikes.

7.1.1. Including vegetation in the safety assessment

The five vegetation effects studied are caused by three types of vegetation: woody vegetation, reed beds and scrubs, and herbaceous vegetation at different locations. The effects are:

1. An increase in water level caused by extra woody vegetation or reed beds and scrubs added to the already existing vegetation along the floodplains upstream or downstream of the dike trajectory or, to a lesser extent, on the foreshore.
2. An increase in erosion resistance due to the root strength of herbaceous vegetation located on the inner slope.
3. A reduction in wave height due to woody vegetation or reed beds and scrub located on the foreshore of river dikes.
4. An increase in roughness due to herbaceous vegetation located on the outer slope.
5. The decrease in the dike's strength due to woody vegetation toppling over on the hinterland.

The method for including vegetation effects in the computation of the failure probability, considering two failure mechanisms consisted of determining the parameters of their respective limit state functions that could be affected by vegetation. Based on the literature, these parameters were then modified according to the vegetation characteristics present on the dike cross-section of interest. The same limit state function with the modified parameters was then used to compute the failure probability with vegetation effects.

The failure mechanism overtopping/overflow was affected by four of the five effects, each of which had an impact on one parameter.

1. The increase in water level influenced the water level parameter, which was modified by increasing it with a constant value.
2. The erosion resistance of vegetation on the inner slope impacted the critical discharge, which was modified by increasing or decreasing its mean value.
3. The reduction in wave height influenced the computed wave height parameter, which was modified by decreasing it by a percentage.
4. The roughness on the outer slope affected the roughness influence factor, which was modified by reducing its value.

For internal erosion, two of the five vegetation effects were relevant, the first had an impact on one parameter, the second had two consequences impacting three parameters. This is explained below. There is no global limit state function for this failure mechanism, instead, vegetation effects impacted the three limit state functions of the sub-mechanisms.

1. The first effect is the increase in water level, which impacted the water level parameter present in all three sub-mechanisms, which was modified by increasing its value by a constant.
2. The second effect, a tree toppling over on the hinterland, had two consequences:
   (a) Decrease in local blanket thickness, affecting the aquitard thickness of two sub-mechanisms: uplift and heave. This parameter was modified by decreasing its mean value.
   (b) Change in exit point location, affecting two parameters: the piezometric head pa-

rameter of the uplift and heave sub-mechanisms and the seepage length parameter in the piping sub-mechanism. Both parameters were modified in the same way by increasing them by a constant.

The effects of vegetation were thus modeled by modifying the relevant parameters, changing their value or modifying their distribution. An advantage of this method is its easy application as the limit state functions are unchanged, the negative side is that it still needs to be validated to check its accuracy.

7.1.2. Creating a framework to find the best location for vegetation

A framework was created for combining all vegetation effects in the computation of the total failure probability, considering different magnitudes of each effect. A Bayesian Belief Network (BBN) was used for this purpose due to its ability to graphically visualize the situation. BBNs can also store a large amount of information and, therefore, quickly compute a large number of different failure probability scenarios, which was very useful when processing results. The framework proved to be very efficient, with multiple scenarios being computed in a matter of a few milliseconds. Only the calibration of the BBN required to construct the conditional probability tables took a few hours. The time required for this process depends on the number of vegetation parameters taken into account, the number of states per root node, and the failure probability without vegetation.

BBNs are powerful tools that can compute many different types of calculations (not all utilized in this study). In general, BBNs are mostly used in studies for inference purposes, which were only marginally conducted in this thesis, but can be used in more depth in future studies. Furthermore, BBNs have the capacity to improve from observations, which can be used to improve the accuracy of their conditional probability tables. Finally, the root nodes were assumed to be all uniformly distributed, but more realistic conditions can be obtained with field data or satellite observations. This proves the potential of the framework.

The BBN was created to study the dominant cross-section of a dike section. However, the advantage of using a BBN is that more cross-sections can be eventually added in order to obtain the *full picture* of the dike trajectory. Similarly, other failure mechanisms can be added together with more vegetation root nodes. Eventually, the BBN could provide a global overview of the effects of vegetation on the whole trajectory of a dike considering all the failure mechanisms. This could help localize the optimal positions for certain vegetation types and the quantity that needs to be maintained to ensure their most beneficial effects.

7.1.3. Dealing with vegetation on upper river dikes

Three case studies located in the upper-river areas of the Netherlands (Culemborg, Grebbedijk, and Duursche Waarden) were chosen to demonstrate the use of the framework. All three case studies showed similar trends, therefore, general conclusions were carefully made for dikes in upper-river areas based on the assumed values given to the vegetation parameters.

When considering vegetation effects on the total failure probability, the most important effects are those influencing the dominant failure mechanism, i.e. the one with the highest failure probability. The effects on none dominant failure mechanisms become marginal when considering the total failure probability.

The increase in water level influences most, if not all, failure mechanisms and is therefore the most important effect on the total failure probability. Its impact on the failure probability varies per failure mechanism, having a higher impact on overtopping/overflow than internal erosion. The impact is always negative and considerably significant, a 0.1 m increase leads to approximately 30% increase in total failure probability. However, such a high increase in water level is highly unlikely to be caused by vegetation, as the effect of the existing vegetation was already taken into account. A more likely cause is climate change or the lack of space.

If the dike's cross-section has overtopping/overflow as the dominant failure mechanism and has an average wave height in the dominant wind direction lower than 0.1 m, it can be expected that the largest effects of vegetation are the increase in water level and the erosion resistance of the inner slope. The former has a negative impact and the latter a positive one. Both can compensate each other to have an overall neutral effect. The effects of the wave height reduction and roughness on the outer slope can be expected to be marginal, mainly because of the very low original wave heights. Therefore, in this case, large vegetation on the foreshore has limited impact on the wave height but can be kept for ecological purposes as long as it does not increase the water level. If it increases the water level, a high grass quality, or other herbaceous vegetation, that is well maintained may compensate for it. Considering vegetation on the outer slope, it has a marginally positive effect and can, therefore, be kept without much affecting the failure probability.

When the dominant failure mechanism is internal erosion, the only dominant vegetation effect is an increase in water level. There is no other vegetation effect that can compensate for this increase in failure probability. Considering vegetation on the hinterland, more specifically the effect of a tree toppling over, the consequences on the failure probability are nonexistent or marginally negative due to the low probability of occurrence considered in this study (1%), although this value was considered conservative. Two consequences of a tree toppling over were studied: a reduction in local blanket thickness and a change in the exit point location. The former influenced significantly and negatively the sub-mechanisms uplift and heave. However, internal erosion is a fully-dependent system, i.e. its probability is equal to the lowest of the three sub-mechanisms. For all three case studies, piping had the lowest failure probability and, therefore, a decrease in local blanket thickness had no impact on internal erosion. The second consequence, a change in exit point location, had a large impact on piping and only a marginal on uplift and heave. Therefore, if a tree does topple over, it influences significantly internal erosion's failure probability. However, it should be kept in mind that a tree cannot have a positive impact on internal erosion, as it does not reduce the load nor increase the strength of a dike. Therefore, the effect of a tree can only be considered if its effect is negative, i.e. if located closer to the toe of the dike than the none vegetated case. In conclusion, the effect of trees on internal erosion is marginal due to the low probability of a tree toppling over and because the exit point without vegetation is usually at the toe of the dike.

Overall, using the framework, this study shows that vegetation certainly can have an important effect on the failure probabilities of river dikes. It all depends on the dominant failure mechanism and the characteristics of the cross-section, i.e. whether it has high wave heights, whether piping is the sub-mechanism with the lowest failure probability, etc. Depending on the situation, vegetation can have a positive impact. However, the relevance of the impact of vegetation on dike strongly depends on its initial failure probability without vegetation compared to its safety requirement.

7.2. Recommendations

From the results obtained, the effect of erosion resistance of the inner slope showed the most promising results, i.e. a high positive impact on the failure probability of overtopping/overflow. Therefore, it is highly recommended to study this effect in more detail. Studies are especially lacking in how different roots of vegetation lead to different distributions of the critical discharge parameter. In general, the parameter affected by this effect is still very uncertain, even though it is one of the most important parameters in the limit state function. Therefore, studying it more can also be beneficial to reduce this uncertainty. In practice, it can be inferred that it is important to ensure that vegetation with strong roots is placed on the inner slopes of dikes. High maintenance of this vegetation is also required to ensure the maximum positive impact. For a dike's cross-section with low wave height, i.e. overflow dominant, good erosion protection of the inner slope is especially important. Overall, this parameter has the potential to compensate for an increase in water level, which is the most important negative effect.

In general, it is recommended to further study the effects of different types and locations of vegetation on dikes considering different failure mechanisms. More importantly, it is important to understand their effect on the parameters of the limit state functions that they influence and quantifying that effect. Finding the right way to modify a parameter will lead to more accuracy in the framework.

It is also recommended to extend the study to eventually obtain the whole picture of how vegetation affects the process of assessing/designing dikes. This way, eventually, the water authorities can include complete guidelines on how to properly assess/deal with vegetation on dikes, i.e. what are the effects that are important and need to be taken into account. This can be done by studying the limit state function of other failure mechanisms and understanding which of their parameters are affected by vegetation and how they can be modified to account for that. Once this is determined, the framework can be extended by:

- Adding more vegetation effects, i.e. more root nodes in the BBN. This does not necessarily mean adding more state variables, therefore it does not need to add much more computational time.
- Adding more failure mechanisms.
- Including more cross-sections.

It is recommended to also apply this framework to river dikes with higher wave heights, coastal dikes, and estuaries dikes. This will allow an understanding of which effects are dominant depending on the type of dike under study.

The framework can be further improved by:

- Taking the dependence of the stochastic variables into account.
- Making the BBN dynamic to include the time dependence of vegetation effects.
- Using field observations to improve its accuracy and validity.

Lastly, it would be useful to validate these results with field experiments or physical models. This could be done by considering just one case study and testing whether the limit state functions are still valid with vegetation present. An alternative method consists of preparing two dikes (one with vegetation and one without) and making detailed observations under different conditions.

Bibliography

Actueel hoogtebestand netherland [Accessed: 07/2020]. (n.d.). https://www.ahn.nl/ahn-viewer

Beheerplan natura 2000 rijntakken (038) (tech. rep.). (2018). Provincie Gelderland.

Berendse, F., van Ruijven, J., Jongejans, E., & Keesstra, S. (2015). Loss of plant species diversity reduces soil erosion resistance. *Ecosystems*, *18*, 881–888.

Chbab, H. (2015). *Basisstochasten WTI-2017 Statistiek en statistische onzekerheid* (tech. rep.). Deltares.

Correction wording flood risks for the Netherlands in IPCC report [https://www.pbl.nl/en/correction-wording-flood-risks (Accessed on 19/10/2020)]. (2017).

De Baets, S., Poesen, J., Gyssels, G., & Knapen, A. (2006). Effects of grass roots on the erodibility of topsoils during concentrated flow. *Geomorphology*, *76*, 54–67.

De Baets, S., Poesen, J., Knapen, A., & Galindo. (2007). Impact of root architecture on the erosion-reducing potential of roots during concentrated flow. *Earth Surface Processes and Landforms*, *32*, 1323–1345.

De Baets, S., Poesen, J., Reubens, B., Wemans, K., De Baerdemaeker, J., & Muys, B. (2008). Root tensile strength and root distribution of typical mediterranean plant species and their contribution to soil shear strength. *Plant and soil*, *305*(1-2), 207–226.

de Groot, B., & Hordijk, D. (2015). *Beslisschema voorlanden - toelichting bij het schema & doorkijk gewenste technische ontwikkelingen* (tech. rep.). Rijkswaterstaat, WVL.

de Groot, S. (2002). *Ecological restoration of aquatic and semi-aquatic ecosystems in the netherlands (nw europe)* (P. Nienhuis & R. Gulati, Eds.). SPRINGER.

de Vries, M., & Dekker, F. (2009). *Ontwerp groene golfremmende dijk fort steurgat bij werkendam* (tech. rep. Z4832.00). Deltares.

de Vries, M., Penning, E., van Geest, G., Genseberger, M., van Steeg, P., & Morris, J. (2015). *Kwantificering van effect van golfremming door vegetatie op uiterwaarden* (tech. rep. 1220539-000-ZWS-0006). Deltares.

Dekking, F. M., Kraaikamp, C., Lopuhaä, H. P., & Meester, L. E. (2005). *A modern introduction to probability and statistics*. Springer, London.

Duits, M. (2019). *Hydra-nl* (2.7). HKV.

Fathi-Maghadam, & Kouwen. (1997). Nonrigid, nonsubmerged, vegetative roughness on floodplains. *Journal of Hydraulic Engineering*, *123*(1), 51–57.

Hasofer, A. M., & Lind, N. C. (1974). Exact and invariant second-moment code format. *Journal of the Engineering Mechanics division*, *100*(1), 111–121.

Järvelä, J. (2002a). Determination of flow resistance of vegetated channel banks and floodplains, 311–318.

Järvelä, J. (2002b). Flow resistance of flexible and stiff vegetation: A flume study with natural plants. *Journal of Hydrology*, *269*, 44–54.

Jiménez Cisneros, B. E., & Oki, T. (2014). *AR5 Climate Change 2014 Impacts, Adaptation, and vulnerability Chapter 3* (tech. rep.). IPCC.

Jongejan, R. (2016). Factsheet : Het lengte-effect. *Kennisplatform Risicobenadering (KPR)*.

Jongenjan, R. (2017). *WBI2017 Code Calibration* (tech. rep.). Rijkswaterstaat.

Klein Breteler, M., van Steeg, P., & Camarena Calderon, R. (2016). *Gebruik van vegetatie ten behoeve van reductie golfoverslag bij dijken* (tech. rep. 1230042-004-ZWS-0007). Deltares.

Kok, M., Jongejan, R., Nieuwjaar, M., & Tanczos, I. (2016). *Grondslagen voor hoogwaterbescherming* (tech. rep. ISBN/EAN: 978-90-8902-151-9). Ministerie van Infrastructuur en Milieu.

Kovats, S., & Valentini, R. (2014). *AR5 Climate Change 2014 Impacts, Adaptation, and vulnerability Chapter 23* (tech. rep.). IPCC.

Lanzafame, R., & Sitar, N. (2018). *Reliability analysis of the influence of woody vegetation on levee performance* (tech. rep.). California Levee Vegetation Research Program.

Leyer, I., Mosner, E., & Lehmann, B. (2012). Managing floodplain-forest restoration in european river landscapes combining ecological and flood-protection issues. *Ecological Applications - Ecological Society of America*, *22*, 85–97.

Losada, I., Maza, M., & Lara, J. (2016). A new formulation for vegetation-induced damping under combined waves and currents. *Coastal engineering*, *107*, 1–13.

Makaske, B., Maas, G., van den Brink, C., & Wolfert, H. (2011). The influence of floodplain vegetation succession on hydraulic roughness: Is ecosystem rehabilitation in dutch embanked floodplains compatible with flood safety standards? *Ambio*, *40*(4), 370–376.

Nakicenovic, N. (2000). *IPCC Special Report Emissions Scenarios Summary for policy makers* (tech. rep.). WMO UNEP.

Neapolitan, R. (2004). *Learning bayesian networks* (Vol. 38). Pearson.

Netica. (2010). Norsys Software Corp.

Openturns [Accessed: 07/2020]. (n.d.). http://www.openturns.org/

Pearl, J. (1995). From bayesian networks to causal networks, In *Mathematical models for handling partial knowledge in artificial intelligence*. Springer.

Rijkswaterstaat. (2017a). *Regeling veiligheid primaire waterkeringen 2017 - bijlage iii sterkte en veiligheid* (tech. rep.). Ministerie van Infrastructure en Milieu.

Rijkswaterstaat. (2017b). *Schematiseringshandleiding piping WBI 2017* (tech. rep.). Ministerie van Infrastructuur en Milieu.

Riskeer. (2019). Deltares.

Roth, L., Trahan, A., Aflaki, R., Berko4, K., & Poosti, A. (2017). Risk analysis of vegetation on levees. *Journal of Chemical Information and Modeling*, *53*(9), 1689–1699.

Schematiseringshandleiding grasbekleding (tech. rep.). (2019). Rijkswaterstaat Ministerie van Infrastructuur en Waterstaat.

Schiereck, G., & Van der Kleij, W. (1998). *Grondslagen voor waterkeren* (tech. rep.). Technische Adviescommissie voor de Waterkeringen (TAW).

Schreiber, J. (2018). Pomegranate: Fast and flexible probabilistic modeling in python. *Journal of Machine Learning Research*, *18*(164), 1–6.

Schweckendiek, T., Vrouwenvelder, A., & Calle, E. (2014). Updating piping reliability with field performance observations. *Structural safety*, *47*, 13–23.

Sellmeijer, H., López de la Cruz, J., van Beek, V., & Knoeff, H. (2011). Fine-tuning of the backward erosion piping model through small-scale, medium-scale and ijkdijk experiments. *European Journal of Environmental and Civil Engineering*, *15*.

Smale, A. (2019). *Memo kennisplatform risicobenadering: Ontwerpen met kansverdelingen voor kritieke overslagdebieten*.

Smale, A., & Borsboom, M. (2016). *Vegetatie als maatregel voor reductie benodigde kruinhoogte voor het traject tiel waardenburg* (tech. rep. 1220539-001-ZWS-0004). Deltares.

Ston, B., & Shen, H. (2002). Hydraulic resistance of flow in channels with cylindrical roughness. *Journal of hydraulic engineering*, *128*(5), 500–506.

Stuip, J., Bos, A., Boeters, R., Botman, B., Brinkman, J., van Ellen, T., van Meeteren, C., Nijburg, C., Paas, W., Pijning, L., Schiereck, G., Schippers, W., Wevers, A., Verkade, G., & Koolen, J. (1999). *Natuurvriendelijke oevers* (tech. rep.). Rijkswaterstaat.

Suzuki, T. (2011). *Wave dissipation over vegetation fields* (Doctoral dissertation). Delft univeristy of technology.

Theodoridis, S. (2015). *Machine learning: A bayesian and optimization perspective - chapter 14*.

Trung, L. H. (2014). *Overtopping on grass covered dikes - resistance and failure of the inner slopes* (Doctoral dissertation). Delft University of Technology.

Uninet [Assessed: February 2020]. (n.d.). https://www.tudelft.nl/en/eemcs/the-faculty/departments/applied-mathematics/applied-probability/risk/software/uninet/

Users Guide WAQUA: General Information. (2016). Rijkswaterstaat.

van der Meer, J., Verheij, H., Hoffmans, G., Paulissen, M., Steendam, G., & van Hoven, A. (2012). *Technisch rapport toetsen grasbekledingen op dijken* (tech. rep. No. 1206016-000). Deltares.

van der Meer, J., Allsop, N., Bruce, T., De Rouck, J., Kortenhaus, A., Pullen, T., Schüttrumpf, H., Troch, P., & Zanuttigh, B. (2018). *EurOtop Manual on wave overtopping of sea defences and related structures. An overtopping manual largely based on European research, but for worldwide application.* (Second Edition 2018).

Van Rossum, G., & Drake Jr, F. L. (1995). *Python reference manual*. Centrum voor Wiskunde en Informatica Amsterdam.

van Hasselt, & van Everdingen. (1998). *Technish rapport erosiebestendigheid van grasland als dijkbekleding* (tech. rep.). Technische Adviescommissie vor de Waterkeringen.

van Houwelingen, A. (2012). *Boment fase 3 gedetaileerde toets* (tech. rep.) [registratienummer : LW-AF20122371]. Deltares. registratienummer : LW-AF20122371.

van Velzen, E., Jesse, P., Cornelissen, P., & Coops, H. (2003). *Stromingsweerstandvegetatie in uiterwaarden* (1st ed.). Rijkswaterstaat.

van Wesenbeeck, B., Mulder, J., Marchand, M., Reed, D., de Vries, M., de Vriend, H., & Herman, P. (2014). Damming deltas: A practice of the past? towards nature-based flood defenses. *Estuarine, Coastal and Shelf Science*.

Vannoppen, W., Poesen, J., Peeters, P., De Baets, S., & Vandevoorde, B. (2016). Root properties of vegetation communities and their impact on the erosion resistance of river dikes. *Earth surface processes and landforms*, *41*, 2038–2046.

Vastila, K., & Jarvela, J. (2014). Modeling the flow resistance of woody vegetation using physically based properties of the foliage and stem. *Water Resources Research*, *50*, 229–245.

Vegetatielegger [https://maps.rijkswaterstaat.nl/geoweb55/index.html?viewer=Vegetatielegger (Accessed = 01/05/2020)]. (2020).

Vegetatiemonitor [Accessed in June 2020]. (n.d.). Deltares and Rijksoverheid. https://vegetatiemonitor.netlify.app/%5C#/veld

Venema, J., Schelfhout, H., & van der Meulen, M. (2014a). *Toetsmethode grienddijk fort steurgat - achtergrondrapport* (tech. rep. 1206002-000-GEO-0024). Deltares.

Venema, J., Schelfhout, H., & van der Meulen, M. (2014b). *Toetsmethode grienddijk fort steurgat - hoofdrapport* (tech. rep. 1206002-000-GEO-0023). Deltares.

Vergouwe, R. (2016). *The national flood risk analysis for the netherlands*. Rijkswaterstaat VNK Project Office.

Verheij, H., & Sprengers, C. (2012). *Quick scan golfremmende vegetatie bij stroomlijn* (tech. rep. 1206002-000-GEO-0005). Deltares.

Verheij, H. (1995). *Golfdemping door riet* (tech. rep.). Rijkswaterstaat.

Vrouwenvelder, A. (1999). *Theoriehandleiding PC-RING deel C*. TNO.

Vuik, V., van Vurena, S., Borsjed, B., van Wesenbeecka, K., & S.N, J. (2018). Assessing safety of nature-based flood defenses: Dealing with extremes and uncertainties. *Coastal Engineering*, *139*, 47–64.

Waterveiligheidsportaal [https://waterveiligheidsportaal.nl/#/nss/nss/norm (Accessed on 01/04/2020)]. (2020).

WBI2017 Handboek voor de toezichthouder (tech. rep.). (2017). Ministerie van Infrastructure en Waterstaat.

Wu, F., SHEN, H., & Chou, Y. (1999). Variation of roughness coefficients for unsubmerged and submerged vegetation. *Journal of hydraulic Engineering*, *125*(9), 934–942.

Young, I. R., & Verhagen, L. (1996). The growth of fetch limited waves in water of finite depth. part 2. spectral evolution. *Coastal Engineering*, *29*(1-2), 79–99.

Zanetti, C., Vennetier, M., Mériaux, P., Royet, P., & Provansal, M. (2009). Managing woody vegetation on earth dikes: Risks assessment and maintenance solutions. *Procedia Environmental Sciences*, *9*, 196–200.

Nomenclature

α	Slope of outer slope [deg]
α_i	One parameter influenced by vegetation, unit is case dependent
$\Delta\phi$	Actual local head difference [m]
$\Delta\phi_{c,u}$	Critical local head difference [m]
η	Drag coefficient [-]
γ_β	Influence factor for oblique wave attack [-]
γ_v	Influence factor for a vertical wall on top of the crest [-]
γ_b	Influence factor of a berm [-]
$\gamma_{f,\,veg}$	Influence factor for roughness adjusted by vegetation [-]
γ_f	Influence factor for the permeability and roughness of the outer slope [-]
γ_s	Volumetric weight of sand grains [kN/mş]
γ_w	Saturated volumetric weight of water [kN/mş]
γ_{sat}	Saturated volumetric weight of the blanket [kN/m^3]
λ	damping factor [-]
λ_h	Leakage factor [-]
$\mu_{d,veg}$	Mean local aquitard thickness adjusted by vegetation [m]
μ_d	Mean local aquitard thickness [m]
$\mu_{qc,veg}$	Mean critical velocity adjusted by vegetation [l/(s m)]
μ_{qc}	Mean critical velocity [l/(s m)]
ν	Kinematic viscosity of water [m^2/s]
ϕ_{exit}	piezometric head at exit point[m]
ϕ_{veg}	Average vegetation diameter [m]

$\boldsymbol{\alpha}$ Set of parameters influenced by vegetation, unit is case dependent

d_{70} 70%-fractile of the grain size distribution [m]

$H_{c,p}$ Critical head difference [m]

$x_{exit,\ veg}$ Distance of the exit point from the center of the levee footprint with vegetation [m]

x_{exit} Distance of the exit point from the center of the levee footprint [m]

θ Bedding angle [deg]

$\xi_{m-1,0}$ Breaker parameter [s/$\sqrt{m}$]

f Function of a limit state function, unit is case dependent

g General function of any parameter dependent on vegetation characteristic, unit is case dependent

g_i Specific function of a parameter dependent on vegetation characteristic, unit is case dependent

loc Vegetation parameter for location of the tree [m]

u Flow velocity [m/s]

B Width of the levee [m]

C_d Vegetation parameter modeling the effect of vegetation on the local aquitard thickness [-]

$C_{\gamma f}$ Vegetation parameter modeling the effect of vegetation on the roughness factor [-]

C_{hw} Vegetation parameter modeling the effect of vegetation on the water level [m]

C_{qc} Vegetation parameter modeling the effect of vegetation on the mean critical discharge [-]

D Thickness of the aquifer [m]

d Thickness of the aquitard [m]

D_{veg} Density of vegetation [veg/m^2]

d_w Water depth [m]

d_{70m} Reference value of d70 [m]

F Fetch of the wind [m]

g gravitational acceleration constant [m/s^2]

h_b Bottom level [m]

h_p Hinterland phreatic level [m]

$h_{w,\ veg}$ Water level increased by vegetation [m]

h_w River water level [m]

h_c Crest height of the dike [m]

$H_{m0,\ veg}$ Wave height reduced by vegetation [m]

H_{m0} Wave height [m]

h_{veg} Average vegetation height [m]

i exit gradient [-]

i_c Critical heave gradient [-]

k Hydraulic conductivity of the aquifer [m/s]

k_h Hydraulic conductivity of the aquitard [m/s]

L Seepage length [m]

L_f Length of the effective foreshore [m]

L_{veg} Seepage length with vegetation [m]

m_p Model factor piping [-]

m_u Model factor uplift [-]

O wave angle in degrees [deg]

P() Probability [-]

q Water discharge [l/(s m)]

q_c Critical discharge [l/(s m)]

q_{max} Maximum discharge [l/(s m)]

$q_{overflow}$ Overflowing discharge [l/(s m)]

$q_{overtopping}$ Final overtopping discharge [l/(s m)]

q_{storm} Discharge that will go over the dike during certain conditions [l/(s m)]

R_c Freeboard of the dike [m]

T_p Wave period [sec]

U_{10} Wind speed at 10 m above ground level [m/s]

WC Wave height coefficient [-]

X Any variable [-]

X_{pai} Parent of X [-]

Z Limit state function, unit is case dependent

Z_h Limit state function of heave [-]

$Z_{OT/OF}$ Limit state function of overtopping/overflow [l/(s m)]

Z_p Limit state function of piping [m]

Z_u Limit state function of uplift [m]

A

Reliability techniques

This appendix presents the different reliability techniques that can be used to assess dikes using their respective limit state function. It starts with presenting the deterministic approach (Section A.1), followed by the First Order Reliability Method (FORM) (Section A.2) and finally the Monte Carlo (MC) method (Section A.3). The use of the deterministic approach provides a simple first estimation of the effect of vegetation in a faster way than more complex methods. However, this technique does not allow for the computation of the failure mechanism overtopping/overflow. Therefore, MC simulations were employed for this purpose, since the FORM analysis were not appropriate either due to convergence issues. FORM offers, on the other hand, a faster alternative for computing failure probabilities than MC and was, therefore, employed for the calculations regarding internal erosion. Furthermore, FORM allows for the computation of the design point (explained below), which provides a better physical understanding of the problem.

A.1. Deterministic approach

In this reliability technique, all stochastic variables are transformed to a deterministic value and the limit state function is then easily computed. The deterministic values for the hydraulic boundary conditions, which are the water levels and the wind speeds, are found based on the required failure probability for a cross-section and a specific failure mechanism. These values can be extracted from the Dutch governmental program called "*Hydra-NL*" , which give deterministic values that already include model and statistic uncertainty (Duits, 2019). All other stochastic variables need to be transformed into their respective characteristic values, which are computed by using the inverse of the 5% or 95% of the exceedance probability, depending on whether the variable is a load or strength, respectively. For normally distributed variables Equation A.1 can be used, and for log-normally distributed variables Equation A.2. All the deterministic values were then implemented in the limit state functions presented in Section 2.2.1 for overtopping/overflow and Section 2.2.2 for internal erosion.

$$X_k = \begin{cases} \mu_X - \lambda\sigma_X, & \text{if strength variable} \\ \mu_X + \lambda\sigma_X, & \text{if load variable,} \end{cases} \tag{A.1}$$

$$X_k = \begin{cases} \exp\left(\mu_m - t_{n-1}\sigma_m\sqrt{(1-a)+\frac{1}{n}}\right), & \text{if strength variable} \\ \exp\left(\mu_m + t_{n-1}\sigma_m\sqrt{(1-a)+\frac{1}{n}}\right), & \text{if load variable,} \end{cases} \tag{A.2}$$

$$\sigma_m^2 = \ln\left[1 + \left(\frac{\sigma_X}{\mu_X}\right)^2\right], \tag{A.3}$$

$$\mu_m = \ln(\mu_X) - \frac{1}{2}\sigma_m^2, \tag{A.4}$$

where:

- X_k: characteristic value.
- μ_X: mean value.
- σ_X: standard deviation.
- μ_X: mean value of log-normal distribution.
- σ_X: standard deviation of log-normal distribution.
- λ: normal distribution factor, here takes a value of 1.64.
- t_{n-1}: student t-factor, here takes a value of 1.76.
- a: ratio between the local and regional variation, here takes a value of 0.
- n: number of observations, here takes a value of 15.

For the overtopping and overflow failure mechanisms, this method was used to compute, using the limit state functions, the discharge of the water flowing over the dike. For internal erosion, this method was used to compute the factor of safety, see Equation A.5, where a value smaller than one represents an increased failure probability and vice versa. Some characteristics of this method are mentioned in Table A.1.

$$FS = \frac{R_d}{S_d}, \tag{A.5}$$

where:

- FS [-]: factor of safety.
- R_d: design strength value, the unit depends on the failure mechanisms under study.
- S_d: design load value, the unit depends on the failure mechanisms under study.

Table A.1: Advantages and disadvantages of a deterministic approach.

Advantages	Disadvantages
• Fast and easy computation. • Can be standardized.	• Often a too simplistic approach, leading to a possibly conservative assessment. • Low precision.

A.2. First Order Reliability Method (FORM)

This method is a semi-probabilistic analysis because the mean and the covariance matrix of the stochastic variables are taken into account to determine the failure probability. The stochastic variables are transformed into the standard normal space. These are then replaced in the limit state function, transforming it to a uniform-space, which is then divided into two parts: The safe domain and the unsafe domain, by a line where the limit state is 0. The shortest distance between this line and the origin is the reliability index, which denotes the highest probable point of failure (called the design point) and is used to obtain the failure probability (see Equation A.6). In general, the higher the reliability index, the lower the failure probability. In this research, the reliability index (β) according to Hasofer and Lind was used (Hasofer and Lind, 1974), due to its advantage of being invariant with respect to the formulation of the limit state equations compared to other techniques.

$$\mathrm{P}_f = \Phi(-\beta), \tag{A.6}$$

where:

- P_f [-]: failure probability.
- Φ [-]: Cumulative Density Function (CDF) of the standard normal space.
- β [-]: reliability index or beta value.

When variables are not normally distributed, transforming them into the standard normal space is more difficult. Therefore, they first need to be converted to a normal distribution. This is done in such a way that the Probability Density Function (PDF) and the Cumulative Density Function (CDF) of the variable and its transformed normal distribution are equal at the design point. Multiple methods are available to solve for the reliability index. For this study, the program Open Turns in python was used ("OpenTurns", n.d.).

An important advantage of using this method is its ability to give the points of the joint probability distribution with the highest probability of failure. This combination of variables can provide a physical meaning to the problem. Furthermore, with this method, *alpha* values can be derived, which provide the contribution of each variable to the failure probability and are an extremely powerful tool to determine the most dominant parameters. The *alpha* parameter with the highest absolute value contributes the most to failure. These values are computed using the normalised partial derivative to each variable, see Equation A.7. The advantages and limitations of this method are summarised in Table A.2.

$$\alpha_i = \frac{\frac{\partial g(\mathrm{U}_i)}{\partial x}}{\sum_{n=1}^{n} \frac{\partial g(\mathrm{U}_i)}{\partial x}}. \tag{A.7}$$

Table A.2: Advantages and disadvantages of a level II (semi-probabilistic) analysis.

Advantages	Disadvantages
• Fast computation. • Unique solution. • Provides alpha values and design point.	• Does not find a solution if the limit state function is too curved. • Does not converge when the derivatives are zero.

A.3. Monte Carlo (MC) analysis

This method is a fully probabilistic analysis as it uses the distribution of all stochastic variables to compute the failure probability. MC is a simulation method. To calculate the failure probability, it draws random variables from each distribution and calculates whether there is failure ($Z < 0$) or not ($Z > 0$). The probability is then taken as the fraction between the number of failures divided by the number simulations, see Equation A.8.

$$P_f = \frac{N_f}{N}, \tag{A.8}$$

where:

- P_f [-]: failure probability.
- N_f [-]: number of failures.
- N [-]: total number of simulations.

Below are the steps taken to conduct a Monte Carlo simulation.

1. Draw a random number between 0 and 1 as many times as there are random variables.
2. For each random variable, take the inverse of this random number.
3. Replace these new values in the limit state functions.
4. If the limit state function is negative, count N_f+1.
5. Repeat 1 to 4 until convergence.
6. Divide N_f by the number of times this was repeated.

Reaching convergence with MC can be time consuming, and sometimes proper convergence is hard to reach. Typically, the results should not change too much and a good criterion is to employ a parameter, called the coefficient of variation that can be calculated with Bernouilli's theorem and gives Equation A.9 (Dekking et al., 2005). It is assumed that convergence is achieved once this parameter reaches a value lower than 0.05.

$$V_{pf} = \frac{1}{\sqrt{NP_f}}. \tag{A.9}$$

With MC simulations, the smaller the failure probability, the more simulations are required to get a low coefficient of variation, and, thus, the more computation time. A rough estimate is that approximately 1 million samples are required, which makes the computational time relatively high. Some techniques have been developed to accelerate this process, such as importance sampling (Theodoridis, 2015).

Table A.3: Advantages and disadvantages of a level III analysis.

Advantages	Disadvantages
• Easy computation for variables with any distribution.	• High computational cost. • Usually different results every run.

B

Equations for wave parameters and breaker parameter

The case studies are all located in river areas, therefore, their waves are mainly ship and wind waves. It is expected that wind waves are the dominant ones during a flood. Thus the empirical equations of Young and Verhagen (1996) were used to calculate the parameters of those wind waves, see Equation (B.3) for the wave height and (B.4) for the wave period (Young and Verhagen, 1996).

$$\tilde{d_w} = \frac{g\, d_w}{U_{10}^2}, \tag{B.1}$$

$$\tilde{F} = \frac{g\, F}{U_{10}^2}, \tag{B.2}$$

$$H_{m0} = 0.24 \frac{U_{10}^2}{g} \left[\tanh\left(0.343 \tilde{d_w}^{1.14}\right) \tanh\left(\frac{4.41 \times 10^{-4}\, \tilde{F}^{0.79}}{\tanh\left(0.343 \tilde{d_w}^{1.14}\right)} \right) \right]^{0.572}, \tag{B.3}$$

$$T_p = 7.69 \frac{U_{10}}{g} \left[\tanh\left(0.1 \tilde{d_w}^{2.01}\right) \tanh\left(\frac{2.77 \times 10^{-7}\, \tilde{F}^{1.45}}{\tanh\left(0.1 \tilde{d_w}^{2.01}\right)} \right) \right]^{0.187}, \tag{B.4}$$

where:

- d_w [m]: water depth.
- F [m]: fetch of the wind.
- U_{10} [m/s]: wind speed at 10 m height.
- g [m/s^2]: gravitational acceleration constant.

The breaker parameter $\xi_{m-1,0}$ takes the type of breaking wave into account and can be found with Equation (B.5).

$$\xi_{m-1,0} = \frac{\tan\alpha}{\sqrt{\frac{H_{m0}}{1.56\,(0.9T_p)^2}}}. \tag{B.5}$$

C

Dominant wind direction

Before computing the failure probabilities of overtopping and overflow, the dominant wind direction needed to be found, this was done using a deterministic analysis (see Appendix A). By doing this, a considerable amount of computational time is saved, because all future computations can then consider only one wind direction instead of all 16 of them. The dominant wind direction is found by computing only the overtopping discharge since overflow is not influenced by the wind. Therefore, the overtopping discharge was computed for each wind direction and then multiplied by its probability of occurrence. Figures C.1 to C.3 shows the results in a graphs where the y-axis represents the overtopping discharge (going from 0 to 2 l/(s m)), the x-axis the water level, and each colour line represents one wind direction. The one with the highest discharge is the dominant wind. For Culemborg, this wind is the one with direction 270°N (Figure C.1), for Grebbedijk 247.5°N (Figure C.2), and for the Duursche Waarden 225°N (Figure C.3). From these figures, it can be observed that the Grebbedijk has the largest overtopping discharge, followed by the Duursche Waarden and Culemborg.

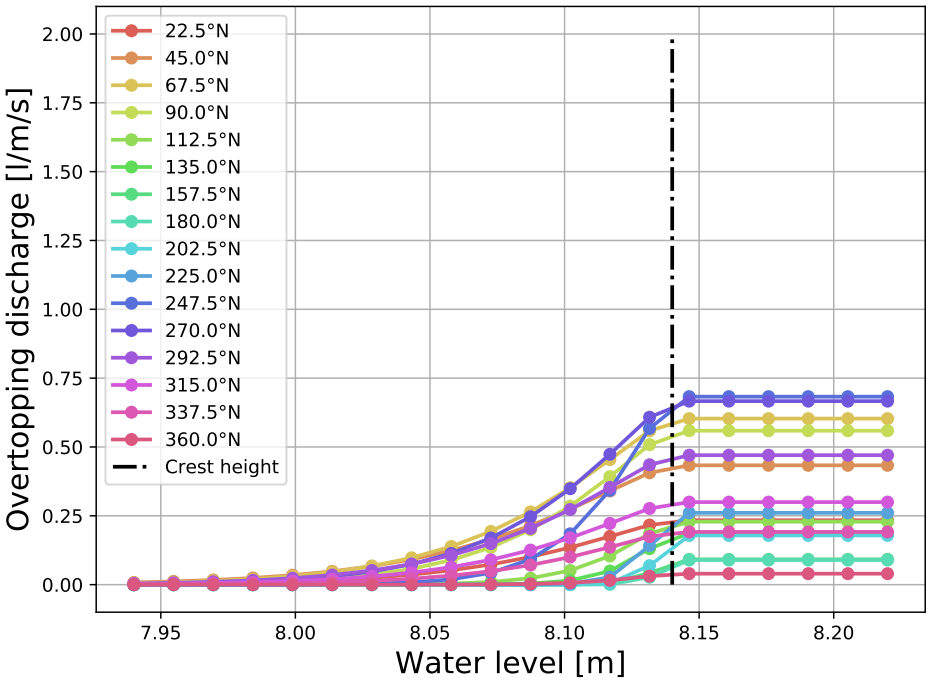

Figure C.1: Overtopping/overflow graph for different wind directions, Culemborg.

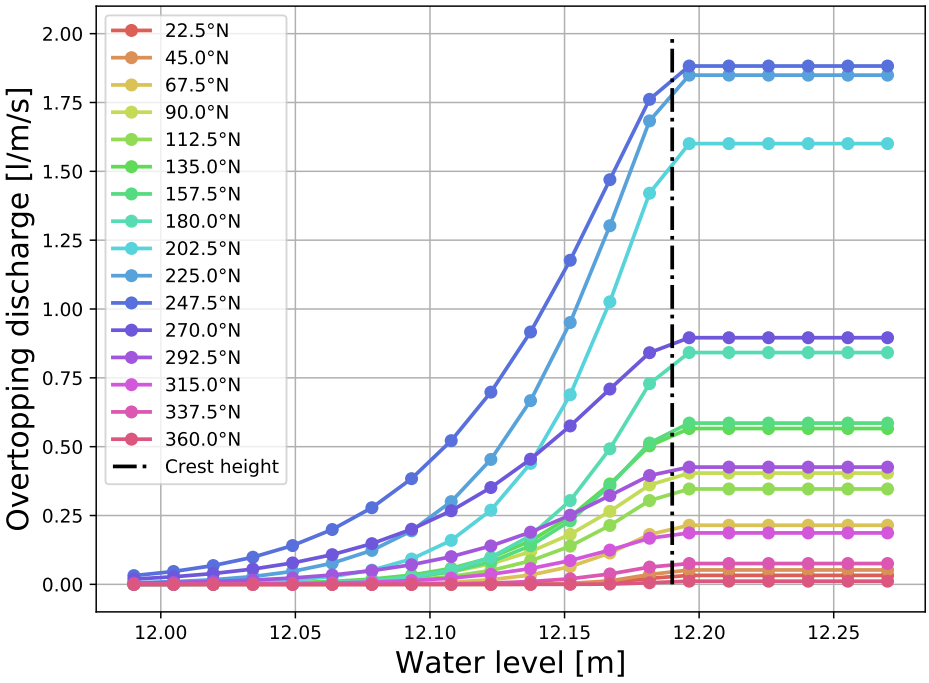

Figure C.2: Overtopping/overflow graph for different wind directions, Grebbedijk.

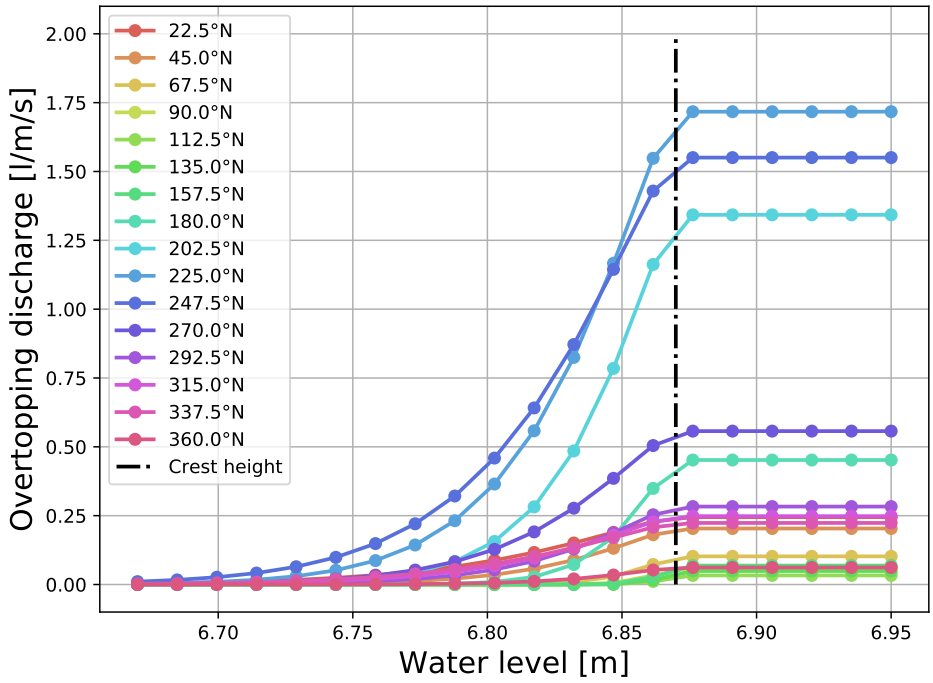

Figure C.3: Overtopping/overflow graph for different wind directions, Duursche Waarden.

D

Failure probability without vegetation

This Appendix presents a more thorough analysis of all case studies without vegetation effects. It uses all three reliability techniques mentioned in Appendix A to get a better understanding of both failure mechanisms individually.

D.1. Overtopping/overflow

The analysis starts with a presentation of two types of graphs for overtopping/overflow without considering vegetation. The first type of graph presents the results of a deterministic approach and the second of a FORM analysis. In the deterministic analysis, for this particular failure mechanism, no failure probability can be computed. Instead, the results are presented in terms of overtopping discharge, overflow discharge or both, expressed in l/(s m) on the y-axis. Therefore, the critical discharge is not yet considered, neither are the distributions of the variables, which are assigned design values. The water level is represented on the x-axis. In the FORM analysis, the graph is a fragility curve, which is a graph that consider probability on the y-axis and the load, in this case the water level, on the x-axis. The failure probabilities in the fragility curves are conditionalized by the water level. Therefore, it is important to keep that in mind when using the probabilities on the y-axis, i.e. the distribution of the water level is not yet taken into account. Now the critical discharge parameter is taken into account, together with the mean and standard deviation of the stochastic variables.

The deterministic analysis (see the three graphs on the first row of Figure D.1), show the overtopping and overflow discharges on the y-axis going from 0 to 40 l/(s m). The second type of graphs, using the FORM analysis (see the three graphs on the lower row of Figure D.1), shows the conditional failure probability, going from 10^{-20} to 1. The x-axes of both types of fragility curves indicate water levels from 0.2 m below the crest height to 0.08 m above it. The range of water level was chosen because if water levels are much lower they are less interesting as no overtopping occurs, and if they are much higher mainly overflow takes place, which is not much affected by vegetation. These graphs and scales were used throughout the analysis of this failure mechanism.

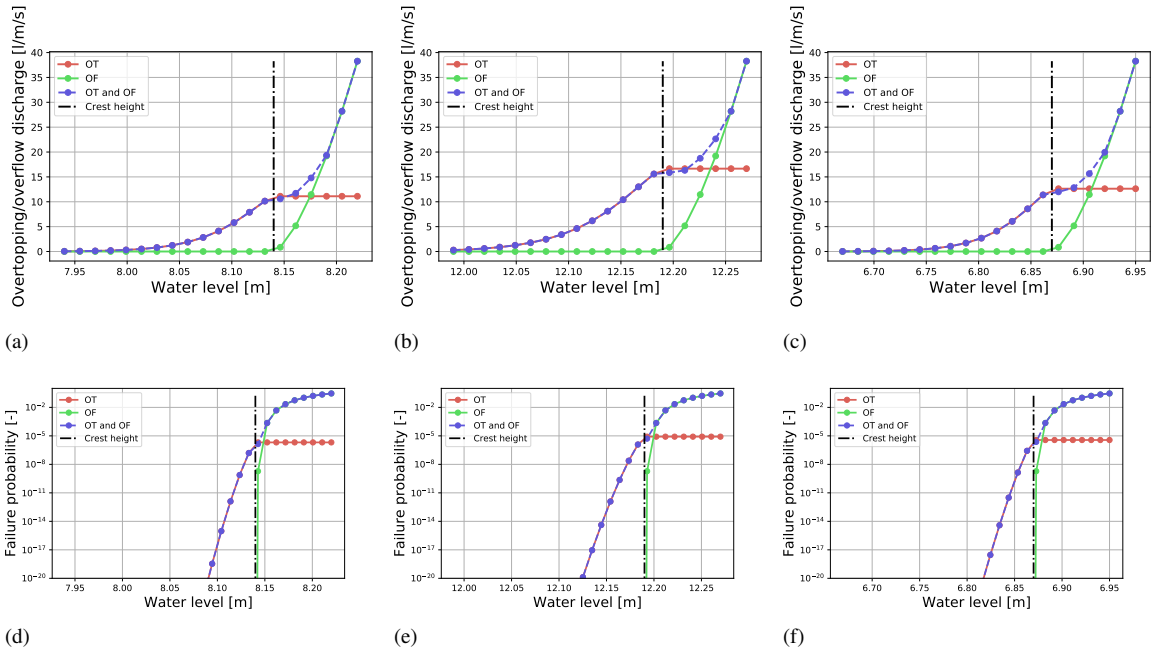

Figure D.1: Fragility curves representing overtopping (in red), overflow (green) and combination of overtopping and overflow (in blue). The top three graphs are found using a deterministic approach, the bottom three a FORM analysis. Results are found using the case study's respective dominant wind direction: (a) and (d) Culemborg, (b) and (e) Grebbedijk, (c) and (f) Duursche Waarden.

The failure mechanisms overtopping and overflow were for now considered separately (red and green lines, respectively) and then combined (purple line) to better understand the mechanisms, which would later on facilitate the understanding of how vegetation affects this failure mechanism. It can be observed that the overtopping discharge and the failure probability gradually increases with higher water levels until the water level reaches the crest height. The discharge and probability then become constant. This behavior is explained by the definition of overtopping, which is the amount of water that topples over a dike due to a wave. Once the water level exceeds the crest height all of the wave's discharge goes to the landside, thus the maximum discharge of the wave passes to the other side and this value is constant no matter how much more the water level increases.

For overflow, the discharge is zero when the water level is below the crest height, and once it exceeds it (negative freeboard) the discharge increases exponentially. This behavior is also explained by the definition of overflow, which is the amount of water that flow continuously over the dike, this amount is zero when the water level has not exceeded the crest height, as no water can flow over the dike continuously. When the water level increases above the crest height, water flows continuously over the dike. This amount increases the more the water level increases.

In the combined case any water flowing over the crest is considered. Therefore, the line first follows the overtopping line (water level is below the crest, the only water flowing over the dike comes from the waves), then there is a transition period (small amount of water flows continuously over the crest, and a lot of the wave's discharge flows over that), and finally, it follows the overflow line (water level is much higher than the crest, the waves are not felt anymore, and overflow dominates). The EuroTop manual provides guidelines on this transition period (see

Chapter 4), however, this guideline leads to a discontinuity between the transition period and the moment only overflow occurs (van der Meer et al., 2018). Therefore, in order to smooth out the curve, a small adjustment was made: during the transition period the overtopping discharge was multiplied by a factor (see Equation(D.1)), which would take a value of one when the freeboard is zero, and become zero the moment only overflow needs to be considered. This marginal change is not expected to influence much the failure probability.

$$f = \frac{h_w - h_{lim}}{h_c - h_{lim}} \tag{D.1}$$

Where:

- f [-]: factor used to multiply the overtopping discharge during the transition period.
- h_{lim} [m]: water level for which no overtopping should be taken into account anymore at the end of the transition period ($h_{lim} = h_c + 0.3\ H_{m0}$)

Finally, the distribution of the water level was added, which can be done with a FORM or a MC analysis. Using a FORM analysis, which was the faster option, was not possible mainly due to two reasons:

- The derivative of the limit state function with respect to the water level is zero and, thus, it does not allow for convergence. For overflow, water levels below the crest height lead to a zero derivative and the water level is mostly under the crest, whereas for overtopping this is because the waves are very small.
- The distribution of the water level is the problem. Since it is not normally distributed, it needs to be transformed using a mean and a standard deviation based on the PDF and CDF of the water level. The values coming out of the CDF and PDF for high water levels (close to the design point) are basically zero and, thus, the gradient is roughly zero and convergence cannot be found in those areas.

A MC analysis can be performed. The probabilities presented are, from now on, no longer conditionalized on the water levels, as their distribution is now taken into account. The empirical distribution of the water level was taken from the governmental program *Hydra-NL* for the year 2050 and was fitted to a Gumbel distribution as it is commonly done in practice. However, the fit was based on the mean and standard deviation of the water level instead of the required failure probability. Therefore, the fit is conservative and the failure probabilities presented below are higher than in reality. This was, however, necessary because using the empirical fit would provide extremely low probabilities, which would cost a high amount of computational time when using a MC analysis. Furthermore, fitting the distribution using the required failure probability and the "Decimeringshoogte" proved to be more erroneous than using the mean and the standard deviation, the failure probabilities were even higher. This adjustment to reduce computational time is considered acceptable as this study only looks at relative changes rather than properly assessing the dike.

In order to obtain reliable results, the coefficient of variation of the MC analysis needs to be lower than 0.05, see Section 4.1 and Equation (4.3). Therefore, one million simulations were made for the Culemborg and Grebbedijk case studies, and 13 million for the Duursche Waarden because of its lower failure probabilities, which required more simulations to achieve a roughly

similar coefficient of variation. The outcome of the MC is presented in Table D.1 together with the coefficients of variation found from Equation (4.3).

Table D.1: Approximate failure probability considering one cross section and the overtopping/overflow mechanism without vegetation effects for each case study.

	Culemborg	Grebbedijk	Duursche Waarden
Failure probability of overtopping and overflow considering one cross section [-]	6e-04	2e-03	3e-05
Number of simulations in million	1	1	13
Coefficient of variation [-]	0.04	0.022	0.05

The MC analysis, unlike FORM, does not allow for the computation of the design point, which can be very useful to better understand the failure mechanism. However, some techniques exist to still get the "alpha" values or sensitivity indices to quantify the correlation between the input variables and the output variable. In this study, the FAST sensitivity indices from OpenTurns were used, which are based on the Fourier decomposition ("OpenTurns", n.d.). The FAST indices range from zero to one and the closer the index is to one, the greater the importance of that variable. The values of these indices per variable and case studies are presented in Table D.2, where it can be noted that the dominant variable in overtopping/overflow is by far the critical discharge. The second most important variable is the wind speed, closely followed by the water level. The bottom level is the variable with the smallest influence. From this table it can be expected that the vegetation effect of the erosion resistance of the inner slope, which influences the critical discharge, is probably going to have a considerable impact on the failure probability.

Table D.2: FAST sensitivity indices per variables for each case study.

	Culemborg	Grebbedijk	Duursche Waarden
Bottom level [m]	7.38e-05	4.03e-04	8.77e-05
Critical discharge [l/(s m)]	6.52e-01	5.59e-01	7.07e-01
Water level [m]	1.27e-04	2.26e-03	2.20e-05
Wind speed [m/s]	3.48e-04	2.95e-04	3.43e-05

D.2. Internal erosion

The analysis starts with a presentation of two types of fragility curves for internal erosion without considering vegetation. The first type uses a deterministic approach and the second a FORM analysis. The deterministic analysis presents the results in terms of safety factors, which is the strength divided by the load. The FORM analysis computes failure probabilities. The fragility curves have the water level on the x-axis, going from 3 m below the crest height to 1 m above it. This wider range in the x-axis compared to overtopping/overflow is because, for

internal erosion, failure does not only occur when the water level is close to the crest height, usually it happens before. Figure D.2 presents the results of the deterministic analysis (top three graphs) and the FORM analysis (three lower graphs) for all three sub failure mechanisms of internal erosion (uplift in red, heave in green and piping in purple).

It can be noticed that the factor of safety decreases, and consequently the failure probability increases, for all three sub-mechanisms with increasing water level. This is because the higher the water level the larger the pressure difference between the river side and the land side and, thus, the load increases. It can be observed that the sub-mechanism piping has the highest factor of safety, hence lowest failure probability, for all three case studies and is, thus, the safest and dominant sub-mechanism. Looking at all three case studies, Culemborg seems to be the safest against these failure mechanisms, followed by Duursche Waarden. It is also noted that for all three case studies the safety factor for uplift and heave are relatively similar.

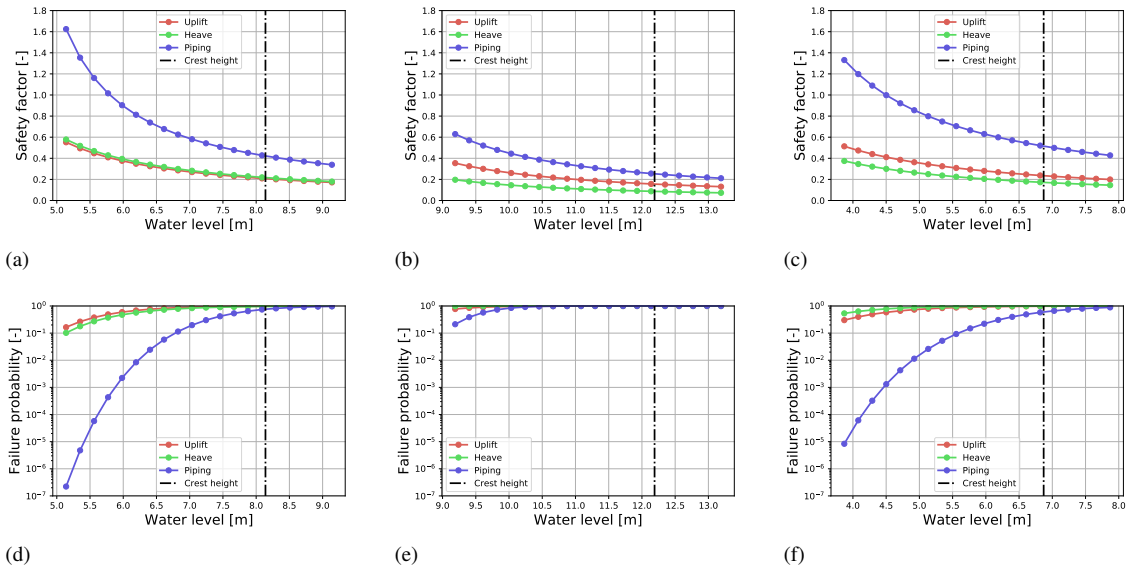

Figure D.2: Fragility curves without vegetation effects found using a deterministic approach (top three graphs) and a FORM analysis (lower three graphs) considering only the failure mechanism internal erosion. The red line represents uplift, the green heave and the purple piping. All three case studies are presented: (a) and (d) Culemborg, (b) and (e) Grebbedijk, (c) and (f) Duursche Waarden.

To obtain the full failure probability of internal erosion, the distribution of the water level can be added using a MC or a FORM analysis. The latter was chosen due to its lower computational time and the results are gathered in Table D.3. The first row of this table shows the failure probability when considering the empirical distribution of the water level and the second considering the conservative fitted Gumbel distribution. Because the failure probabilities are higher for this failure mechanism, the empirical distribution could be used but it can be seen that both are in the same order of magnitude.

Table D.3: Failure probability (P_f) of each sub-mechanism of internal erosion for all case studies considering the empirical water distribution and the more conservative fitted Gumbel distribution according to the mean.

		Culemborg	Grebbedijk	Duursche Waarden
P_f with empirical distribution of the water level [-]	Uplift	1.28e-01	3.93e-01	3.30e-01
	Heave	1.02e-01	6.63e-01	5.44e-01
	Piping	3.85e-03	2.09e-01	3.40e-03
P_f with Gumbel distribution for the water level fitted with the mean [-]	Uplift	1.01e-01	4.76e-01	3.73e-01
	Heave	7.48e-02	7.61e-01	5.91e-01
	Piping	4.12e-03	1.82e-01	1.75e-03

An advantage of the FORM analysis is that the design points and the importance factors, which are the squared "alpha" values, can be computed, for each sub-mechanism and case study, see Table D.4. The higher the importance factor, the more influence the parameter has on the failure probability. For uplift and heave, the dominant parameter is clearly the water level and the blanket thickness is next, which means that the reduction in blanket thickness is expected to influence these two mechanisms significantly. For piping, the water level is also the dominant parameter now followed by the hydraulic conductivity of the aquifer, and finally the blanket thickness is of smaller importance.

Table D.4: Design point and importance factors (imp. factor) for each sub-mechanism and case study.

		Culemborg		Grebbedijk		Duursche Waarden	
		Design point	Imp. factor	Design point	Imp. factor	Design point	Imp. factor
Uplift	k	6.89e-04	1.92e-03	5.3e-04	2e-03	2.66e-04	1.98e-02
	D	2.46e01	5.68e-04	2.94e01	1.24e-04	4.64e01	4.64e-03
	d	3.82	1.06e-01	1.87	9.67e-02	3.31	5.33e-01
	k_h	8.68e-07	3.2e-03	8.89e-07	2.05e-03	8.67e-07	2.27e-02
	L_f	1.99e01	8.05e-05	4.99	1.39e-04	1.99e01	1.1e-04
	h_p	3.49	5.63e-03	7.00	5.69e-03	1.49	1.18e-02
	y_{sat}	1.43e01	4.18e-02	1.76e01	1.64e-02	1.59e01	1.41e-01
	m_u	9.79e-01	2.06e-02	9.92e-01	1.11e-02	9.83e-01	7.59e-02
	h_w	5.44	8.20e-01	8.67	8.66e-01	3.97	1.91e-01
Heave	k	6.97e-04	3.58e-03	5.16e-04	1.08e-02	2.56e-04	2.38e-02
	D	2.47e01	6.45e-04	2.93e01	2.52e-03	4.6e01	2.75e-03
	d	3.69	1.47e-01	2.1	5.63e-01	3.73	5.69e-01
	k_h	8.65e-07	3.08e-03	9.137e-07	1.15e-02	9.01e-07	2.06e-02
	L_f	1.99e01	1.08e-04	5.00	1.25e-05	1.99e01	1.11e-03
	h_p	3.49	4.97e-03404	7.01	4.75e-02	1.5	1.7e-02
	i_c	4.58e-01	7.4e-02	5.13e-01	3.02e-01	4.96e-01	3.27e-01
	h_w	5.55	7.66e-01	8.29	6.23e-02	3.89	3.93e-02
Piping	k	1.08e-03	1.41e-01	5.66e-04	3.74e-02	5.09e-04	2.81e-01
	D	2.58e01	9.29e-03	2.97e01	2.95e-03	4.83e01	8e-03
	d	3.4	8.32e-02	1.87	9.34e-03	2.87	8.94e-02
	L_f	1.97e01	1.63e-03	5.00	3.15e-05	1.96e01	0.00278
	h_p	3.48	7.45e-03	6.99	3.15e-03	1.47	0.0128
	d_{70}	2.66e-04	1.01e-02	3.01e-04	5.98e-03	3.22e-04	4.11e-02
	m_p	9.09e-01	7.7e-02	9.80e-01	1.8e-02	8.8e-01	1.39e-01
	h_w	6.64	6.7e-01	9.43	9.23e-01	5.06	4.25e-01

E

One vegetation effect on overtopping/overflow

In this Appendix four of the five vegetation effects influencing this failure mechanism are studied more thoroughly. The results are, when possible, presented with fragility curves, which are graphs that consider the safety factor or failure probability on the y-axis and the load, in this case the water level, on the x-axis. The failure probabilities in the fragility curves are conditionalized by the water level. Therefore, it is important to keep that in mind, i.e. the distribution of the water level is not yet taken into account. The overall failure probabilities of each failure mechanism are computed using a FORM or a MC analysis. These results are presented in three different graphs denoted a, b and c. The different y-axis of these graphs are listed below and all have the same x-axis, which depends on the vegetation effect under study.

(a) The first type of graphs presents on the y-axis the failure probability on a logarithmic scale.
(b) The second type of graphs considers the reliability index (see Equation (E.1)) on the y-axis. In this case, an increase in failure probability is denoted by a decrease in reliability index.
(c) The third type depicts the percentage difference in failure probability (see Equation (E.2)) on the y-axis. For this type of graphs an increase in probability is shown by a negative value, and a positive value indicates a reduction in failure probability. Special attention should be paid to these graphs as the scale of the y-axis is sometimes changed to better perceive some effects.

$$\beta = \Phi^{-1}(\mathrm{P}_{f\,\mathrm{veg}}), \tag{E.1}$$

$$\Delta \mathrm{P}_f = 100 \frac{\mathrm{P}_{f\,\mathrm{no\ veg}} - \mathrm{P}_{f\,\mathrm{veg}}}{\mathrm{P}_{f\,\mathrm{no\ veg}}}, \tag{E.2}$$

where:

- β [-]: reliability index or beta factor.
- Φ^{-1} [-]: inverse CDF of the standard normal distribution.

- ΔP_f [%]: difference in failure probability.
- $P_{f\,\text{no veg}}$ [-]: failure probability without vegetation. For overtopping/overflow this means that there is no increase in water level, no wave reduction (WC=1), the roughness factor is one and the critical discharge is log-normally distributed with mean 100 and standard deviation 120. For internal erosion this means that there is no increase in water level and no tree toppling over, i.e. no decrease in blanket thickness and the exit point is at the toe of the dike.
- $P_{f\,\text{veg}}$ [-]: failure probability with vegetation. For overtopping/overflow this means a change in water level, WC, roughness factor and/or critical discharge. For internal erosion this means a change in water level, blanket thickness and/or exit point.

E.0.1. Increase in water level

The effect of an increase in water level could only be studied showing the overall failure probability, because the results could not be presented with fragility curves. Two changes in water level were made:

1. First, different water level distributions based on different assessment years were extracted from *Hydra-NL*. The distribution of the current water level, 2017, and the predicted water levels of 2050 and 2100 (based on the KNMI W+, they include climate change) were chosen (Duits, 2019). These data were fitted to a Gumbel distribution using their mean and standard deviation values. As mentioned above, this fitting leads to a conservative estimation of the water level distribution. Figure E.1 shows the difference in the Cumulative Density Functions (CDF) for the three years considered. It can be observed that the further away the year of assessment, the higher the probabilities of higher the water levels, thus, there will most probably be an increase in failure probability.

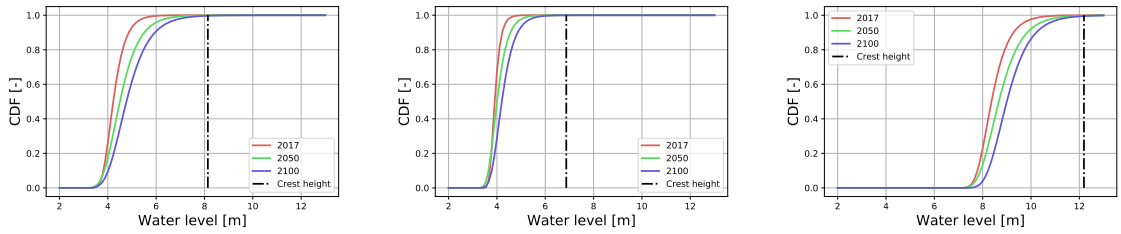

(a) (b) (c)

Figure E.1: Water level CDF fitted by a Gumbel distribution using the mean and the standard deviation of the empirical data, which differs per year. In red the data of the year 2017 is used, in green the predicted data for 2050 and finally in purple the predicted data from 2100. All three case studies are represented: (a) Culemborg, (b) Grebbedijk, (c) Duursche Waarden.

The results of the MC analysis for those different assessment years are presented in Figure E.2, where all three case studies are depicted as dashed-dotted lines. The dotted lines indicate the required failure probability for a cross section considering this failure mechanism. In Figure E.2(c), the difference in failure probability is based on the water level of the year 2050. It can be noted that, in Figure E.2(b), there is a point missing for the Duusche Waarden in the year 2017. This is because the failure probability for that year is extremely small, close to zero.
Significant differences are observed when different assessment years are taken for the as-

sessment of each dike section. Looking at Figure E.2(a), the failure probability using the water levels of 2017 or 2100 changes from approximately 5e-06 to 5e-03 (i.e. a thousand-fold) for Culemborg, and from 0 to 4e-04 for the Duursche Waarden. Only the Grebbedijk has a less impressive change going from approximately 3e-06 to 5e-05. Figure E.2(b) shows the same gradient, between the water levels of 2050 and 2100. The Duursche Waarden shows the steepest gradient followed closely by Culemborg and Grebbedijk. In Figure E.2(c) it looks like the failure probabilities in 2017 are all 100% lower than the ones in 2050 for all case studies. This is probably because the failure probabilities of 2017 are so low compared to 2050 that when taking the difference almost no change is perceived. Finally, the Duursche Waarden shows the biggest percentage increase in the failure probability (750%) in 2100, followed by Culemborg (300%) and Grebbedijk (100%).

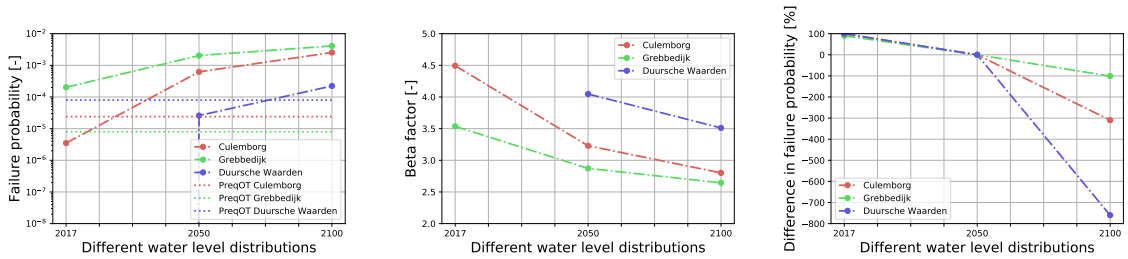

(a) (b) (c)

Figure E.2: Results of a change in water level distribution for the failure mechanisms of overtopping/overflow using an MC analysis: (a) shows the failure probability in log-scale, the dashed dotted line shows the computed failure probability and the dotted line shows the required failure probability. Ideally the required failure probability is above the computed one, however, the latter is overly conservative due to the Gumbel fit. (b) shows the same results but now in terms of reliability index (β), which is found using the inverse CDF of the standard normal distribution. (c) shows the percentage difference in failure probability with respect to the year 2050.

2. Secondly, a simple constant increase in the distribution of the water level of the assessment year 2050, going from 0 to 0.2 m, was made. Figure E.3 shows this effect. This change had a significant impact on the failure probability, although less than choosing a different year of assessment. For a constant increase of 0.2 m, Figure E.3(a) shows an increase in failure probability but in the same order of magnitude, Culemborg's failure probability goes from approximately 6e-05 to 1e-05. In Figure E.3(b) the reliability index changes marginally and Figure E.3(c) shows an increase in failure probability of approximately 45%, 40% and 80% for an increase of 0.2 m for Culemborg, Grebbedijk and Duursche Waarden respectively. Here again, the Duursche Waarden seems to be the most impacted by the increase in failure probability, whereas Culemborg and Grebbedijk seem to have approximately the same impact.

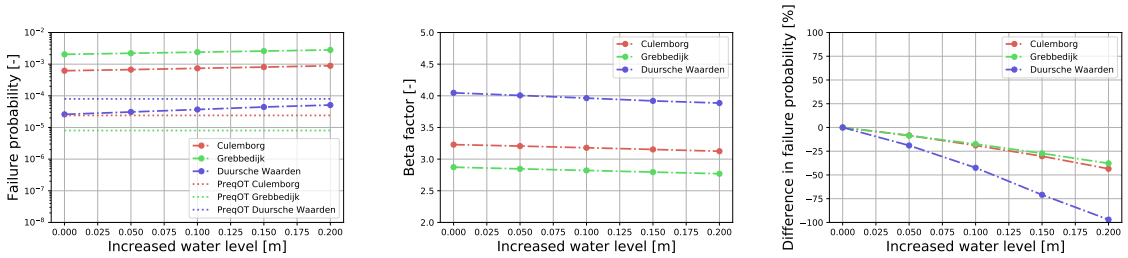

(a) (b) (c)

Figure E.3: Results of a constant increase in water level for the failure mechanisms of overtopping/overflow using an MC analysis: (a) shows the failure probability in log-scale, the dashed dotted line shows the computed failure probability and the dotted line shows the required failure probability. Ideally the required failure probability is above the computed one, however, the latter is overly conservative due to the Gumbel fit. (b) shows the same results but now in terms of reliability index (β), which is found using the inverse CDF of the standard normal distribution. (c) shows the percentage difference in failure probability with respect to the year 2050.

It can be concluded that a change in water level has a significant impact on Dutch upper-river dikes. Especially the assessment year considered is of high importance, which shows that the impact on the failure probability of any increase in water level due to vegetation is notably less than using the water level distribution of a later year.

E.0.2. Increased cohesion

The second effect, erosion resistance of the inner slope, could only be studied by a FORM and a MC analysis. It was studied by modifying the parameters of the critical discharge in order to simulate a change in erosion resistance of the inner slope. Its parameters were changed based on the two sets of parameters recommended by the WBI (see Table 2.2) for wave heights between 0 and 1 m. The first set is a log-normal distribution with a mean of 100 l/(s m) and a standard deviation of 120 l/(s m), the second has a mean of 225 l/(s m) and a standard deviation of 250 l/(s m). The mean of both sets was increased and decreased by 20%, to simulate a slightly higher and lower than average grass quality respectively, leading to six different sets of parameters studied.

The results presented in a fragility curve from a FORM analysis are presented in Figure E.4, where it can be concluded that the choice in parameters of the critical discharge influences the conditional failure probability for every water level. Therefore, it can already be concluded that this effect is of high importance. Looking at the water level when equal to the crest height, a critical discharge with a log-normal distribution (mean and standard deviation of 225 and 250 l/(s m)) has a failure probability of approximately 10^{-5} for Culemborg and if the mean is reduced by 20%, the failure probability is approximately 10^{-9}, i.e. ten thousand times smaller. From the graph, it looks like Grebbedijk is the case study that is most impacted by this effect, as it has the biggest difference between the red line and the purple line, followed by Duursche Waarden and Culemborg.

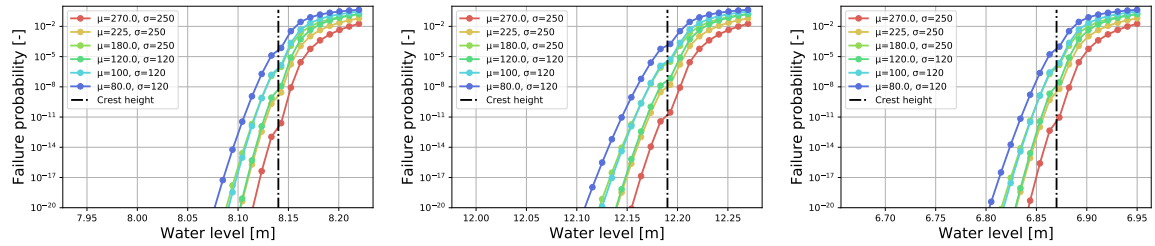

(a) (b) (c)

Figure E.4: Fragility curves with different parameters for the critical discharge found using a FORM analysis considering only the failure mechanism overtopping/overflow. All three case studies are presented: (a) Culemborg, (b) Grebbedijk, (c) Duursche Waarden.

The results of the MC analysis, which include the water level distribution, are shown in Figure E.5. Looking at Figures E.5(a) and (b), the failure probabilities considering different parameters are of the same order of magnitude, and the reliability indices do not show a large increase with lower mean values. The percentage difference graph, Figure E.5(c), which has a y-axis now going from -20% to 50%, shows that up to a 30% change in failure probability can be observed when changing the parameters of the critical discharge for Duursche Waarden, and 20% for the two other case studies. It seems Duursche Waarden is the most impacted by this effect once again.

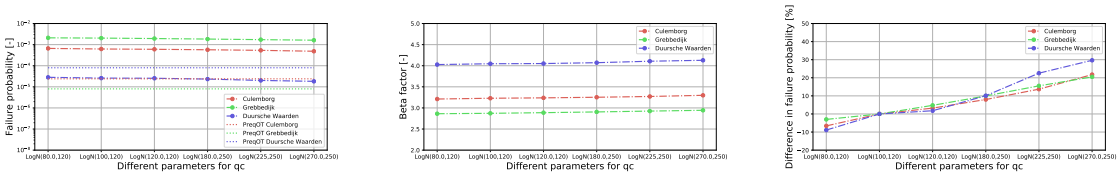

(a) (b) (c)

Figure E.5: Results of differing critical discharge parameters for the failure mechanisms of overtopping/overflow using an MC analysis: (a) shows the failure probability in log-scale, the dashed dotted line shows the computed failure probability and the dotted line shows the required failure probability. Ideally the required failure probability is above the computed one, however, the latter is overly conservative due to the Gumbel fit. (b) shows the same results but now in terms of reliability index (β), which is found using the inverse CDF of the standard normal distribution. (c) shows the percentage difference in failure probability with respect to the year 2050.

As a conclusion, this effect has an important effect on the failure probability and should definitely be studied further. Its quantitative impact is in the same order of magnitude as the increase in water level.

E.0.3. Wave height reduction

The effects of up to a 50% wave height reduction were studied using a deterministic, FORM, and MC analyses. The results in terms of fragility curves found with a deterministic and a FORM analysis are presented in Figure E.6, in the first and second rows, respectively. Looking at the deterministic analysis, it is observed that the influence of the wave height increases with increasing wave water level and is zero when the water levels are higher than the crest height. This increase in effect is because the wave heights are higher with higher water levels, so a reduction has a higher impact. When the water levels are higher than the crest, only overflow

occurs, which explains why the wave height reduction has no effect. Looking at water levels at the crest height, it can be observed that approximately 5, 8 and 7 l/(s m) discharge reduction can be achieved with 50% wave reduction for Culemborg, Grebbedijk and Duursche Waarden, respectively.

The FORM results, seem to show an opposite effect, the impact is higher for the lower water level. This is because the critical discharge is taken into account, thus there is a limit in the amount of water that can flow over the dike. Therefore, when the water levels are close to the crest, high overtopping discharge are observed, and reducing those might not be enough to be below the limit imposed by the critical discharge, hence smaller effects due to wave reduction are observed. Looking at the different case studies, and the difference between the purple line (no wave reduction) and the red line (50% wave reduction), it can be concluded that Grebbedijk would benefit the most from wave height reduction, followed by Duursche Waarden and Culemborg. This can be explained by the higher overtopping discharges found for Grebbedijk, which imply higher wave heights and, thus, a change of 50% wave height has a stronger impact.

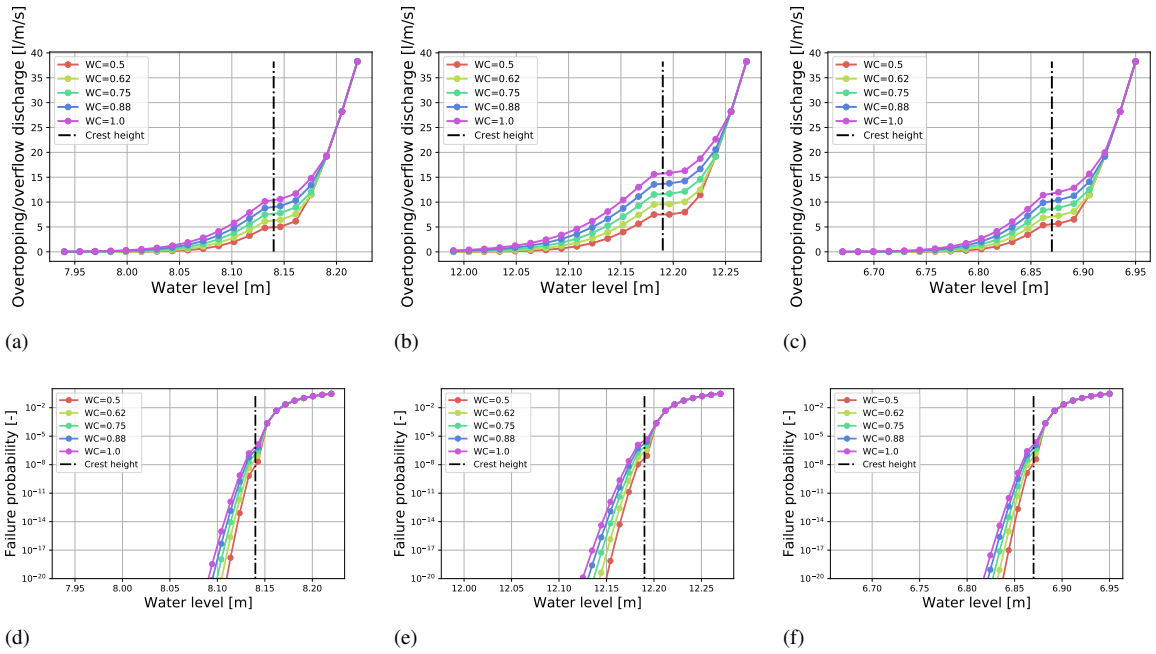

Figure E.6: Fragility curves with different wave height reduction found using a deterministic approach (top three graphs) and a FORM analysis (lower three graphs) considering only the failure mechanism overtopping/overflow. All three case studies are presented: (a) and (d) Culemborg, (b) and (e) Grebbedijk, (c) and (f) Duursche Waarden.

The results of the MC analysis, which considers the distribution of the water levels, are presented in Figure E.7 with the x-axis showing different vegetation scenarios represented by the wave coefficient. Figures E.7(a) and (b) show no change due to a wave height reduction. This difference compared to the results of fragility curves is due to the distribution of the water levels now being considered. The changes that were perceived in the previous analysis were very close to the crest height, the probability of these high water levels are extremely low and, therefore, any change is unseen because it is multiplied by a very small probability. Looking at Figure E.7(c), where the y-axis goes from -2% to 5%, it is possible to see that there is a

difference between each wave reduction but relatively marginal, with only up to 1% decrease in failure probability for a 50% wave height reduction. This vegetation effect seems to have approximately the same order of magnitude on each case study.

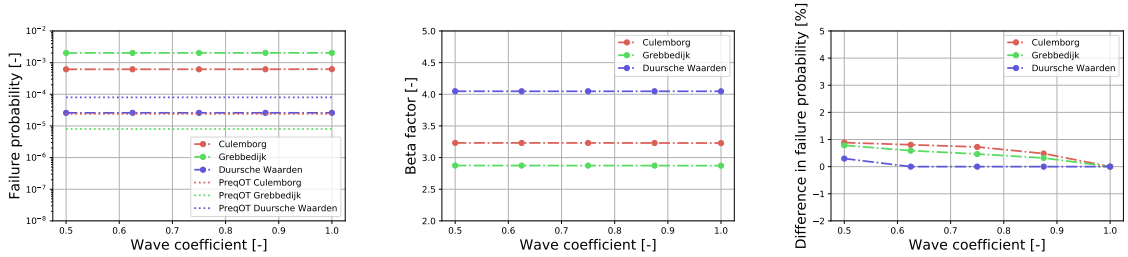

(a) (b) (c)

Figure E.7: Results of a decrease in wave height for the failure mechanisms of overtopping/overflow using an MC analysis: (a) shows the failure probability in log-scale, the dashed dotted line shows the computed failure probability and the dotted line shows the required failure probability. Ideally the required failure probability is above the computed one, however, the latter is overly conservative due to the Gumbel fit. (b) shows the same results but now in terms of reliability index (β), which is found using the inverse CDF of the standard normal distribution. (c) shows the percentage difference in failure probability with respect to the year 2050.

It can be concluded that the effect of wave height reduction for dike in the upper-river areas is marginal, due to their initially low wave height.

E.0.4. Increased roughness

The effect of an increased roughness on the outer slope was simulated by lowering the roughness factor up to a value of 0.8, the former being the scenario with the highest roughness. The results represented by fragility curves using a deterministic and a FORM analysis are found in Figure E.8, where it can be concluded that improving the roughness of the outer slope has a smaller effect than reducing the wave height. With a roughness factor of 0.8, looking at the upper figures and water levels approximately 0.05 m lower than the crest height, around 1, 2 and 1 l/(s m) discharge reduction can be achieved for each case study, respectively. The decrease in the roughness factor does not have the same effect for each water level since no effect is observed for the cases next to the crest height, higher, and a few centimeters lower. From the lower graphs, with the FORM analysis, it can be observed that low roughness factors provide lower failure probabilities and that the effect is higher with lower water levels, and when the water level is at the crest height no effect is observed. This is explained because the higher the water level, the more the grass on the outer slope is drowned and, thus, the smaller effect it can have. Looking at the difference between the purple line (no change in the roughness factor) and the red line (roughness factor of 0.8) for each case study, Grebbedijk benefits the most from a reduction roughness factor, followed by Duursche Waarden and Culemborg. These differences can be explained by the fact that the Grebbedijk has the highest overtopping discharge and, thus, the change in roughness has the most influence.

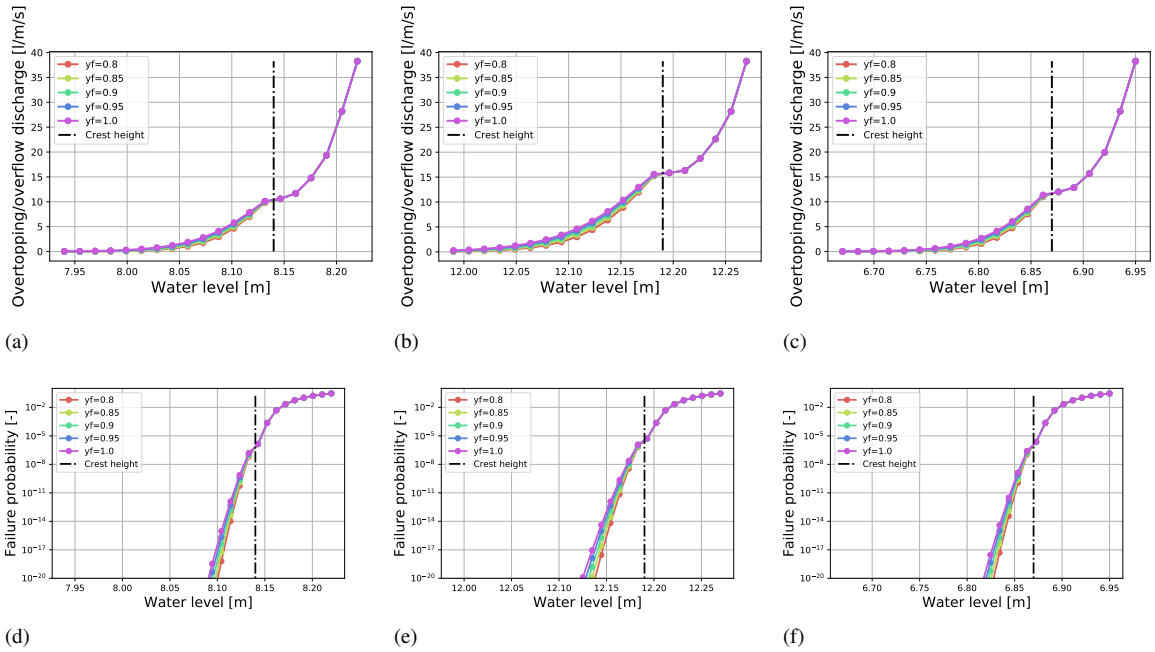

Figure E.8: Fragility curves with different roughness factors found using a deterministic approach (top three graphs) and a FORM analysis (lower three graphs) considering only the failure mechanism overtopping/overflow. All three case studies are presented: (a) and (d) Culemborg, (b) and (e) Grebbedijk, (c) and (f) Duursche Waarden.

The results of the MC analysis are presented in Figure E.9, where the x-axis shows different vegetation scenarios represented by different roughness factors. From Figures E.9(a) and (b) it can be noticed that the change in failure probability is marginal. Figure E.9(c), where the y-axis goes from -2% to 5%, reinforces this observation by showing that a difference of less than 0.2 % approximately is observed. The percentage difference is the highest for Culemborg, whereas it is everywhere zero for Duursche Waarden.

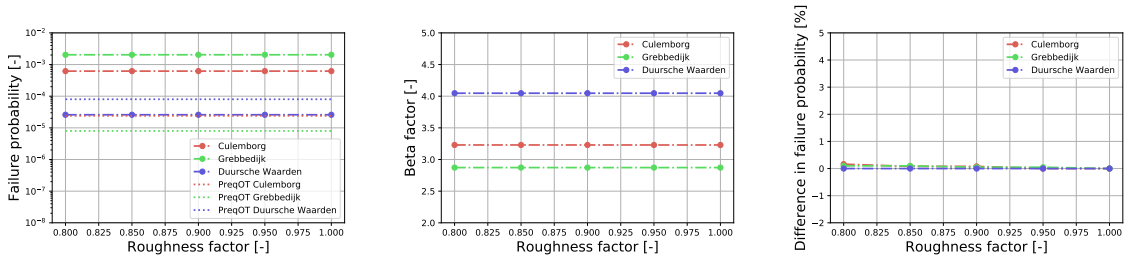

Figure E.9: Results of a decrease in roughness factor for the failure mechanisms of overtopping/overflow using an MC analysis: (a) shows the failure probability in log-scale, the dashed dotted line shows the computed failure probability and the dotted line shows the required failure probability. Ideally the required failure probability is above the computed one, however, the latter is overly conservative due to the Gumbel fit. (b) shows the same results but now in terms of reliability index (β), which is found using the inverse CDF of the standard normal distribution. (c) shows the percentage difference in failure probability with respect to the year 2050.

It can be concluded that the effect of roughness is not relevant for upper-river dikes due to their low wave heights. High wave only occur at high water levels, which drowns the vegetation and

therefore its roughness is not felt anymore. An overview of the individual effects of vegetation on the failure probability overtopping/overflow are found in Table E.1.

Table E.1: Overview of the studied effects of vegetation on the failure mechanism overtopping/overflow.

Effect studied	Results
Increase in water level. A constant increase up to 0.2 m was added to the water level distribution.	*High negative impact.* With 0.2 m increase there was between a 50% and 100% increase in failure probability. The failure probability went from 6.2e-04, 2e-03 and 2.6e-05 to 8.9e-04, 2.8e-03 and 5.1e-05. The reliability when from 3.23, 2.87 and 4.05 to 3.12, 2.87 and 3.88 for Culemborg, Grebbedijk and Duursche Waarden respectively. Thus 0.1 change in reliability index for the first two and 0.6 for the second.
Erosion resistance of the outer slope. The parameters of the critical discharge were increased and decreased by 20% to analyse the effect of an above and below than average grass quality respectively.	*High positive or negative impact.* The changes in failure probability ranged from approximately -10% or -5% to 30%, 20%, a positive value was a positive impact and vice versa. Looking at the lowest critical discharge and the highest the failure probability went from 4.8e-04, 1.6e-03 and 1.8e-05 to 6.6e-04, 2.1e-03 and 2.8e-05 for Culemborg, Grebbedijk and Duursche Waarden respectively. The reliability indexes changed from 3.3, 2.9 and 4.13 to 3.2, 2.86 to 4.03 for Culemborg, Grebbedijk and Duursche Waarden respectively.
Wave height reduction. The wave height computed was multiplied with a wave coefficient ranging from 0 to 0.5 to simulate the effect of up to 50% wave height reduction.	*Low positive impact.* Not more than 1% decrease in failure probability was observed. For a 50% decrease of wave height the failure probabilities went from 6.15e-04,2.022e-03 and 2.58e-05 to 6.205e-04, 2.038e-03 and 2.59e-05 for Culemborg, Grebbedijk and Duursche Waarden respectively. The reliability index went from 3.23, 2.875 and 4.0478 to 3.229, 2.872 and 4.0471 for Culemborg, Grebbedijk and Duursche Waarden respectively.
Increased roughness on outer slope. The effect of a rougher slope was analysed by changing the roughness factor, which took values from 0.8 to 1. The former representing the scenario with the highest roughness and the latter the scenario with no change due to vegetation effect.	*Negligible positive impact.* Less than 0.1% change in failure probability. Looking at the different between 0.8 and 1 in roughness factor the failure probability went from 6.195e-04 and 2.036e-03 to 6.205e-04 and 2.038e-03 for Culemborg and Grebbedijk respectively. The reliability index changed from 3.2297 and 2.8725 to 3.2293 and 2.8722 for Culemborg and Grebbedijk respectively. The Duursche Waarden felt no effect.

F One vegetation effect on internal erosion

In this Appendix two of the five vegetation effects influencing this failure mechanism are studied more thoroughly. The results are presented in the same way as explained in Appendix E.

F.0.1. Increase in water level

The effect of a constant increase in water level could not be studied with fragility curves and, thus, a FORM analysis was performed, which included the distribution of the water level. Figure F.1 presents results, the left graph contains the failure probability, the middle one the reliability index and the right one the difference in failure probability. The lines in each graph represent the total failure probability of internal erosion, i.e. the minimum failure probability between uplift, heave and piping. All three case studies are presented in these graphs.

A constant increase in water level has negative impact on the failure probability, however, it does stay in the same order of magnitude. An increase in failure probability of approximately 75%, 20% and 100% can be observed with 0.2 m higher water levels for Culemborg, Grebbedijk and Duursche Waarden, respectively. Looking at the reliability index, the gradient of each plot seems to be approximately the same. Comparing all case studies, Culemborg and Duursche Waarden seem to have the same effect.

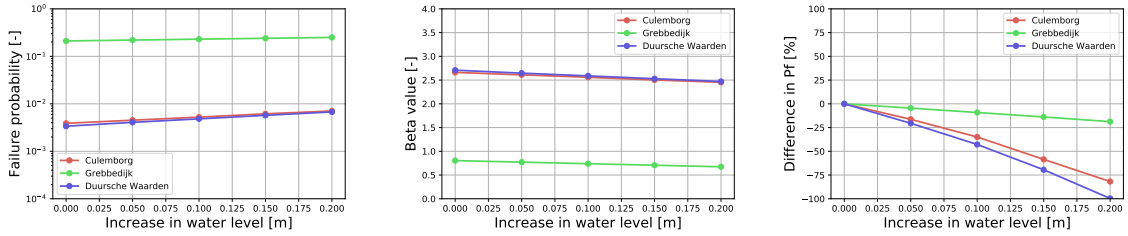

(a) (b) (c)

Figure F.1: Results of a constant increase in water level for the failure mechanisms of internal erosion using a FORM analysis: (a) shows the failure probability in log-scale. (b) shows the same results but now in terms of reliability index, which is found using the inverse CDF of the standard normal distribution. (c) shows the percentage different in failure probability with respect to the year 2050.

In conclusion, the impact of an increase in water level is negative for all case studies. For an

increase of up to 0.2 m, the failure probability stays in the same order of magnitude. When compared to overtopping/overflow, the impact of the same increase in water level seems similar.

F.0.2. Tree or other large vegetation topples over in the hinterland

The effect of a tree toppling over on the hinterland has two effects, which are analysed individually below. It is important to keep in mind that the following effects are conditionalized on a tree toppling over.

Reduction in blanket thickness

One of the effects of a tree toppling over in the hinterland is that the blanket thickness can be locally reduced, this parameter is denoted with the symbol d. This was studied first with fragility curves using a deterministic and a FORM analysis for the sub-mechanism uplift and heave. The last sub-mechanism, piping, is not influenced by a local reduction in the blanket thickness and, therefore, it was not considered. The results are shown in Figures F.2 and F.3, where different amount of reduction in local blanket thickness are presented in different colors. The legend "d-0.44m" means that this particular line represents the situation for a decrease in local blanket thickness of 0.44 m. From this figure, it can be concluded that this effect has the same significant impact on both uplift and heave. Furthermore, it can be observed that a reduction of the blanket thickness of 50% (2.22 m for Culemborg, 1 m for Grebbedijk and 1.9 m for Duursche Waarden) leads to a safety factor of zero and, thus, a failure probability of one, for all case studies. The impact is not constant for each water level, it impacts lower water level more than higher ones. This can be explained because above a certain limit, the difference in water level between the river and the land-side is already so high that increasing it does not have a large influence.

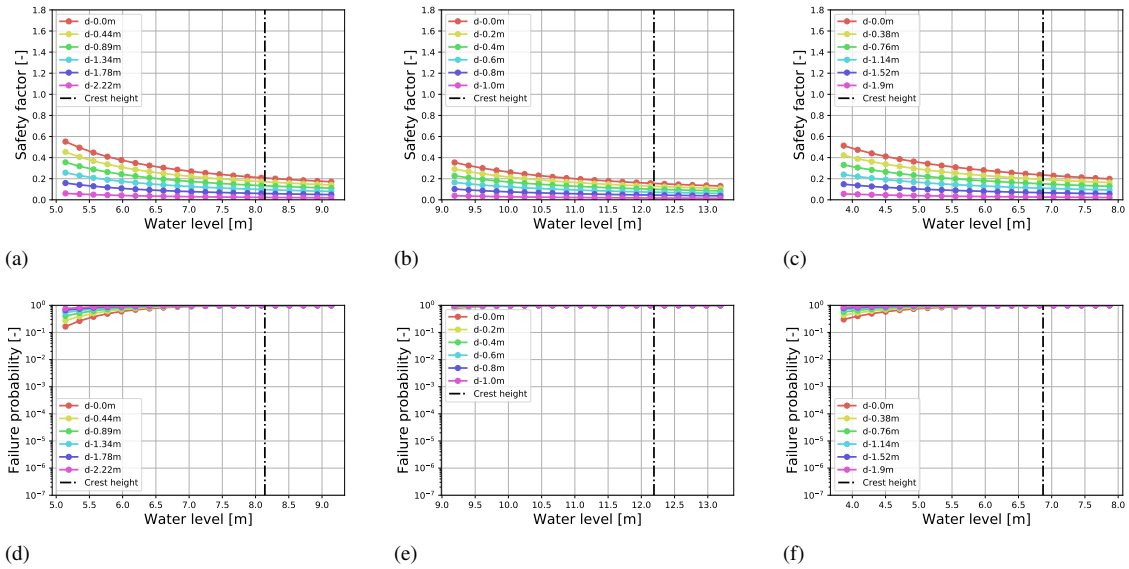

Figure F.2: Fragility curves with different blanket thickness reduction found using a deterministic approach (top three graphs) and a FORM analysis (lower three graphs) considering only the sub-mechanism uplift. All three case studies are presented: (a) and (d) Culemborg, (b) and (e) Grebbedijk, (c) and (f) Duursche Waarden.

Figure F.4 presents the effect of the reduced blanket thickness when considering the distribution of the water level and all three sub-mechanisms. The amount of reduction in local blanket

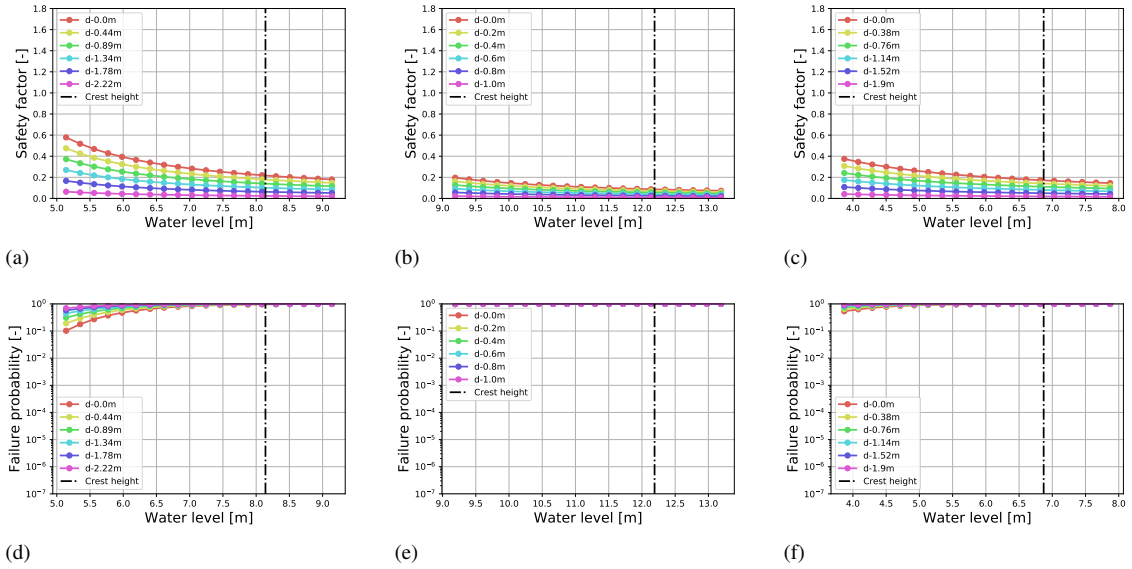

Figure F.3: Fragility curves with different blanket thickness reduction found using a deterministic approach (top three graphs) and a FORM analysis (lower three graphs) considering only the sub-mechanism heave. All three case studies are presented: (a) and (d) Culemborg, (b) and (e) Grebbedijk, (c) and (f) Duursche Waarden.

thickness was not similar for all case study due to their varying original blanket thickness. The reduction was based on a percentile reduction for all case study, from 0% decrease to 50% decrease. Therefore, the decrease in blanket thickness is different per case study. The failure probability is found taking the minimum failure probability of all three sub-mechanism. From this graph, it can be concluded that the reduction in blanket thickness has no effect on internal erosion, because the dominant mechanism (piping) is not influenced by this effect.

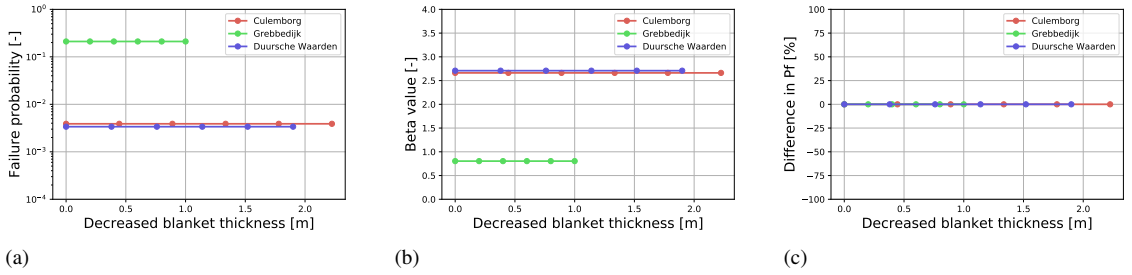

Figure F.4: Results of a decrease in blanket thickness for the failure mechanisms of internal erosion using a FORM analysis: (a) shows the failure probability in log-scale. (b) shows the same results but now in terms of reliability index, which is found using the inverse CDF of the standard normal distribution. (c) shows the percentage different in failure probability with respect to the year 2050.

It can be concluded that a local reduction in blanket thickness increases considerably the probability of having a crack (uplift) and sand boils (heave), however the probability of having an erosion channel (piping), which is the dominant mechanism, is not changed. Therefore, the effect does not influence the overall probability of failure of internal erosion, i.e. all three sub-mechanisms must occur simultaneously to have internal erosion.

Change in exit point

The last effect studied is the change in location of the exit point due to a tree or large vegetation falling over at up to 20 m from the toe of the dike. This effect impacts uplift and heave due to a change in the hydraulic head and piping due to a change in seepage length. The further away the exit point is located, the lower the hydraulic head and the longer the seepage length, which are both advantageous. This effect is first studied using fragility curves and looking at each sub-mechanism individually. The fragility curves are created with a deterministic approach and a FORM analysis.

Figures F.5 and F.6 show the results when considering only uplift and heave, respectively. From these figures, it can be concluded that this effect is marginal for both sub-mechanisms. A slight increase in safety factor, and thus decrease in failure probability, can be observed especially at low water levels. Compared to the decrease in blanket thickness effect studied previously, the magnitude of this effect seems marginal.

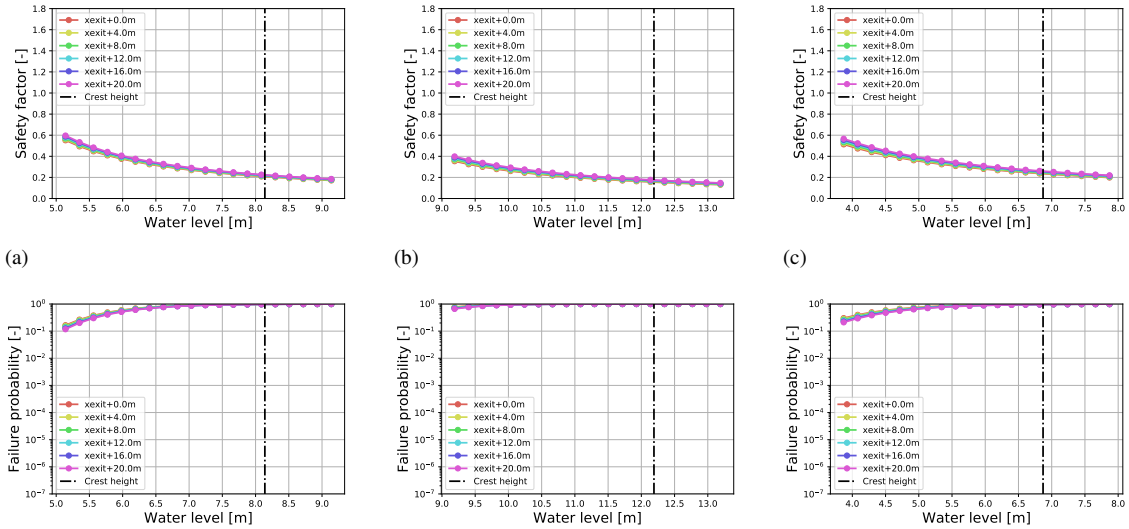

Figure F.5: Fragility curves with different exit point location found using a deterministic approach (top three graphs) and a FORM analysis (lower three graphs) considering only the sub-mechanism uplift. All three case studies are presented: (a) and (d) Culemborg, (b) and (e) Grebbedijk, (c) and (f) Duursche Waarden.

A change in the exit point location has also an influence on the sub-mechanism piping, it changes the seepage length. If the location is further away, the seepage length increases, i.e. the erosion channel needs to cover a longer length before failure occurs, thus, the safety factor increases (see Figure F.7). The changes in safety factors are considerably higher than for uplift and heave. A safety factor reduction of roughly 0.4, 0.2 and 0.3 are observed with water levels around 6 m and an exit point 20 m from the toe of the dike for Culemborg, Duursche Waarden and Grebbedijk, respectively. The effect is not constant over the water levels, probably again because of this “limit” in water level difference that, if exceeded, not much difference is observed.

Figure F.8 presents the effect of a change in exit point, using a FORM analysis, when considering all three sub-mechanisms and the distribution of the water level. It can be deducted that all three case studies are positively impacted in a significant manner by an increase in exit point

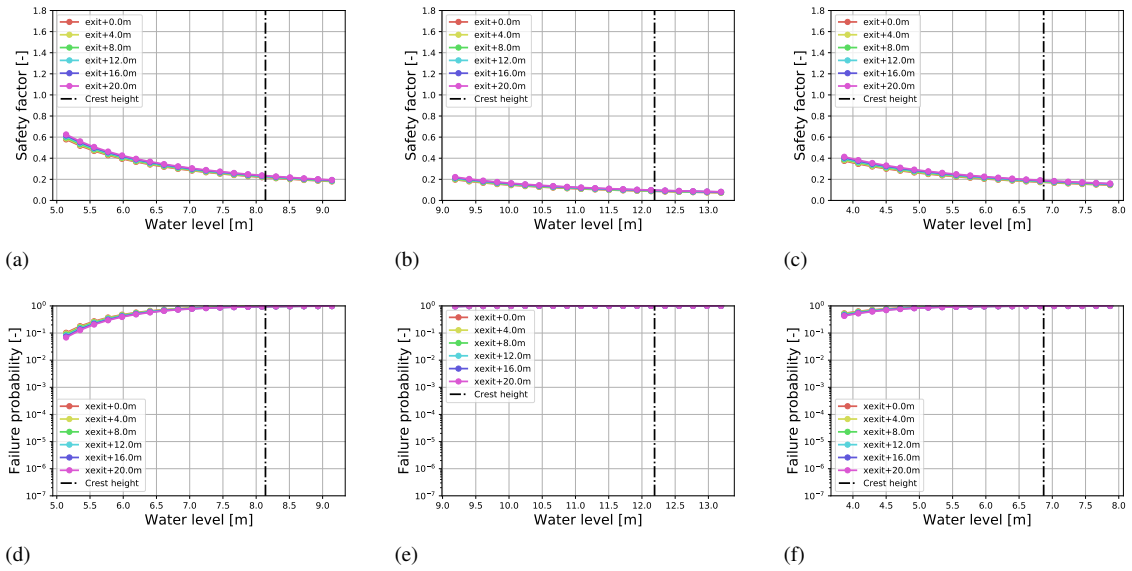

Figure F.6: Fragility curves with different exit point location found using a deterministic approach (top three graphs) and a FORM analysis (lower three graphs) considering only the sub-mechanism heave. All three case studies are presented: (a) and (d) Culemborg, (b) and (e) Grebbedijk, (c) and (f) Duursche Waarden.

distance between zero up to 20 m from the toe of the dike. The case study of Grebbedijk seems the least affected by this change, followed by Culemborg and Duursche Waarden.

It can be concluded that if a tree falls over on the hinterland and becomes the new exit point, all three sub-mechanisms are influenced. The dominant sub-mechanism, piping, is significantly and positively impacted the further away the tree is from the toe of the dike, i.e. the erosion channel needs to cover more distance before failure.

However, if the tree falling is further away from the toe of the dike, its positive effect should not be confused with a strengthening of the dike. If the exit point is further way nothing guaranties that another exit point closer to the toe will not occur. Therefore, the impact of a new exit point, if further way than the case without a tree toppling over, should not be taken into account. It should only be taken into account if it impacts negatively internal erosion, i.e. when the tree is closer to the toe of the dike than the exit point without vegetation. Furthermore, this effect is only felt if a tree topples over. Therefore, the probabilities of this effect need to include this probability of a tree toppling over. An overview of the individual effects of vegetation on the failure probability internal erosion are found in Table F.1.

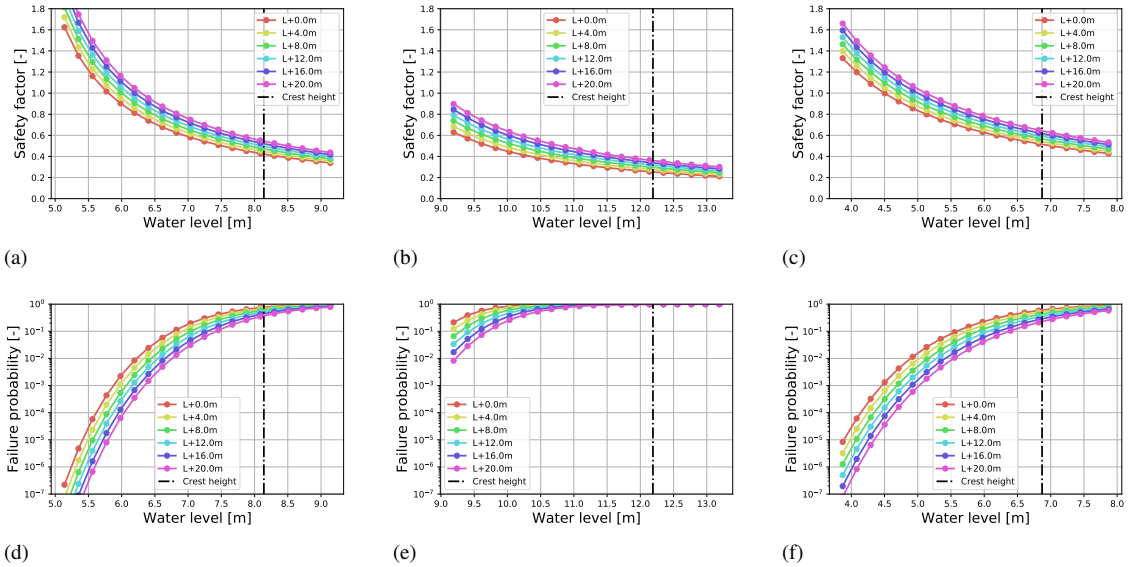

Figure F.7: Fragility curves with different exit point location found using a deterministic approach (top three graphs) and a FORM analysis (lower three graphs) considering only the sub-mechanism piping. All three case studies are presented: (a) and (d) Culemborg, (b) and (e) Grebbedijk, (c) and (f) Duursche Waarden.

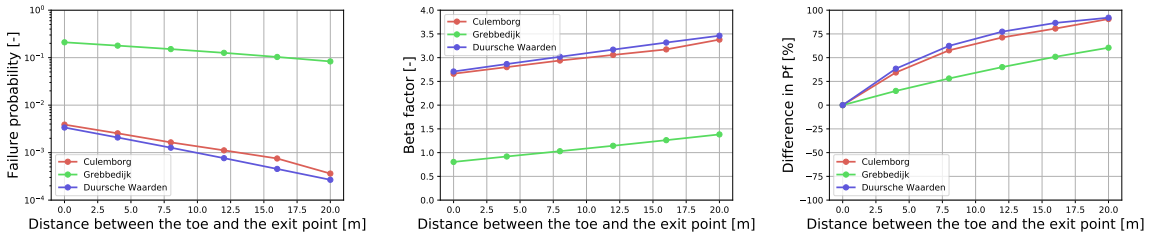

Figure F.8: Results of a increase in exit point location for the failure mechanisms of internal erosion using a FORM analysis: (a) shows the failure probability in log-scale. (b) shows the same results but now in terms of reliability index, which is found using the inverse CDF of the standard normal distribution. (c) shows the percentage different in failure probability with respect to the year 2050.

Table F.1: Overview of the studied effects of vegetation on the failure mechanism internal erosion.

Vegetation effect	Results
Increase in water level. The water level distribution was increased by a constant ranging up to 0.2 m.	*High negative impact*. The failure probability was increased by 20% to 100%. The failure probability for 0.2 m increase goes from 3.9e-03, 2.1e-01 and 3.4e-03 to 7.1e-03, 2.5e-01 and 6.7e-03 for Culemborg, Grebbedijk and Duursche Waarden respectively. The reliability index goes from 2.66, 0.80 and 2.71 to 2.45, 0.67 and 2.47 for Culemborg, Grebbedijk and Duursche Waarden respectively.
Decrease in blanket thickness. This was simulated by reducing the local blanket thickness up to 50% of its original value.	*Negligible negative impact*. No major change was observed. Because the failure probability of internal erosion is the minimum of the failure probability all three sub-mechanisms, which was always piping. The latter is not influenced by this effect
Change in exit point. The effect of a change in exit point was studied by moving at different locations starting at the toe of the dike and up to 20 m from the toe.	*High positive impact - however this is without considering the probability of a tree toppling over or the probability of another crack occurring closer to the toe (no positive impact possible). Therefore, if both effects mentioned above are taken into account this effect has a* ***No impact or a low negative impact***. Considering the higher positive impact, the failure probability was decreased by 60% up to 90%. The failure probability at the toe and at 20 m from the toe goes from 3.9e-03, 2.1e-01 and 3.4e-03 to 3.6e-04, 8.3e-02 and 2.68e-04 for Culemborg, Grebbedijk and Duursche Waarden respectively. The reliability index goes from 2.66, 0.80 and 2.71 to 3.38, 1.38 and 3.46 for Culemborg, Grebbedijk and Duursche Waarden respectively. This significant decrease is also because 20 m is relatively far. Considering a difference between the toe and 5 m from the toe, the decrease in failure probability was between 12% and 35%, which are more realistic and representative values.

G

Case study Culemborg

This appendix presents the results of the framework corresponding to the Culemborg case study. The same BBN was used as presented in Chapter 6.2. The framework was used to analyse the impact of combined vegetation effects on the failure probability. Heat maps are used to present the results, the x and y axes represent a different vegetation parameter whereas the color depicts the normalized failure probability (left graphs) and the normalized beta value (right graphs), see Section 4.3.2. The normalization was conducted with respect to the total failure probability of the Culemborg's cross-section of interest without vegetation, which was estimated as 4.2×10^{-3}. The beta values are normalized by the total beta value without vegetation which is 2.64. The internal erosion failure mechanism is the dominant one for this case study.

Figure G.1 shows the impact on the total failure probability of both an increase in water level and a change in mean critical discharge. It can be observed that the increase in water level is the dominant effect compared to the changes in critical discharge. An increase in water levels of 0.1 m can lead to up to 22% increase in the total failure probability and 2.6% decrease in beta values. The effect of a change in mean critical discharge is no longer as relevant as when it was considered for only overtopping/overflow.

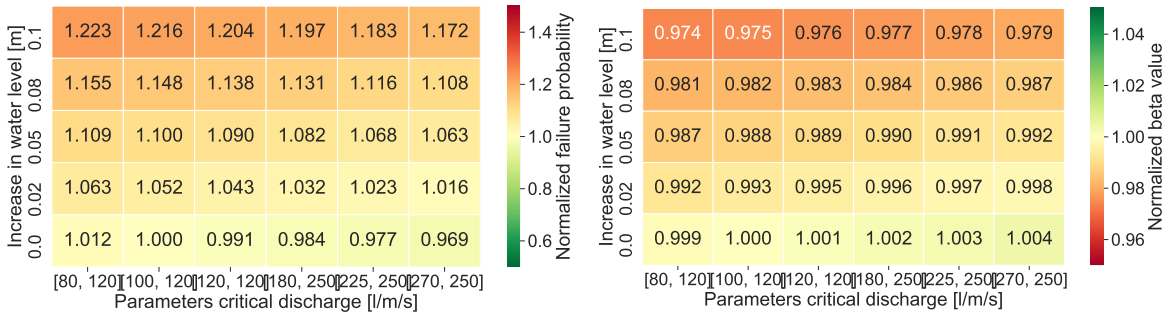

Figure G.1: Quantitative effect of the increase in water level and change in mean critical discharge on the total failure probability (a) and normalized beta value (b) for the Culemborg. It can be observed that an increase in water level is the dominant effect when considering both failure mechanisms.

Considering the effects of wave height reduction and increase in water level (see Figure G.2) it is observed that the increase in water level is the dominant effect with the wave coefficient showing no impact on the total failure probability or total beta value.

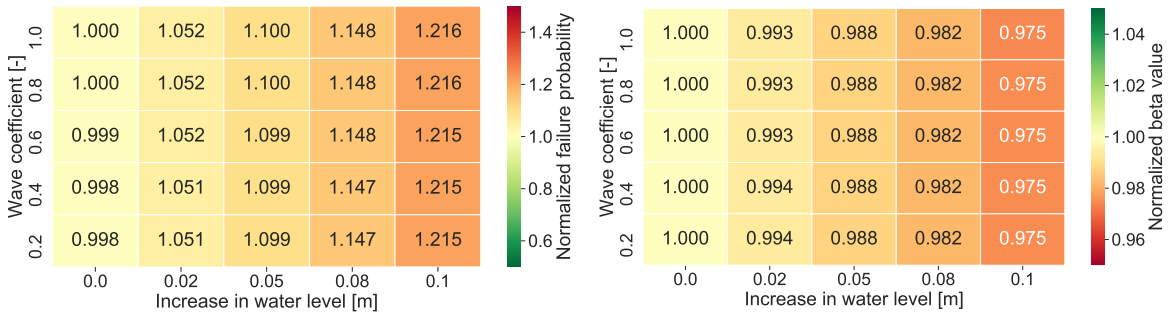

(a) (b)

Figure G.2: Quantitative effect of the decrease in wave height and increase in water level on the total failure probability (a) and normalized beta value (b) for the Culemborg. It can be observed that an increase in water level is the dominant effect and that the decrease in wave height has no impact when considering both failure mechanisms.

When comparing the change in exit point location and the increase in water level (see Figure G.3), it is noticed that the increase in water level has again a dominant impact on the total failure probability and the beta value. Looking at the change in exit point, due to the reference scenario (without vegetation) using an exit point located at the toe of the dike, any new location further away should be ignored. Therefore, no changes are observed with a new exit point location. Other graphs showing the impact of change in exit point with the wave reduction or changes in mean critical discharge are discarded as similar conclusions can be drawn.

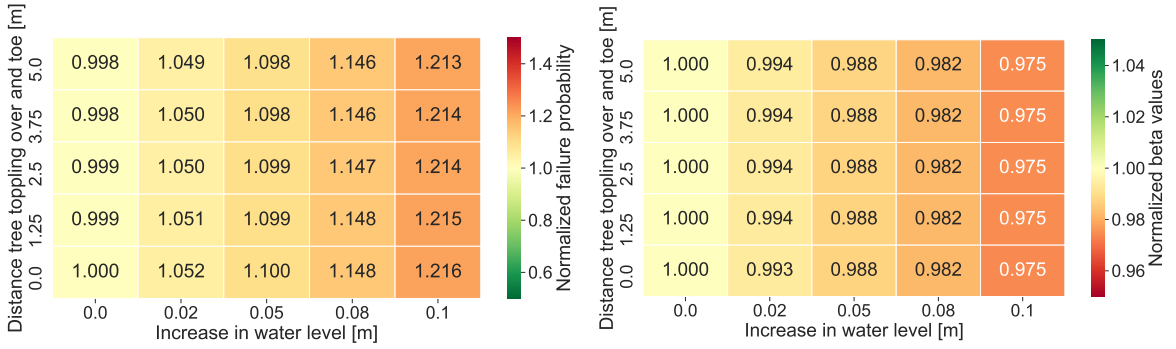

(a) (b)

Figure G.3: Quantitative effect of the change in exit point location and increase in water level on the total failure probability (a) and normalized beta value (b) for the Culemborg. It can be observed that an increase in water level is the dominant effect and that the change in exit point location has a marginal impact when considering both failure mechanisms.

The last heat map, Figure G.4, shows the wave reduction effect with a change in mean critical discharge. Here again it can be seen that the wave reduction effect has no impact on the total failure probability. The change in mean critical discharge shows again marginal effects up to 3.1% decrease in failure probability and a 0.4% increase in beta value.

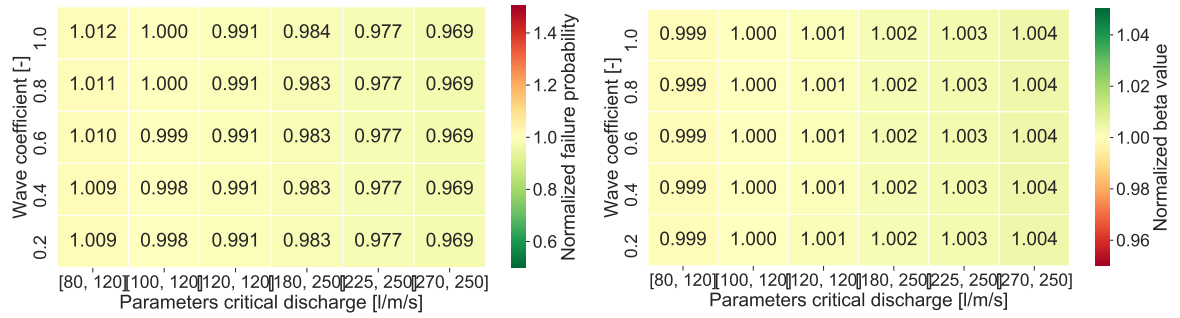

(a) (b)

Figure G.4: Quantitative effect of the reduction of wave height and the change in mean critical discharge on the total failure probability (a) and normalized beta value (b) for the Culemborg. It can be observed that a reduction in wave height has no effect and that a change in mean critical discharge has a marginal impact when considering both failure mechanisms.

The change in mean critical discharge and water level were dominant effects when considering only overtopping/overflow, therefore, it is interesting to analysis there combined effect normalized now on the failure probability of overtopping/overflow without vegetation instead of the total one, which showed that the change in mean critical discharge had no impact. Figure G.5 shows that when considering only overtopping/overflow both effects have a similar but opposite impact which means that they can compensate each other.

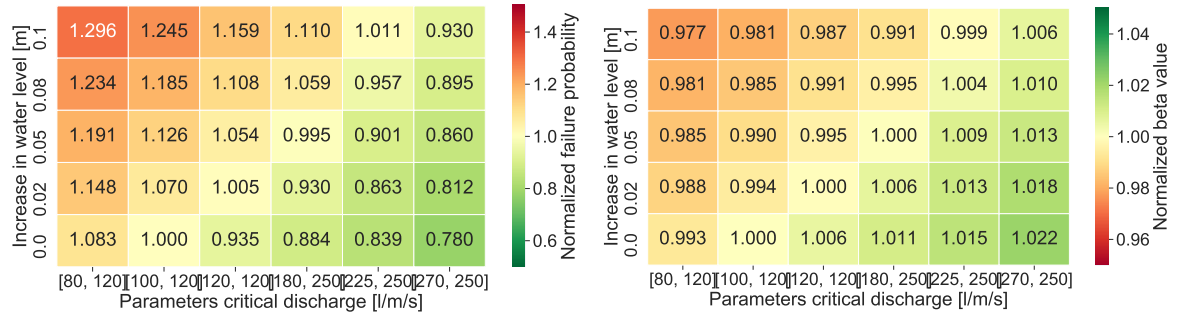

(a) (b)

Figure G.5: Quantitative effect of the increase in water level and the change in mean critical discharge on the overtopping/overflow failure probability (a) and normalized beta value (b) for the Culemborg. It can be observed that an increase in water level and that a change in mean critical discharge can compensate each other.

It is interesting to use the framework to further study those two effects. Inference is used for this purpose, where the marginal distributions of both root nodes: “increase in water level” and “erosion resistance” are analysed given different types of failures: overtopping/overflow, internal erosion, and both. Initially, the marginal distributions are uniformly distributed. The results are presented in Figure G.6, where the y-axis denotes the probability (PDF) and the x-axis the increase in water level for the graph on the left and the change in mean critical discharge for the graph on the right.

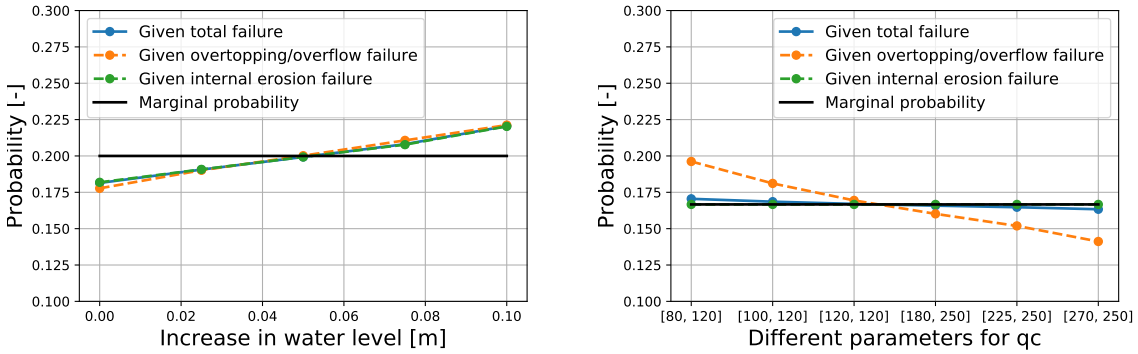

(a) (b)

Figure G.6: Marginal distribution of the increase in water level (a) and the change in mean critical discharge (b) conditionalized on different failure types.

H

Case study Grebbedijk

This appendix presents the results of the framework corresponding to the Grebbedijk case study. The same BBN was used as presented in Chapter 6.2. The framework was used to analyse the impact of combined vegetation effects on the failure probability. Heat maps are used to present the results, the x and y axes represent a different vegetation parameter whereas the color depicts the normalized failure probability (left graphs) and the normalized beta value (right graphs), see Section 4.3.2. The normalization was conducted with respect to the total failure probability of the Grebbedijk's cross-section of interest without vegetation, which was estimated as 4.2×10^{-3}. The beta values are normalized by the total beta value without vegetation which is 2.64. The internal erosion failure mechanism is the dominant one for this case study.

Figure H.1 shows the impact on the total failure probability of both an increase in water level and a change in mean critical discharge. It can be observed that the increase in water level is the dominant effect compared to the changes in critical discharge. An increase in water levels of 0.1 m can lead to up to 22% increase in the total failure probability and 2.6% decrease in beta values. The effect of a change in mean critical discharge is no longer as relevant as when it was considered for only overtopping/overflow.

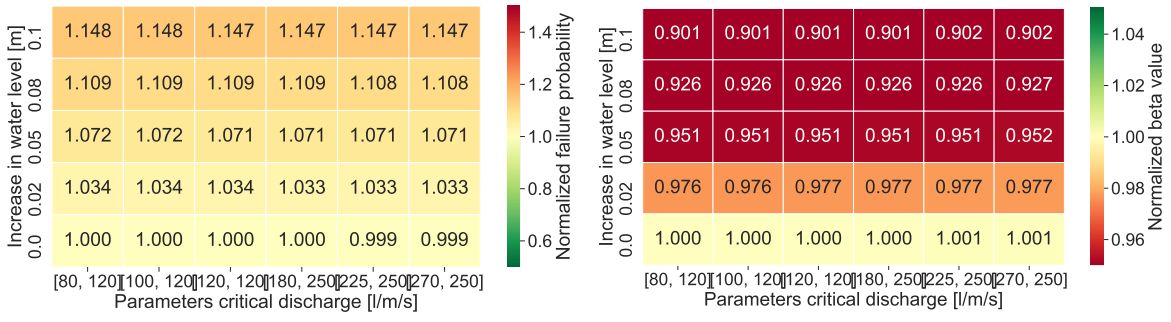

Figure H.1: Quantitative effect of the increase in water level and change in mean critical discharge on the total failure probability (a) and normalized beta value (b) for the Grebbedijk. It can be observed that an increase in water level is the dominant effect when considering both failure mechanisms.

Considering the effects of wave height reduction and increase in water level (see Figure H.2) it is observed that the increase in water level is the dominant effect with the wave coefficient showing no impact on the total failure probability or total beta value.

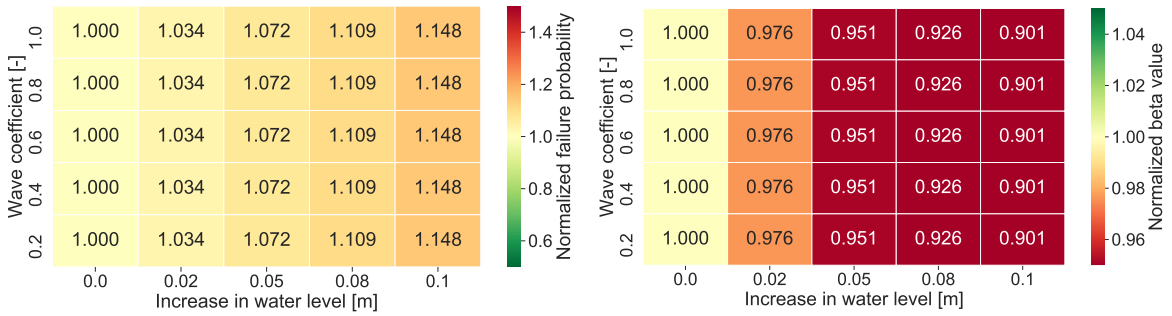

(a) (b)

Figure H.2: Quantitative effect of the decrease in wave height and increase in water level on the total failure probability (a) and normalized beta value (b) for the Grebbedijk. It can be observed that an increase in water level is the dominant effect and that the decrease in wave height has no impact when considering both failure mechanisms.

When comparing the change in exit point location and the increase in water level (see Figure H.3), it is noticed that the increase in water level has again a dominant impact on the total failure probability and the beta value. Looking at the change in exit point, due to the reference scenario (without vegetation) using an exit point located at the toe of the dike, any new location further away should be ignored. Therefore, no changes are observed with a new exit point location. Other graphs showing the impact of change in exit point with the wave reduction or changes in mean critical discharge are discarded as similar conclusions can be drawn.

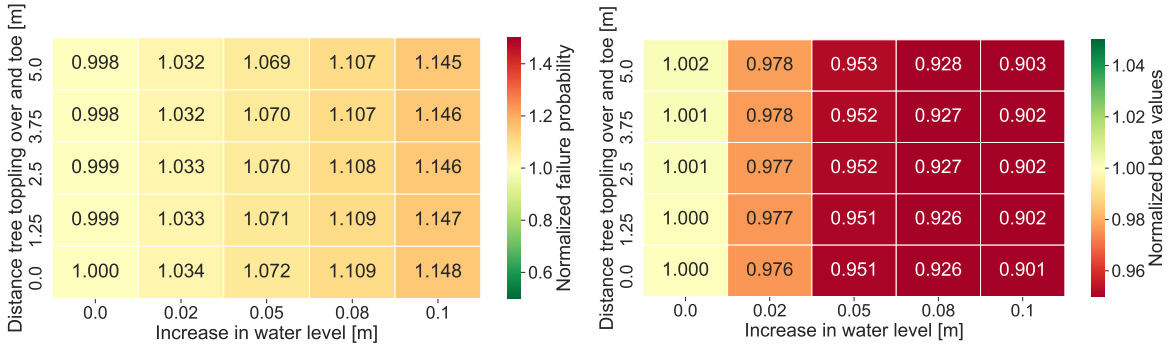

(a) (b)

Figure H.3: Quantitative effect of the change in exit point location and increase in water level on the total failure probability (a) and normalized beta value (b) for the Grebbedijk. It can be observed that an increase in water level is the dominant effect and that the change in exit point location has a marginal impact when considering both failure mechanisms.

The last heat map, Figure H.4, shows the wave reduction effect with a change in mean critical discharge. Here again it can be seen that the wave reduction effect has no impact on the total failure probability. The change in mean critical discharge shows again marginal effects up to 3.1% decrease in failure probability and a 0.4% increase in beta value.

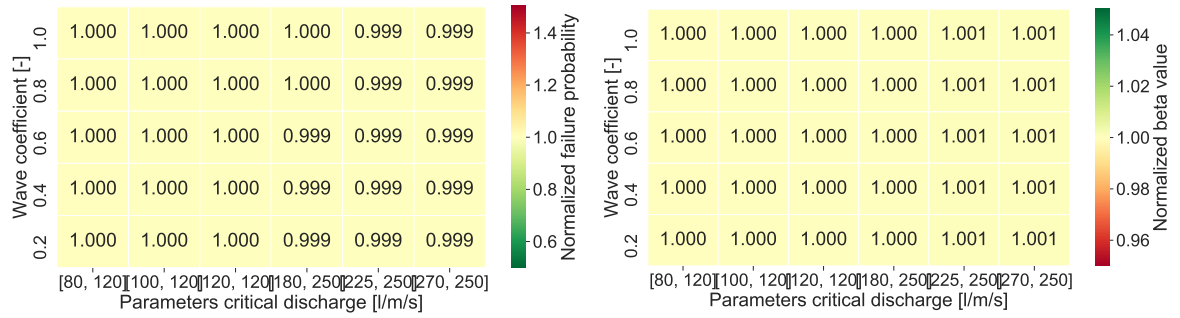

(a) (b)

Figure H.4: Quantitative effect of the reduction of wave height and the change in mean critical discharge on the total failure probability (a) and normalized beta value (b) for the Grebbedijk. It can be observed that a reduction in wave height has no effect and that a change in mean critical discharge has a marginal impact when considering both failure mechanisms.

The change in mean critical discharge and water level were dominant effects when considering only overtopping/overflow, therefore, it is interesting to analysis there combined effect normalized now on the failure probability of overtopping/overflow without vegetation instead of the total one, which showed that the change in mean critical discharge had no impact. Figure H.5 shows that when considering only overtopping/overflow both effects have a similar but opposite impact which means that they can compensate each other.

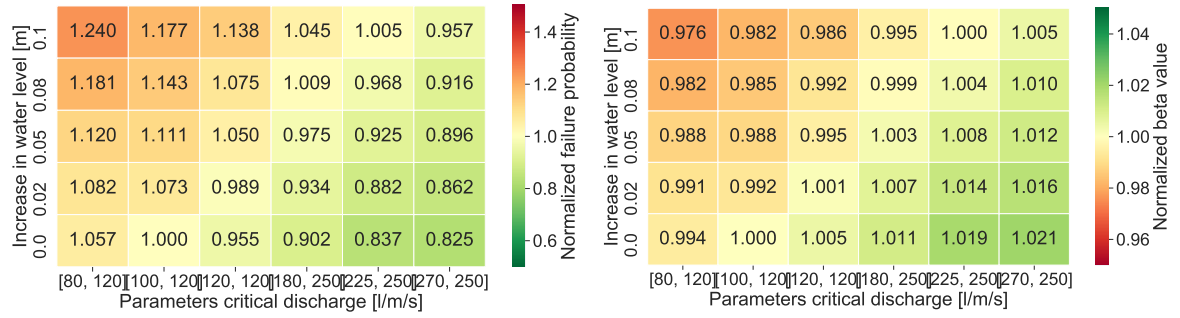

(a) (b)

Figure H.5: Quantitative effect of the increase in water level and the change in mean critical discharge on the overtopping/overflow failure probability (a) and normalized beta value (b) for the Grebbedijk. It can be observed that an increase in water level and that a change in mean critical discharge can compensate each other.

It is interesting to use the framework to further study those two effects. Inference is used for this purpose, where the marginal distributions of both root nodes: “increase in water level” and “erosion resistance” are analysed given different types of failures: overtopping/overflow, internal erosion, and both. Initially, the marginal distributions are uniformly distributed. The results are presented in Figure H.6, where the y-axis denotes the probability (PDF) and the x-axis the increase in water level for the graph on the left and the change in mean critical discharge for the graph on the right.

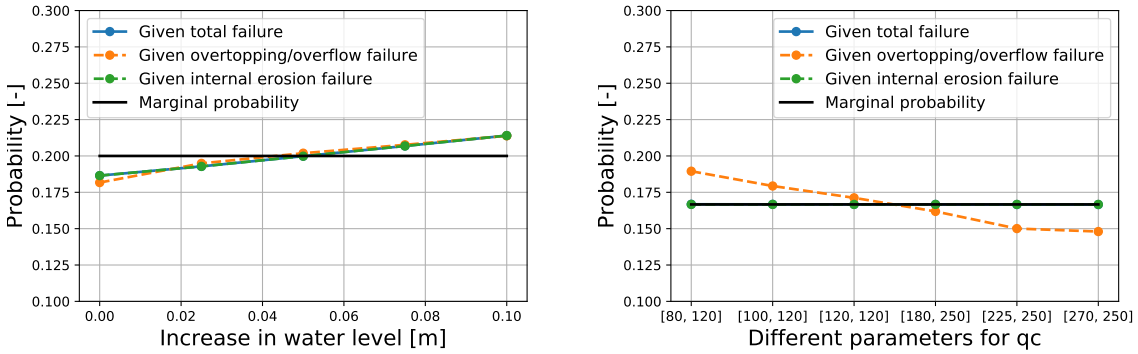

(a) (b)

Figure H.6: Marginal distribution of the increase in water level (a) and the change in mean critical discharge (b) conditionalized on different failure types.

Python code

The code presented below was used to create the framework for all three case studies simultaneously. The data of all case studies were stored in an excel file. The first code, in Section I.1, contains all the limit state functions and gathers the data from the excel sheet. The second code, in Section I.2, contains the MC simulations needed to calibrate the framework and creates the framework.

I.1. Code containing functions + data

```
#!/usr/bin/env python3
# -*- coding: utf-8 -*-
"""
Created on Sat Aug 29 14:13:20 2020

@author: ligayawopereis
"""

import numpy as np
import pandas as pd
import openturns as ot
from scipy.interpolate import interp1d
from scipy import stats as st
from pathlib import Path
from scipy.stats import weibull_min
from scipy.stats import norm
from scipy.stats import uniform
from scipy.stats import lognorm
from scipy.stats import gumbel_r
from scipy.stats import expon
from scipy.stats import rayleigh
from scipy.stats import pareto
from scipy.optimize import curve_fit
import matplotlib.pyplot as plt
from time import perf_counter
from pomegranate import BayesianNetwork

import networkx
```

```
#%% Overtopping and overflow
data = pd.read_excel('Case_studies.xlsx',
                     sheet_name = 'Overtopping and overflow')
data_IE = pd.read_excel('Case_studies.xlsx', sheet_name = 'Internal erosion')


hc = data.hc[dike]
slope = data.slope[dike]
dikenormal = data.Dikenormal[dike] ######
para_hb = [data.hb[dike], 0.3 ]

if dike == 0:
    Fetch = data.Fetch_43
    file = pd.read_excel('Data/43/hw_testmodulus/Water_level.xlsx')

if dike == 1:
    Fetch = data.Fetch_45
    file = pd.read_excel('Data/45/hw_testmodulus/Water_level.xlsx')

if dike == 2:
    Fetch = data.Fetch_53
    file = pd.read_excel('Data/53/hw_testmodulus/Water_level.xlsx')

para_qc = [100,120]
g = 9.81
yb,yf,yv = 1,1,1

F = Fetch[Wind]
Wind_dir = data.Angle[Wind]
para_U10_all = [[data.k_with_uncertainty[Wind], data.u_with_uncertainty[Wind]],
                [data.k_without_uncertainty[Wind],
                 data.u_without_uncertainty[Wind]]]

para_U10 = para_U10_all[0]

Pf_occurence = data.Occurrence

#%% Internal erosion
B     = data_IE.B[dike]        # Width of the levee [m]
para_ysat  = [data_IE.mu_ysat[dike], data_IE.std_ysat[dike]] # Saturated
                            #volumetric weight of the blanket (Normal) [kN/m3]
para_k     = [data_IE.mu_k[dike], data_IE.std_k[dike]] # Hydraulic conductivity
                            #of the aquifer (Normal) [m+NAP]
para_hp    = [data_IE.mu_hp[dike], data_IE.std_hp[dike]] # Hinder land phreatic
                            #level (Normal) [m+NAP]
para_Lf    = [data_IE.mu_Lf[dike], data_IE.std_Lf[dike]] # Length of the
                            #effective foreshore (Lognormal) [m]
para_D     = [data_IE.mu_D[dike], data_IE.std_D[dike]] # Aquifer thickness
                            #(Lognormal) [m]
para_d     = [data_IE.mu_d[dike], data_IE.std_d[dike]] # Blanket thickness at
                            #the exit point (Lognormal) [m]
para_d70   = [data_IE.mu_d70[dike], data_IE.std_d70[dike]] # 70%-fractile of
                            #grain size distribution (Lognormal) [m]

d70m  = 2.08e-04 # Reference value of d70 [m]
```

```
v      = 1.33e-06 # Kinematic viscosity of water [m2/s]
theta  = 37       # Bedding angle [rad]
ys     = 26.5     # Volumetric weight of sand grains [kN/m3]
yw     = 10       # Volumetric weight of water [kN/m3]
n      = 0.25     # Drag coefficient
g = 9.81
para_mu     = [1, 0.1]        # Model factor addressing the uncertainty in the
                              #critical head difference (Normal) [-]
para_mp     = [1, 0.12]       # Model factor addressing the uncertainty in
                              #piping (Normal) [-]
para_ic     = [0.5, 0.1]       # Critical heave gradient (Lognormal) [-]
para_kh     = [1e-06, 1e-06*0.5]     # Hydraulic conductivity aquitard
                                      #(Lognormal) [m/s]

#%% Functions containing the limit state functions

def Log_para(mu,std):
    """
    Returns: The shape and scale parameters of the lognormal distribution.

    """
    v = std**2
    phi = np.sqrt(v+mu**2)
    mean= np.log(mu**2/phi)                # Using this in excel
    sigma= np.sqrt(np.log(phi**2/mu**2)) # Using this in excel
    shape = sigma          # Scipy's shape parameter
    scale = np.exp(mean) # Scipy's scale parameter
    return shape, scale

def Wave_height_MC(MC, F,Uwind,hbottom,hwaterlevel,g):
    Hm0 = np.zeros(MC)
    Tp  = np.zeros(MC)
    for i in range (MC):
        Depth=hwaterlevel[i]-hbottom[i]
        if Depth<=0:
            Depth=0.01
        Ftilde=g*F/Uwind[i]**2
        dTilde=g*Depth/Uwind[i]**2
        hm0first=0.343*dTilde**1.14
        hm0second=(4.41*10**(-4)*Ftilde**0.79)/np.tanh(hm0first)
        tm0first=0.1*dTilde**2.01
        tm0second=(2.77*10**(-7)*Ftilde**1.45)/np.tanh(tm0first)
        Hm0[i]=0.24*Uwind[i]**2/g*(np.tanh(hm0first)*np.tanh(hm0second))**0.572
        Tp[i]=7.69*Uwind[i]/g*(np.tanh(tm0first)*np.tanh(tm0second))**0.187
    return  Hm0, Tp



def OT_OF_Z_MC(MC, Wind_dir,Hm0, Tp,hwaterlevel,qcrit,g,hc,yb,yf,yv,dikenormal
               ,slope):
    Z = np.zeros(MC)
    for i in range (MC):
        Rc=hc-hwaterlevel[i]
        alpha=np.arctan(slope)
        beta=Wind_dir[i]-dikenormal
        if beta>180:
```

```
            beta=beta-360
        ybeta=1-0.0033*abs(beta)
        Xim=np.tan(alpha)/np.sqrt(Hm0[i]/(1.56*(0.9*Tp[i])**2))
        if Rc>0:
            q=(0.026/np.sqrt(np.tan(alpha)))*Xim*np.exp(-((2.5*Rc/(yb*yf*ybeta
              *yv*Xim*Hm0[i]))**1.3))*1000*np.sqrt(g*Hm0[i]**3)
            qmax=np.sqrt(g*Hm0[i]**3)*0.1035*np.exp(-((1.35*Rc/Hm0[i])**1/3))
            *1000
            q=min(q,qmax)
        else:

            if Rc/Hm0[i] > -0.3:
                q=(0.026/np.sqrt(np.tan(alpha)))*Xim*np.exp(-(max((2.5*Rc/(yb
                  *yf*ybeta*yv*Xim*Hm0[i])),0)**1.3))*1000*np.sqrt(g*Hm0[i]**3)
                qmax=np.sqrt(g*Hm0[i]**3)*0.1035*np.exp(-(max((1.35*Rc/Hm0[i])
                ,0)**1/3))*1000
                q=min(q,qmax)
                q = q + 0.54*np.sqrt(g*(abs(Rc))**3)*1000
            else:
                q=0.54*np.sqrt(g*(abs(Rc))**3)*1000
        if qcrit[i] - q < 0:
            Z[i] = 1
    return Z

def MonteCarlo_Piping(MC, data, deterministic_parameters, rootpit, LOC):
    """
    Return the monte carlo for piping.
    """
    B, g, d70m, v, theta, ys, yw,n = deterministic_parameters
    k, hp, ysat, mu, mp, Lf, D, ic, d, d70, kh, hw = data
    lambda_h     = np.zeros(MC)
    lamba        = np.zeros(MC)
    phi_exit     = np.zeros(MC)
    delta_phic   = np.zeros(MC)
    delta_phi    = np.zeros(MC)
    Zu           = np.zeros(MC)
    i_heave      = np.zeros(MC)
    Zh           = np.zeros(MC)
    F1           = np.zeros(MC)
    F2           = np.zeros(MC)
    F3           = np.zeros(MC)
    Hcp          = np.zeros(MC)
    Zp           = np.zeros(MC)
    Pfu          = np.zeros(MC)
    Pfh          = np.zeros(MC)
    Pfp          = np.zeros(MC)
    Pf_tot       = np.zeros(MC)
    L            = np.zeros(MC)
    xexit = B/2+LOC ##################
    for i in range (MC):
        if d[i]-rootpit < 0:
            Zu[i] = -999
            Zh[i] = -999
        else:

            lambda_h[i]     = np.sqrt(max(k[i]*D[i]*d[i]/kh[i],0))
```

```
            lamba[i]        = lambda_h[i]/(Lf[i]+B+lambda_h[i])
            *np.exp((B/2-xexit)/lambda_h[i])
            phi_exit[i]     = hp[i]+lamba[i]*(hw[i]-hp[i])
            delta_phic[i]   = (d[i]-rootpit)*(ysat[i]-yw)/yw
            delta_phi[i]    = phi_exit[i]-hp[i]
            Zu[i]           = mu[i]*delta_phic[i]-delta_phi[i]
            i_heave[i]            = (phi_exit[i]-hp[i])/(d[i]-rootpit)
            Zh[i]           = ic[i]-i_heave[i]

        if Zu[i] < 0:
            Pfu[i] = 1
        if Zh[i] < 0:
            Pfh[i] = 1

        F1[i]           = n*(ys/yw-1)*np.tan(theta/360*2*np.pi)
        L[i]            = B + Lf[i] + LOC
        F2[i]           = d70m/(max(v*k[i]*L[i]/g,0.000000001))**(1/3)
        *(d70[i]/d70m)**0.4
        F3[i]           = 0.91*(D[i]/L[i])**(0.28/((D[i]/L[i])**2.8-1)+0.04)
        Hcp[i]          = F1[i]*F2[i]*F3[i]*L[i]
        Zp[i]           = mp[i]*Hcp[i]-(hw[i]-hp[i]-0.3*d[i])
        if Zp[i] < 0:
            Pfp[i] = 1
        if Pfu[i]+Pfh[i]+Pfp[i] == 3:
            Pf_tot [i] = 1
    return Zu, Zh, Zp, Pfu, Pfh, Pfp, Pf_tot
```

I.2. Main code

```
# -*- coding: utf-8 -*-
"""
Created on Tue Sep 22 12:14:15 2020

@author: lmwop
"""
from time import perf_counter
import seaborn as sns

start_tot = perf_counter()
save=False

for idike in range(3): # Running all three case studies after one another
    dike = idike
    print ()
    print ('DIKE:', dike)

    #Setting dominant wind direction and the number of simulation needed (N)
    if dike ==0:
        Wind = 11
        num = 635000
    if dike ==1:
        Wind = 10
        num = 221000
    if dike ==2:
        Wind = 9
        num = 2000000
```

```
exec(open('functions.py').read())

# Values of the vegetation parameters
WC_inps = np.linspace(0.2,1,5) # Decrease in wave height
adding_hw = np.linspace(0,0.1,5) # Increase in water level
lognorm_qc = [[270,250],[225,250],[180,250],[120,120],[100,120],[80,120]]
                        # Change in critical discharge parameter
LOC_inps = np.linspace(0, 5,  5) # Increase in exit point location

# Water level data used
years = ['2050']
uncertainties=['with']
xx = file['{}_{}'.format(years[0],uncertainties[0])].values.reshape
(len(file.CDF), 1)
yy = file.CDF.values.reshape(len(file.CDF), 1)
hw_CDF = np.concatenate((xx,yy), axis=1)
def fit_gumbel (x, loc, scale):
    return gumbel_r.cdf(x,loc,scale)
para_gum, pop = curve_fit(fit_gumbel, hw_CDF[:,0], hw_CDF[:,1])

# Randomly creating data
U10= weibull_min(para_U10[0], loc=0, scale=para_U10[1]).rvs(num)
hb= norm(para_hb[0], para_hb[1]).rvs(num)
hw= gumbel_r(para_gum[0], para_gum[1]).rvs(num)
qc_tot = []
for i in range (len(lognorm_qc)):
    shape, scale  = Log_para(lognorm_qc[i][0], lognorm_qc[i][1])
    qc_tot.append(lognorm(shape, loc=0, scale = scale).rvs(num))

ysat=norm(loc=para_ysat[0],  scale=para_ysat[1]).rvs(num)
hp=norm(loc=para_hp[0],  scale=para_hp[1]).rvs(num)
mu = lognorm(Log_para(para_mu[0],para_mu[1])[0], loc=0
             , scale=Log_para(para_mu[0],para_mu[1])[1]).rvs(num)
mp = lognorm(Log_para(para_mp[0],para_mp[1])[0], loc=0
             , scale=Log_para(para_mp[0],para_mp[1])[1]).rvs(num)
k  = lognorm(Log_para(para_k[0],para_k[1])[0], loc=0
             , scale=Log_para(para_k[0],para_k[1])[1]).rvs(num)
Lf = lognorm(Log_para(para_Lf[0],para_Lf[1])[0], loc=0
             , scale=Log_para(para_Lf[0],para_Lf[1])[1]).rvs(num)
D  = lognorm(Log_para(para_D[0],para_D[1])[0], loc=0
             , scale=Log_para(para_D[0],para_D[1])[1]).rvs(num)
ic = lognorm(Log_para(para_ic[0],para_ic[1])[0], loc=0
             , scale=Log_para(para_ic[0],para_ic[1])[1]).rvs(num)
d  = lognorm(Log_para(para_d[0],para_d[1])[0], loc=0
             , scale=Log_para(para_d[0],para_d[1])[1]).rvs(num)
d70= lognorm(Log_para(para_d70[0],para_d70[1])[0], loc=0
             , scale=Log_para(para_d70[0],para_d70[1])[1]).rvs(num)
kh = lognorm(Log_para(para_kh[0],para_kh[1])[0], loc=0
             , scale=Log_para(para_kh[0],para_kh[1])[1]).rvs(num)
deterministic_parameters = [B, g, d70m, v, theta, ys, yw,n]

# Conbuting wave height and wave period
Hm0, Tp = Wave_height_MC(num, F,U10,hb,hw,g)

uniq_tot = np.array([])
weights_tot = np.array([])
```

```
start = perf_counter()
print ('starting sampling')
for l in range (len(adding_hw)):
    print ('l',l,'/',len(adding_hw))
    data = [k, hp, ysat, mu, mp, Lf, D, ic, d, d70, kh, hw+adding_hw[l]]
    for kk in range (len(lognorm_qc)):
        qc = qc_tot[kk]
        for i in range (len(WC_inps)):
            rootpit = 0
            for ff in range (len(LOC_inps)):
                LOC = LOC_inps[ff]

                Zu, Zh, Zp, Pfu, Pfh, Pfp, Pf_tot = MonteCarlo_Piping(num
                        , data, deterministic_parameters, rootpit, LOC)
                pf= OT_OF_Z_MC(num, np.ones(num)*Wind_dir,Hm0*WC_inps[i]
                , Tp,hw+adding_hw[l],qc,g,hc,yb,yf,yv,dikenormal,slope)

                total = np.zeros(num)
                for uu in range (num):
                    if Pf_tot[uu] == 1 or pf[uu] ==1:
                        total[uu] = 1
                BBN_LOC = np.ones(num)*round(LOC,2)
                BBN_IE = Pf_tot
                BBN_Wave_coeff = np.ones(num)*round(WC_inps[i],2)
                BBN_qc = ['{}'.format(lognorm_qc[kk])]*num
                BBN_hw = np.ones(num)*round(adding_hw[l],2)
                BBN_OTOF = pf

                inps   = np.array(np.vstack((BBN_Wave_coeff, BBN_qc,BBN_hw
                                    , BBN_OTOF, BBN_LOC, BBN_IE, total)).T)
                uniq, weights = np.unique(inps, axis = 0
                                          , return_counts = True)
                if i ==0 and kk ==0 and  l==0 and ff==0:
                    uniq_tot = uniq
                    weights_tot = weights
                else:
                    uniq_tot = np.concatenate((uniq_tot, uniq), axis=0)
                    weights_tot = np.concatenate((weights_tot, weights)
                    , axis=0)

end = perf_counter()
print ('It took in total for dike',dike,':', (end-start)/60, 'min.')

if save:
    # saving the input matrix
    np.save ('BBN/BBN_combined_uniq_{}.npy'.format(dike),uniq_tot)

    # saving the weight of each row of the input matrix
    np.save ('BBN/BBN_combined_weights_{}.npy'.format(dike),weights_tot)

#Creating the BBN with Pomegranate

labels=['Wave coefficient', 'Critical discharge','hw','OT OF','Loc','IE'
        , 'Total']
# Structure of the BBN
```

```
    imposed=((), # 0 wave coefficient
             (), # 1 qc
             (), # 2 hw
             (0,1,2,), # 3 OT_OF
             (), #4 Loc
             (2,4,),#5 IE
             (3,5,),) #6 total


    a = networkx.DiGraph()
    a.add_nodes_from([0,1,2,3,4,5,6])
    for i, tar in enumerate(imposed):
        [a.add_edge(tari, i) for tari in tar]

    # Create BBN
    BBN = BayesianNetwork.from_structure(uniq, imposed,  weights = weights
                                         , state_names=list(labels))

end_tot = perf_counter()
print ('It took:', (end_tot-start_tot)/3600, 'HOURS')
```

.